CONTRACT NO. A032-067
FINAL REPORT
AUGUST 1994

Experimental Investigation of the Atmospheric Chemistry of Aromatic Hydrocarbons and Long-Chain Alkanes

CALIFORNIA ENVIRONMENTAL PROTECTION AGENCY

AIR RESOURCES BOARD
Research Division

Experimental Investigation of the Atmospheric Chemistry of Aromatic Hydrocarbons and Long-Chain Alkanes

Final Report

Contract No. A032-067

Prepared for:

California Air Resources Board
Research Division
2020 L Street
Sacramento, California 95814

Prepared by:

Co-Principal Investigators

Roger Atkinson
Janet Arey
Ernesto C. Tuazon

Research Staff

Sara M. Aschmann
Isabelle Bridier
Eric S. C. Kwok

Statewide Air Pollution Research Center
University of California
Riverside, California 92521

August, 1994

Disclaimer

The statements and conclusions in this report are those of the contractor and not necessarily those of the California Air Resources Board. The mention of commercial products, their source, or their use in connection with material reported herein is not to be construed as actual or implied endorsement of such products.

Acknowledgments

We express our appreciation to our Project Officer, Bart E. Croes, for many helpful discussions and encouragement throughout this entire program. We thank Ms. Susan I. Waddy for assistance in the fiscal management of this program and special thanks is due to Ms. Christy J. LaClaire for typing and assembling this report.

This report was submitted in fulfillment of ARB Contract Number A032-067 "Experimental Investigation of the Atmospheric Chemistry of Aromatic Hydrocarbons and Long-Chain Alkanes," by the Statewide Air Pollution Research Center, University of California, Riverside, under the sponsorship of the California Air Resources Board and the California Environmental Protection Agency. Work was completed as of May 5, 1994.

Abstract

Two aspects of the atmospheric chemistry of volatile organic compounds have been addressed in this experimental program, and these concern the reactions of the hydroxycyclohexadienyl-type radicals (OH-aromatic adducts) formed from OH radical addition to the aromatic ring of the aromatic hydrocarbons under atmospheric conditions and the atmospheric reactions of the alkoxy radicals formed after OH radical reaction with the alkanes. Product studies of the OH radical-initiated reactions of toluene, *o*-xylene and 1,2,3-trimethylbenzene have been carried out in the absence of NO_x and in the presence of varying concentrations of NO_2. The 2,3-butanedione formation yields from the *o*-xylene reaction show that the OH-*o*-xylene adduct reacts with both O_2 and NO_2. The rate constant ratio for reaction of the OH-*o*-xylene adduct with NO_2 *versus* reaction with O_2 was determined to be k_{NO2}/k_{O2} = 1.3 x 10^5 at 298 K, showing that the OH-*o*-xylene adduct reacts with O_2 in the atmosphere. However, since several product studies of the OH radical reactions with aromatic hydrocarbons have been carried out at part-per-million levels of NO_2, care must be taken in using these laboratory product data for atmospheric purposes.

A series of product studies of the OH radical-initiated reactions of selected alkanes, ketones and alcohols have been carried out to obtain further insights into alkoxy radical isomerization. Product studies with gas chromatographic analyses of the OH radical reaction with 4-methyl-2-pentanone, 2,6-dimethyl-4-heptanone, 2,4-dimethyl-2-pentanol and 3,5-dimethyl-3-hexanol, in the presence of NO_x, have provided unambiguous evidence for alkoxy radical isomerization and these studies and that of *n*-pentane, again using gas chromatography for product analyses, have provided rate constant ratios for the isomerization reaction *versus* alkoxy radical decomposition and reaction with O_2. Preliminary experiments with *in situ* atmospheric pressure ionization mass spectrometry are consistent with the formation of the expected δ-hydroxcarbonyls formed after the alkoxy radical isomerizations, with the apparent importance of isomerization increasing with the carbon number for the *n*-alkane series *n*-butane through *n*-octane.

The experimental data obtained in this Contract provide new information concerning the atmospheric chemistry of aromatic hydrocarbons and alkanes which will allow future detailed chemical mechanisms for the formation of photochemical air pollution to be placed on a firmer scientific basis than is presently the case.

Table of Contents

Page

Disclaimer ii
Acknowledgments iii
Abstract iv
List of Figures vi
List of Tables ix

I. INTRODUCTION AND BACKGROUND 1

A. Introduction 1
B. Background 3

II. PRODUCTS OF THE GAS-PHASE REACTIONS OF AROMATIC HYDROCARBONS 9

A. Experimental 9
B. Results 13
C. Conclusions 33

III. PRODUCTS OF THE GAS-PHASE REACTIONS OF SELECTED KETONES 34

A. Experimental 35
B. Results and Discussion 37
C. Conclusions 58

IV. PRODUCT STUDIES OF THE GAS-PHASE REACTIONS OF THE OH RADICAL WITH SELECTED ALCOHOLS 59

A. Experimental 59
B. Results and Discussion 64

V. PRODUCTS OF THE GAS-PHASE REACTIONS OF OH RADICALS WITH A SERIES OF *n*-ALKANES 66

A. Experimental 66
B. Results and Discussion 69

VI. SUMMARY AND CONCLUSIONS 81

References 83
Glossary of Terms, Abbreviations and Symbols 88

List of Figures

Page

Figure 1. Schematic of the SAPRC ~7900 liter all-Teflon chamber 10

Figure 2. Plot of the amounts of *o*-cresol formed, corrected for reaction with the OH radical (see text), against the amounts of toluene reacted in O_3-alkene-toluene-air mixtures. The alkenes were: o, propene; ▵, α-pinene 15

Figure 3. Plots of the amounts of 2,3-butanedione (biacetyl) formed against the amounts of *o*-xylene and 1,2,3-trimethylbenzene reacted in O_3-alkene-aromatic hydrocarbon-air mixtures. The alkenes were: ▿, propene; o, ▵, α-pinene 16

Figure 4. Plots of the amounts of 2,3-butanedione formed against the amounts of *o*-xylene reacted in irradiated CH_3ONO-NO-NO_2-*o*-xylene-air mixtures. Average NO_2 concentrations (in molecule cm^{-3} units) are given and the differing symbols identify different experiments. o, NTC-150; ●, NTC-162; ▵, NTC-133; ▲, NTC-160; ▿, NTC-146; □, NTC-163; ▼, NTC-161 22

Figure 5. Plot of the 2,3-butanedione formation yields against the average NO_2 concentrations. o, Irradiations of CH_3ONO-NO-*o*-xylene-air mixtures; ▵, Irradiation of a CH_3ONO-NO-NO_2-*o*-xylene-air mixture (NTC-163); □, Irradiation of a CH_3ONO-NO-*o*-xylene-O_2 (4.3%)-N_2 (NTC-164) mixture; ●, Reaction of O_3-alkene-*o*-xylene-air mixtures. [See Table 3 for initial conditions]. (▬), Calculated 2,3-butanedione yield for one atmosphere of air with $k_2 = 2.3 \times 10^{-16}$ cm^3 $molecule^{-1}$ s^{-1}; $Y_{O_2} = 0.185$; $k_3 = 3.0 \times 10^{-11}$ cm^3 $molecule^{-1}$ s^{-1}; $Y_{NO_2} = 0.04$ (see text) 23

Figure 6. Plot of $(Y_{O_2}-Y)[O_2]/[NO_2]$ against Y for the OH radical-initiated reaction of *o*-xylene in the presence of NO_x. Y is the measured 2,3-butanedione yield and Y_{O_2} is the 2,3-butanedione yield from the reaction when the hydroxycyclohexadienyl radical(s) react with O_2. o - Irradiations of CH_3ONO-NO-NO_2-*o*-xylene-air mixtures; ▵, Irradiation of a CH_3ONO-NO-*o*-xylene-O_2 (4.3%)-N_2 mixture (NTC-164) 25

List of Figures
(continued)

Page

Figure 7. Plot of the amounts of 2,3-butanedione formed against the amounts of 1,2,3-trimethylbenzene reacted in irradiated CH_3ONO-NO-NO_2-1,2,3-trimethylbenzene-air mixtures with average NO_2 concentrations of (0.58-2.4) x 10^{13} molecule cm^{-3}. □, NTC-139; ▽, NTC-138; △, NTC-137; o, NTC-132 28

Figure 8. Plot of the amounts of 2,3-butanedione formed against the amounts of 1,2,3-trimethylbenzene reacted in irradiated CH_3ONO-1,2,3-trimethylbenzene-air mixtures. o, NTC-140, 142 and 143; ●, NTC-141. (- - -), 2,3-Butanedione yield from data obtained at NO_2 concentrations in the range (0.16-3.6) x 10^{13} molecule cm^{-3} (Figure 7) 29

Figure 9. Plot of the nitrobenzene formation yield against NO_2 concentration (taken from ref. *35*). (——) Fit with k_2 = 1.7 x 10^{-16} cm^3 $molecule^{-1}$ s^{-1}, k_3 = 2.5 x 10^{-11} cm^3 $molecule^{-1}$ s^{-1} and a nitrobenzene yield from reaction (3) of 0.09 31

Figure 10. Plot of the *m*-nitrotoluene formation yield against the NO_2 concentration (taken from ref. *35*). (——), Fit with k_2 = 5.2 x 10^{-16} cm^3 $molecule^{-1}$ s^{-1}, k_3 = 3.6 x 10^{-11} cm^3 $molecule^{-1}$ s^{-1} and a *m*-nitrotoluene yield from reaction (3) of 0.076 (using k_{1b}/k_1 = 0.92 for toluene (*4*); $k_{3c}k_{1b}/k_1k_3$ = 0.07) 32

Figure 11. Plots of the amounts of acetone and 2-methylpropanal formed, corrected for reaction with the OH radical (see text), against the amounts of 4-methyl-2-pentanone reacted with the OH radical 39

Figure 12. Plots of the amounts of acetone formed, corrected for reaction with the OH radical (see text), against the amounts of 2,6-dimethyl-4-heptanone reacted with the OH radical. Initial NO and NO_2 concentrations (in units of 10^{14} molecule cm^{-3}) were: o, ●, 1.9 and 0.3, respectively; △, ▲, 1.2 and 1.3, respectively; ▽, ▼, 0.7 and 1.5, respectively; □, ■, 2.4 and 0, respectively. ●, ▲, ▼, ■, Analysis ≥1 hr after addition of NO to reacted mixture. Line is from a least-squares analysis of data shown by filled symbols 47

List of Figures
(continued)

Page

Figure 13. Plots of the amounts of acetone [after addition of NO to the reacted mixtures (data shown as ●, ▲, ▼, ■ in Figure 12)] and 2-methyl-propanal, corrected for reaction with the OH radical (see text), against the amounts of 2,6-dimethyl-4-heptanone reacted with the OH radical 49

Figure 14. Schematic of 6500 liter all-Teflon chamber interfaced to SCIEX API mass spectrometer 67

Figure 15. Plots of the amounts of 2- and 3-pentanone formed, corrected for reaction with the OH radical, against the amount of *n*-pentane reacted. o, △ - In air diluent; ●, ▲, in a 75% O_2 25% N_2 mixture 71

Figure 16. Plots of $(\text{yield})^{-1}$ for 2- and 3-pentanone against $[O_2]^{-1}$ 74

Figure 17. API MS spectrum for 4-octanol 77

Figure 18. API MS spectra obtained before (top) and after (bottom) irradiation of a CH_3ONO-NO-*n*-pentane-air mixture 78

Figure 19. API MS spectra obtained before (top) and after (bottom) irradiation of a CH_3ONO-NO-*n*-heptane-air mixture 79

List of Tables

Page

Table 1. Summertime NMOC Concentrations in Ambient Air (0600 hr) in Los Angeles (1987) [from Lurmann and Mains (*15*)] 2

Table 2. Experimental Conditions and *o*-Cresol Formation Yields from the OH Radical-Initiated Reaction of Toluene in Air 17

Table 3. Experimental Conditions and 2,3-Butanedione Formation Yields from the OH Radical-Initiated Reaction of *o*-Xylene 18

Table 4. Experimental Conditions and 2,3-Butanedione Formation Yields from the OH Radical-Initiated Reaction of 1,2,3-Trimethylbenzene 19

Table 5. Experimental Yields of Acetone and 2-Methylpropanal from the Reactions of the OH Radical with 4-Methyl-2-pentanone and 2,6-Dimethyl-4-heptanone at 296 ± 2 K and 740 Torr Total Pressure of Air 40

Table 6. Initially Formed Alkoxy Radicals in the OH Radical-Initiated Reaction of 2,6-Dimethyl-4-heptanone, and the Possible Production of Acetone and 2-Methylpropanal from the Reactions of these Alkoxy Radicals (Reaction Schemes IIa-IIc) 55

Table 7. Experimental and Estimated Relative Importances of Decomposition *versus* Isomerization for Selected Alkoxy Radicals at 298 K 56

Table 8. Measured Formation Yields of 2-Pentanone, 3-Pentanone, 2-Pentyl Nitrate and 3-Pentyl Nitrate at 296 ± 2 K and 760 Torr Total Pressure 72

I. INTRODUCTION AND BACKGROUND

A. Introduction

The interactions, under the influence of sunlight, of non-methane organic compounds (NMOC) emitted into the atmosphere from anthropogenic sources with oxides of nitrogen lead to the formation of photochemical air pollution, manifested by the formation of ozone, PM-10 (leading to visibility degradation), acidic deposition and a spectrum of non-criteria pollutants such as peroxyacetyl nitrate (PAN) and formaldehyde (*1-4*). In California's South Coast Air Basin, emissions from mobile sources are responsible for 50-60% of the 1200-1700 tons per day (for 1987) of anthropogenic reactive organic compounds (*5,6*), with these mobile-source generated non-methane organic compounds being predominantly comprised of alkanes, alkenes and aromatic hydrocarbons (*7-11*).

NMOC emission measurements from gasoline-fueled light duty vehicles show that the percentages of the alkane, alkene and aromatic hydrocarbon emissions are ~55%, ~15%, and ~30%, respectively (*8,10*), and very similar alkane, alkene and aromatic hydrocarbon concentration profiles are observed from roadway (*9*), tunnel (*7*) and ambient urban air (*12-15*) measurements. Table 1 summarizes the NMOC data reported by Lurmann and Mains (*15*) for the 0600 hr sample period in Los Angeles during the 1987 South Coast Air Quality Study, and the alkane, alkene, aromatic hydrocarbon partitioning is 48%, 10% and 22%, respectively, with carbonyls and unidentified NMOC accounting for the remainder. Clearly, on a mass basis the alkanes and aromatic hydrocarbons account for ≥70% of the NMOC emitted into the atmosphere in urban areas.

A detailed knowledge of the atmospheric chemistry of these NMOC emissions is needed to understand the the formation of photochemical air pollution and to develop cost-effective air pollution control strategies (*1,2,4,16-19*). During the past two decades, there have been vast improvements in our understanding of the detailed chemical processes involving anthropogenic NMOC and oxides of nitrogen which occur in urban and, to a lesser extent, in rural air masses. Recently developed and tested chemical mechanisms designed for use in airshed computer models are in general agreement (*16-19*). However, despite this general agreement between

Table 1. Summertime NMOC Concentrations in Ambient Air (0600 hr) in Los Angeles (1987) [from Lurmann and Mains (*15*)].

	Average Concentration	
Reactivity Class	ppbC	%
Unreactive (ethane + acetylene)	61	6.3
Propane	62	6.4
Higher paraffins	366	37.7
Ethylene	34	3.5
Propene	14	1.4
Higher Olefins	54	5.6
Benzene	24	2.5
Toluene	68	7.0
Higher aromatics	117	12.0
Formaldehyde	6.8	0.7
Acetaldehyde	8.4	0.9
Higher aliphatic carbonyls	48	4.9
Unidentified hydrocarbons	139	14.3
TOTAL	972	100

recent chemical mechanisms describing the formation of photochemical air pollution (*17,18*), there are significant areas of uncertainty in the chemistry of the polluted troposphere (*4*). In fact, the similarities among the predictions of the recent chemical mechanisms arise because chemical mechanisms are tested against, and fitted to, smog chamber data which provide "global" bounds on the mechanisms. Thus, those aspects of the chemistry which are uncertain are parameterized and best-fit to the smog chamber data and the general agreement between mechanism predictions is then not surprising.

As a result of chemical mechanism development (*16-19*) and review and evaluation of the literature kinetic, mechanistic and product data (*4*), it is recognized that the major areas of uncertainty in the tropospheric chemistry of anthropogenically emitted NMOC are:

- The chemistry of the $>C_4$ alkanes.
- The chemistry of the aromatic hydrocarbons.
- The products formed from the reactions of O_3 with alkenes, including the formation yields of OH radicals.

In this experimental program, the California Air Resources Board (ARB) contracted to the Statewide Air Pollution Research Center (SAPRC) to study the products formed from the atmospheric transformations of selected long-chain alkanes and aromatic hydrocarbons, using an array of analytical techniques, including *in situ* atmospheric pressure ionization tandem mass spectrometry (API MS/MS). The data obtained have significantly advanced our knowledge of the atmospheric chemistry of these two classes of organic compounds and will place the next generation of chemical mechanisms for use in urban and regional airshed computer models on a firmer basis than was previously the case.

B. Background

As discussed above, two major areas of uncertainty in the chemistry of anthropogenically emitted NMOC concern the chemistry of the $>C_4$ alkanes and of the aromatic hydrocarbons, which comprise a major fraction of the NMOC emitted from vehicles and present in ambient urban air. The present status of the tropospheric chemistry of the $>C_4$ alkanes and of the aromatic hydrocarbons is briefly discussed below [the articles of Carter and Atkinson (*20*), and Atkinson (*4*) provide a more detailed discussion].

Alkane Chemistry. Under tropospheric conditions, the alkanes react essentially only with the OH radical, with the nighttime NO_3 radical reaction being of minor importance.

$$OH + RH \rightarrow H_2O + \dot{R}$$

The alkyl radicals rapidly and exclusively add O_2 to form the alkyl peroxy ($R\dot{O}_2$) radicals

$$\dot{R} + O_2 \xrightarrow{M} R\dot{O}_2$$

The important tropospheric reactions of these alkyl peroxy radicals are with NO and HO_2 and, to a lesser extent, organic peroxy radicals. The reaction with NO can form either the corresponding alkoxy ($R\dot{O}$) radical plus NO_2 or the alkyl nitrate

$$R\dot{O}_2 + NO \xrightarrow{M} \begin{cases} R\dot{O} + NO_2 \\ RONO_2 \end{cases}$$

with the formation yield of the nitrate increasing with increasing pressure and decreasing temperature, and being dependent on whether the $R\dot{O}_2$ radical is primary, secondary or tertiary (*4,21,22*). For the secondary $R\dot{O}_2$ radicals formed from the *n*-alkanes, the alkyl nitrate yield at 298 K and 760 torr total pressure of air increases monotonically from 8% for *n*-butane to 33% for *n*-octane (*21*).

The reactions of the $R\dot{O}_2$ radicals with HO_2 radicals become important when the NO mixing ratio falls below ~30 parts-per-trillion (at these low NO mixing ratios $R\dot{O}_2$ radicals are not important for the formation of O_3 but are important in the chemistry of downwind urban and rural airmasses)

$$R\dot{O}_2 + HO_2 \rightarrow ROOH + O_2$$

Under conditions where O_3 formation is occurring, the major reaction is with NO leading in large part to the formation of the corresponding alkoxy radical. The alkoxy radicals can react by thermal decomposition, thermal isomerization and reaction with O_2. For example, for the 2-pentoxy radical formed from *n*-pentane

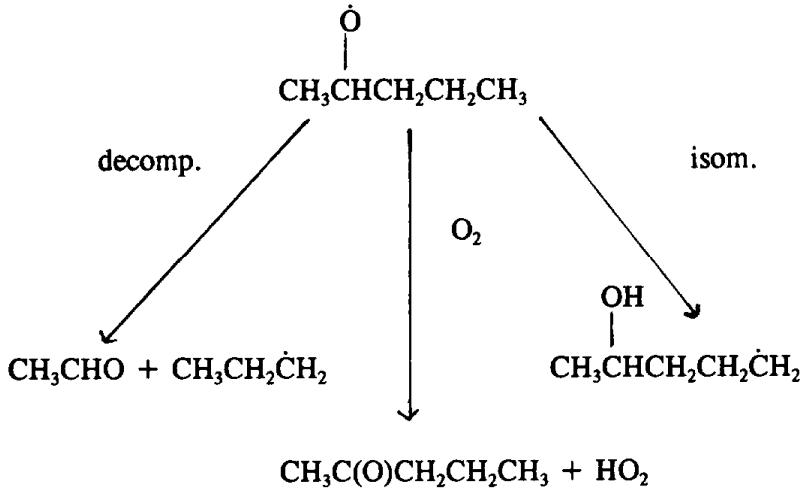

The uncertainty concerns the importance of the isomerization pathway and the subsequent reactions as well as the relative importance of the decomposition, isomerization, and O_2 reactions (*4*). In agreement with thermochemical estimates (*4,20,21*), there is evidence that the isomerization reaction occurs [for example, from a lack of the products expected from the RȮ + O_2 reaction in the *n*-butane photooxidation system (*23-25*)], but there is no *direct* experimental evidence of this reaction pathway, and the reactions subsequent to the isomerization step are not known nor are the final products observed. As discussed by Carter and Atkinson (*20*), this isomerization reaction is estimated to account for the majority of the reactions of the alkoxy radicals formed from the long-chain alkanes. Thus, the reaction sequence, including the number of NO to NO_2 conversions, the extent of organic nitrate formation from the δ-hydroxyalkyl peroxy radicals and the carbonyl compounds formed, has a significant effect on ozone formation from this class of organic compounds (*20,22*).

Aromatic Hydrocarbons. As for the alkanes, under tropospheric conditions the aromatic hydrocarbons react essentially only with the OH radical. The rate constants for these reactions are well known, and the reactions proceed by two pathways; H atom abstraction from the C-H bonds of the alkyl substituents or (for benzene) of the ring C-H bonds, and reversible OH radical addition to the aromatic ring to form hydroxycyclohexadienyl or alkyl-substituted hydroxycyclohexadienyl radicals (*4,26,27*). For example, for toluene

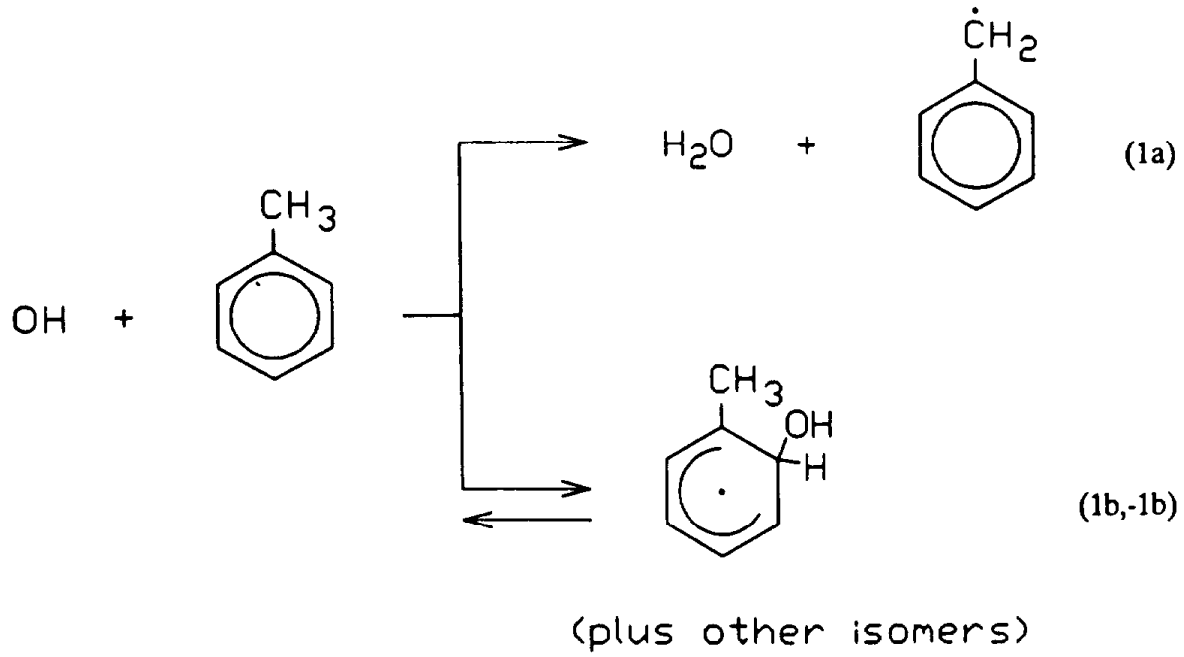

The H atom abstraction pathway is relatively minor for benzene and the methyl-substituted benzenes, with $k_{1a}/(k_{1a} + k_{1b}) \leq 0.1$ at 298 K (*4*), and the reactions subsequent to the formation of the benzyl-type radicals from reaction (a) appear to be reasonably well understood. For example, for the benzyl radical:

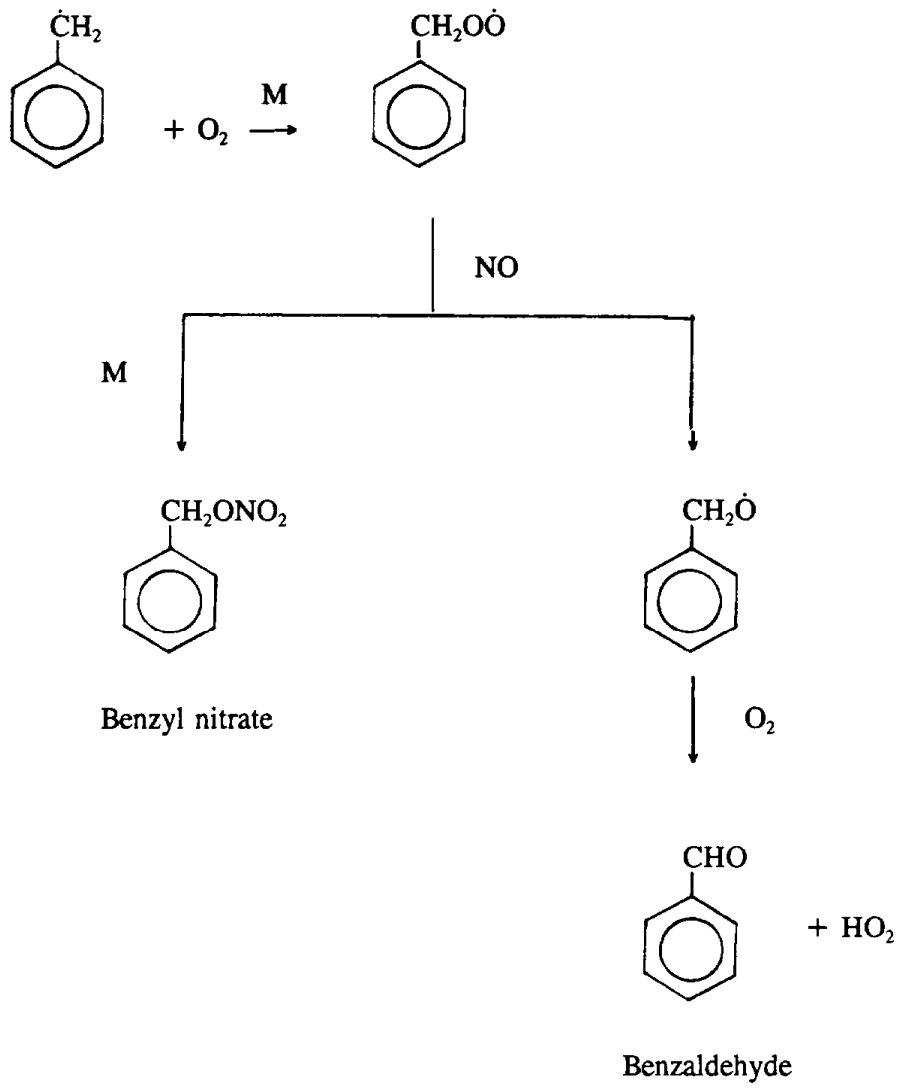

The major fraction of the OH radical-initiated reaction proceeds through the intermediate formation of a hydroxycyclohexadienyl-type radical, ultimately leading to the formation of ring-retaining compounds, such as phenols and nitroaromatics, and ring-cleavage compounds such as α-and γ-dicarbonyls and other unsaturated carbonyl compounds.

The reactions subsequent to OH radical addition to the aromatic ring to form the hydroxycyclohexadienyl radical(s) are, however, presently not well understood (*4*). There have been a number of studies to determine the rate constants for the reactions of the

hydroxycyclohexadienyl and methylhydroxycyclohexadienyl radicals with O_2, NO and NO_2 (*27-34*), and Zetzsch and coworkers (*27,31,34*) have shown that the important reactions are with O_2 and NO_2. The room temperature rate constants for the reactions of the hydroxycyclohexadienyl and methylhydroxycyclohexadienyl radicals with O_2 and NO_2 (*27,34*) are (cm^3 $molecule^{-1}$ s^{-1} units) $(1.6 \pm 0.6) \times 10^{-16}$ and $(5.6 \pm 1.5) \times 10^{-16}$ for reaction with O_2 at 299 K, respectively (*34*), and $(2.75 \pm 0.2) \times 10^{-11}$ and $(3.6 \pm 0.4) \times 10^{-11}$ for reaction with NO_2 at 300-305 K, respectively (*27*). These rate constants lead to the expectation that the hydroxycyclohexadienyl radical will react at equal rates with O_2 and NO_2 in an atmosphere of air for an NO_2 concentration of 3×10^{13} molecule cm^{-3}, and for the methylhydroxycyclohexadienyl radical at an NO_2 concentration of 8×10^{13} molecule cm^{-3}.

Previous studies of the aromatic ring-retaining products formed from the OH radical-initiated reactions of benzene, toluene and the xylenes in the presence of NO_x showed, however, no change in the major products formed or in their formation yields over a range of NO_2 concentrations such that the expected reactions of the hydroxycyclohexadienyl radicals ranged from being mainly with O_2 to being mainly with NO_2 (*35,36*). These product data (*35,36*), especially those for nitrobenzene from benzene and m-nitrotoluene from toluene (*35*), were interpreted as indicating that the dominant reaction of the hydroxycyclohexadienyl radicals were with NO_2 for NO_2 concentrations $> 1.5 \times 10^{13}$ molecule cm^{-3}.

In this study, we have experimentally investigated selected aspects of the atmospheric chemistry of organic compounds with the aim being to elucidate the reactions under tropospheric conditions of the alkoxy radicals formed from alkanes (and related compounds) and of the hydroxycyclohexadienyl radicals formed from the aromatic hydrocarbons.

Sections II through V describe the experimental studies carried out to investigate the selected aspects of the atmospheric chemistry of alkanes and aromatic compounds.

II. PRODUCTS OF THE GAS-PHASE REACTIONS OF AROMATIC HYDROCARBONS

The formation of selected ring-retaining and ring-opened products from the OH radical reactions with toluene, o-xylene and 1,2,3-trimethylbenzene were investigated as a function of the NO_2 concentration, including in the absence of NO_x. The data obtained, in particular the formation of 2,3-butanedione (biacetyl) from o-xylene, are consistent with the kinetic data of Zetzsch and coworkers (*27,34*), and indicate that under ambient atmospheric conditions the hydroxycyclohexadienyl radicals formed from the simple monocyclic aromatic hydrocarbons will react predominantly with O_2.

A. Experimental

Experiments were carried out at 296 $\pm$ 2 K and atmospheric pressure (735 Torr) of purified air or (air + O_2) in a 7900 liter all-Teflon chamber (NTC; New Teflon Chamber) equipped with two parallel banks of blacklamps (Figure 1). OH radicals were generated in the presence of NO_x from the photolysis of CH_3ONO-NO-NO_2-air (or air + O_2) mixtures

$$CH_3ONO + h\upsilon \rightarrow CH_3O + NO$$

$$CH_3O + O_2 \rightarrow HCHO + HO_2$$

$$HO_2 + NO \rightarrow OH + NO_2$$

The initial reactant concentrations (in units of 10^{13} molecule cm^{-3}) for the experiments carried out in air were: for toluene, CH_3ONO, 9.4-40.2; NO, 9.2-27.7; NO_2, 0-12.1; toluene, 2.25-2.28; for o-xylene, CH_3ONO, 0.85-23.8; NO, 1.0-22.0; NO_2, 0-5.3; o-xylene, 2.15-2.53; and for 1,2,3-trimethylbenzene, CH_3ONO, 1.0-23.8; NO, 0-8.4; NO_2, 0; 1,2,3-trimethylbenzene, 2.48-2.63. Irradiations were carried out at 20% of the maximum light intensity for 6-18 mins (toluene), 3-9 mins (o-xylene) or 0.25-5 mins (1,2,3-trimethylbenzene). In addition, an irradiation of an o-xylene (2.20 x 10^{13} molecule cm^{-3})-CH_3ONO (9.2 x 10^{12} molecule cm^{-3})-NO (1.06 x 10^{13} molecule cm^{-3}) mixture was carried out in a 4.3% O_2/95.7% N_2 mixture at 20%

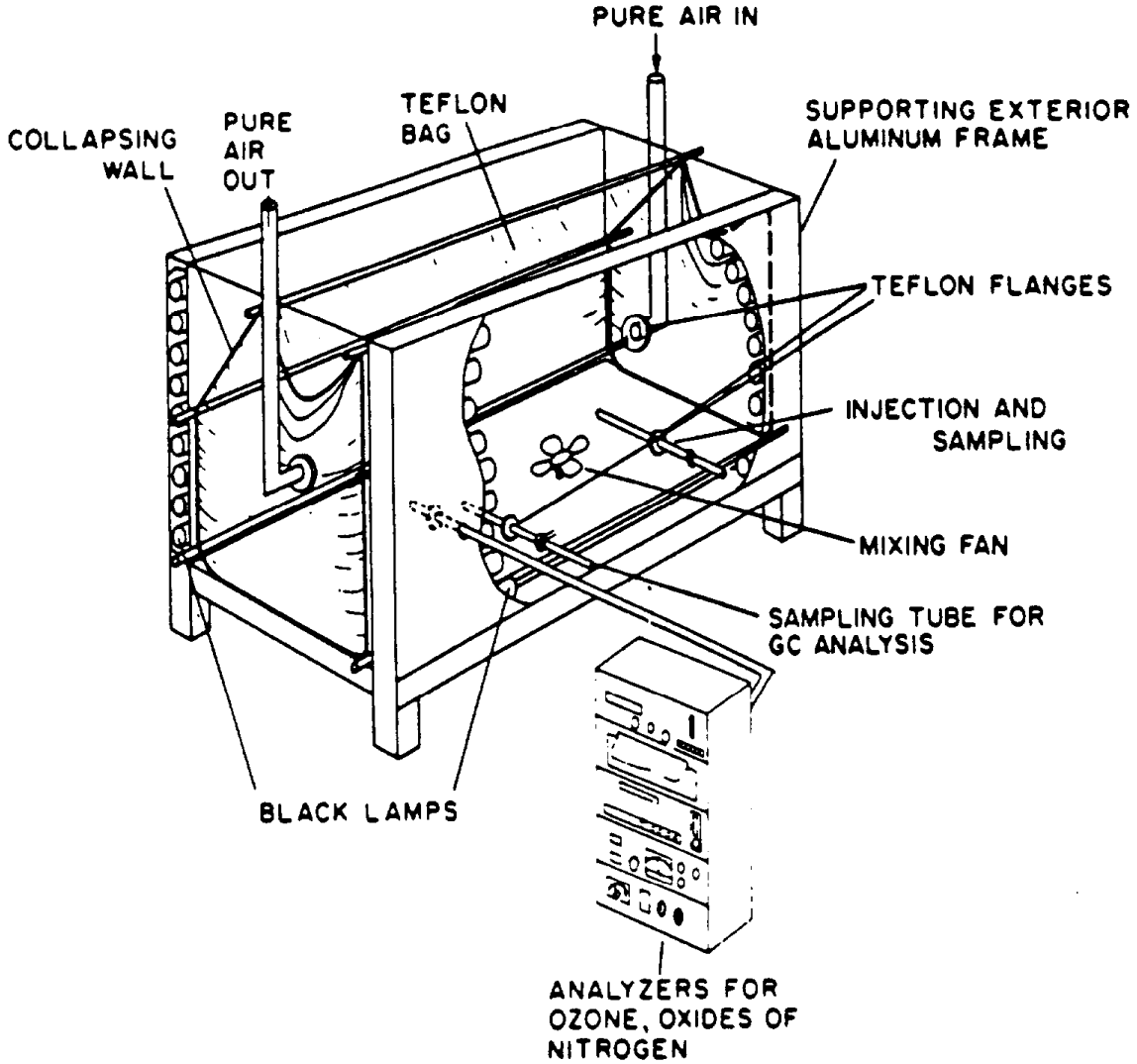

Figure 1. Schematic of the SAPRC ~7900 liter all-Teflon chamber.

maximum light intensity for 3-9 mins. OH radicals were also generated in the absence of NO_x from the dark reactions of O_3 with propene or α-pinene in air (*38,39*), with initial reactant concentrations (in units of 10^{13} molecule cm^{-3}) of: propene or α-pinene, 4.8; toluene, *o*-xylene or 1,2,3-trimethylbenzene, 4.3-5.0; and 6-8 additions of O_3 (at initial concentrations in the chamber of 5 x 10^{12} molecule cm^{-3} per addition) were made to the chamber during an experiment.

The aromatic hydrocarbons and selected products (*o*-cresol from toluene and 2,3-butanedione from *o*-xylene and 1,2,3-trimethylbenzene) were analyzed by gas chromatography with flame ionization detection (GC-FID). Gas samples of 100 cm^3 volume were collected from the chamber onto Tenax-TA solid adsorbent, with subsequent thermal desorption at 250 °C onto a 30 m DB-5.625 megabore column held at 0 °C and then temperature programmed at 8 °C min^{-1}. GC-FID calibration factors for *o*-xylene, 1,2,3-trimethylbenzene and 2,3-butanedione were determined by introducing known amounts of these organic compounds into the NTC. Calibration factors for toluene, *o*-cresol and 2,3-dimethylphenol were determined by adding known amounts in methanol solution to Tenax solid adsorbent cartridges. This and previous (*35*) studies indicate quantitative collection and thermal desorption efficiencies for these compounds using Tenax solid adsorbent. Selected analyses were also carried out by combined gas chromatography-mass spectrometry (GC/MS) using a Hewlett Packard 5890 GC interfaced to a HP 5970 mass selective detector operating in the scanning mode. For these GC/MS analyses, gas samples collected on Tenax-TA solid adsorbent were thermally desorbed at 250 °C onto a 50 m HP-5 fused silica capillary column held at -50 °C and temperature programmed to 200 °C at 10 °C min^{-1}.

Irradiations of 2,3-butanedione (1.2 x 10^{13} molecule cm^{-3})-air, CH_3ONO (2.5 x 10^{13} molecule cm^{-3})-air and CH_3ONO (2.5 x 10^{13} molecule cm^{-3})-NO (1.32 x 10^{13} molecule cm^{-3})-air mixtures were also conducted at 20% of the maximum light intensity for 10-30 mins to determine the photolysis lifetimes of 2,3-butanedione and methyl nitrite under the light intensity and spectral distribution conditions used for the CH_3ONO-NO-NO_2-aromatic hydrocarbon-air irradiations. 2,3-Butanedione was analyzed as described above, and CH_3ONO was analyzed by GC-FID using a 1 cm^3 gas sampling loop and 30 m DB-5 megabore column temperature programmed from -25 °C at 6 °C min^{-1}. NO concentrations during the experiments and the

initial NO_2 concentrations were monitored using a Thermo Environmental Instruments, Inc. Model 42 chemiluminescence NO-NO_2-NO_x analyzer. NO_2 concentrations during the CH_3ONO-NO-NO_2-aromatic-air irradiations were calculated from the initially measured NO and NO_2 concentrations and the assumption (*35*) that ([NO] + [NO_2]) remained constant during these irradiations.

As noted above, the GC-FID systems were calibrated for the aromatic hydrocarbon reactants and the *o*-cresol, 2,3-dimethylphenol and 2,3-butanedione products. Measured pressures of 2,3-butanedione, as measured using a MKS Baratron 0-100 Torr pressure sensor, were introduced into a 2.0 liter Pyrex bulb and the contents flushed into the chamber with a stream of N_2 gas. Measured volumes of liquid *o*-xylene and 1,2,3-trimethylbenzene were introduced into a 1 liter Pyrex bulb and the contents flushed into the chamber by a stream of N_2 gas. The volume of the chamber was determined during these calibrations by introducing a measured volume of *trans*-2-butene into the chamber and measuring its concentration using a pre-calibrated GC/loop injection system. Known solutions of toluene, *o*-cresol and 2,3-dimethylphenol in methanol solution were spiked onto Tenax solid adsorbent with subsequent thermal desorption for the GC-FID calibrations of these compounds. Consistency of the initial concentrations of reactants and the product formation yields in replicate experiments served to validate the calibration factors during the series of experiments conducted. The NO-NO_x analyzer was calibrated using a National Institute of Standards and Technology NO in N_2 mixture. All analytical instruments were maintained as recommended and their performance routinely checked on a daily basis.

The chemicals used, and their stated purities, were: 2,3-butanedione (99%), *o*-cresol (99+%), 2,3-dimethylphenol (97%), α-pinene (99+%), toluene (99+%), 1,2,3-trimethylbenzene, and *o*-xylene (97%), Aldrich Chemical Company; and propene ($\geq$99.0%) and NO ($\geq$99.0%), Matheson Gas Products. NO_2 was prepared prior to use by reacting NO with an excess amount of O_2. Methyl nitrite was prepared and stored as described previously (*37*), and O_3 was obtained as needed from a Welsbach T-408 ozone generator. For the majority of the experiments, purified air (relative humidity ~5%) was used as the diluent gas; a low O_2 concentration experiment was carried out in a purified air/O_2 mixture corresponding to 4.3% O_2.

B. Results

The photolysis of a 2,3-butanedione-air mixture led to 5% loss of 2,3-butanedione after 30 mins irradiation at 20% of the maximum light intensity, and a least-squares analysis of the data yielded a 2,3-butanedione decay rate due to photolysis of $(2.5 \pm 0.8) \times 10^{-5}\ s^{-1}$, where the indicated error is two least-squares standard deviations. Hence <2% photolysis loss of 2,3-butanedione would occur during the ≤9 min duration CH_3ONO-NO-air irradiations of *o*-xylene and 1,2,3-trimethylbenzene. Photolysis of CH_3ONO-NO-air and CH_3ONO-air mixtures at 20% of the maximum light intensity led to photolysis lifetimes of CH_3ONO of 16.2 ± 0.9 mins and 14.5 ± 1.4 mins, respectively, with an average value of 15 mins.

Toluene, *o*-xylene and 1,2,3-trimethylbenzene were observed to react in dark propene-aromatic hydrocarbon-O_3-air and α-pinene-aromatic hydrocarbon-O_3-air mixtures, with the formation of *o*-cresol from toluene and 2,3-butanedione from *o*-xylene and 1,2,3-trimethylbenzene being observed (and focussed on). The fractions of toluene, *o*-xylene and 1,2,3-trimethylbenzene reacted in these O_3-alkene-air mixtures at the end of the reactions were 5-6%, 11-14%, and 24-25%, respectively, which can be compared to ~9% reaction of cyclohexane in similar systems with all reactant concentrations a factor of two lower (*38,39*). Assuming that approximately the same (integrated amounts of OH radicals)/(reactant hydrocarbon concentrations) occur in these various O_3-alkene-air systems, then the fractions of cyclohexane or aromatic hydrocarbons reacted should be approximately proportional to the OH radical reaction rate constants. The literature rate constants for the reactions of the OH radical with toluene, *o*-xylene, 1,2,3-trimethylbenzene and cyclohexane at room temperature are (in 10^{-12} $cm^3\ molecule^{-1}\ s^{-1}$ units) 6.0, 13.7, 32.7 and 7.5, respectively (*4,26*), in general agreement with the percentages of these compounds reacting. This general agreement suggests that the OH radical reactions with the aromatic hydrocarbons in these O_3-alkene-air mixtures occur by both H-atom abstraction and OH radical addition, since the H-atom abstraction pathways account for ≤10% of the total reactions (*26*). This then means that (despite the absence of NO_x in these systems) the methylhydroxycyclohexadienyl radicals formed from the OH radical addition pathway must react further rather than back-decompose to reactants via reaction (-1b).

Plots of the amounts of *o*-cresol formed from toluene and of 2,3-butanedione from *o*-xylene and 1,2,3-trimethylbenzene against the amounts of aromatic hydrocarbon reacting in O_3-

alkene-air mixtures are shown in Figures 2 and 3. Taking into consideration the small fractions of reaction occurring for toluene and *o*-xylene, reasonably good straight line plots are observed, with no obvious difference between the data obtained with propene or α-pinene as the alkene for the experiments with toluene and *o*-xylene. The product yields obtained from least-squares analyses are given in Tables 2, 3, and 4, respectively. In the case of *o*-cresol, the measured concentrations were corrected for secondary reaction with the OH radical as described previously (*40*), using rate constants for the OH radical reactions with toluene and *o*-cresol of 5.96×10^{-12} cm^3 $molecule^{-1}$ s^{-1} and 4.2×10^{-11} cm^3 $molecule^{-1}$ s^{-1}, respectively (*4,26*). Measured NO_x concentrations during these experiments were $<2 \times 10^{11}$ molecule cm^{-3}.

The product yield data from the OH radical reactions in the presence of NO_x are discussed by the individual aromatic hydrocarbon below.

Toluene. Two experiments were carried out using the irradiation of CH_3ONO-NO-air mixtures to generate OH radicals, with the initial CH_3ONO and NO_x concentrations being varied from 9×10^{13} molecule cm^{-3} each to 4.0×10^{14} molecule cm^{-3} each (Table 2). Plots of the amounts of *o*-cresol formed, corrected for reaction with the OH radical, against the amounts of toluene reacted were good straight lines, and the *o*-cresol yields obtained from least-squares analyses are given in Table 2 together with the average NO_2 concentrations during these experiments. The average NO_2 concentrations were calculated from $[NO_2]_{av} = \Sigma_1^n[NO_2]/n$ where n is the number of NO_2 measurements taken (typically 6). The *o*-cresol yields increase from 0.123 ± 0.022 in the absence of NO_x to 0.145 ± 0.007 at 3.5×10^{13} molecule cm^{-3} of NO_2 to 0.160 ± 0.008 at 1.7×10^{14} molecule cm^{-3} of NO_2, where the indicated errors are two least-squares standard deviations and do not take into account the uncertainties in the GC-FID calibration factors for toluene and *o*-cresol (estimated to be $\pm 5\%$ and $\pm 10\%$, respectively).

Reinspection of the data from our previous study of the ring-retaining products of the OH radical reaction with toluene in the presence of NO_x (*35*), by analysis of the individual CH_3ONO-NO-toluene-air irradiations conducted, also shows evidence for an increase in the *o*-cresol formation yield from toluene with increasing average NO_2 concentration, from 0.17 at 2.4×10^{13} molecule cm^{-3} of NO_2 to 0.20-0.21 at average NO_2 concentrations $\geq 3.5 \times 10^{14}$ molecule cm^{-3}. Although the measured *o*-cresol formation yields determined here are $\sim 20\%$ lower than our previous data (*35*) (and are within the combined experimental uncertainties), the trend with

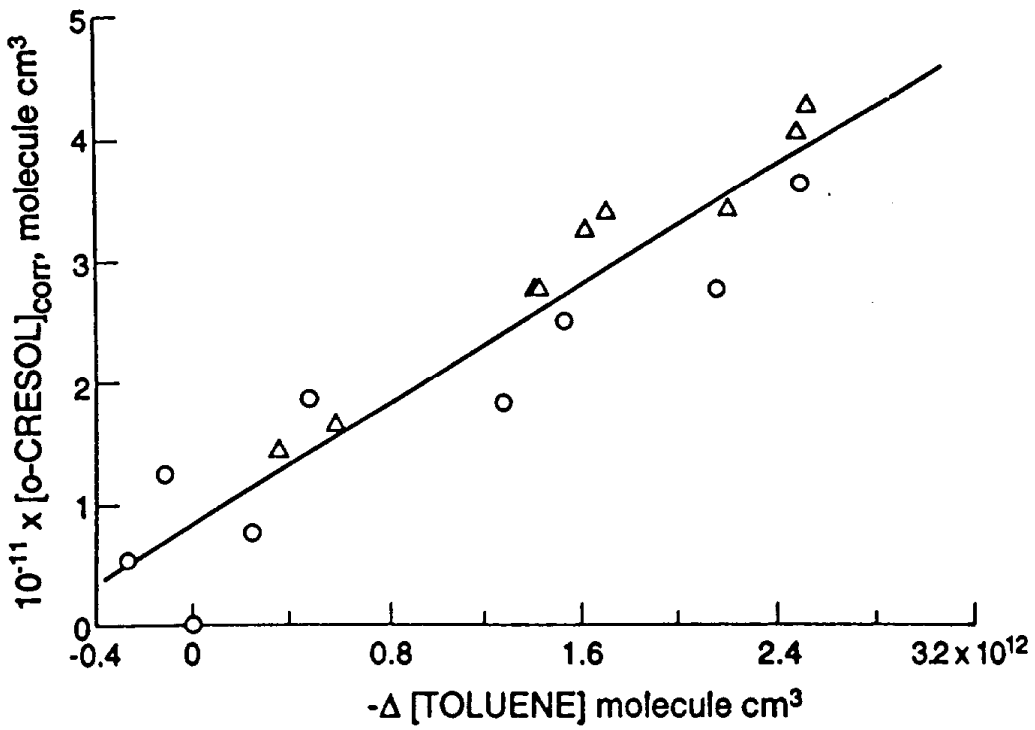

Figure 2. Plot of the amounts of *o*-cresol formed, corrected for reaction with the OH radical (see text), against the amounts of toluene reacted in O_3-alkene-toluene-air mixtures. The alkenes were: o, propene; Δ, α-pinene.

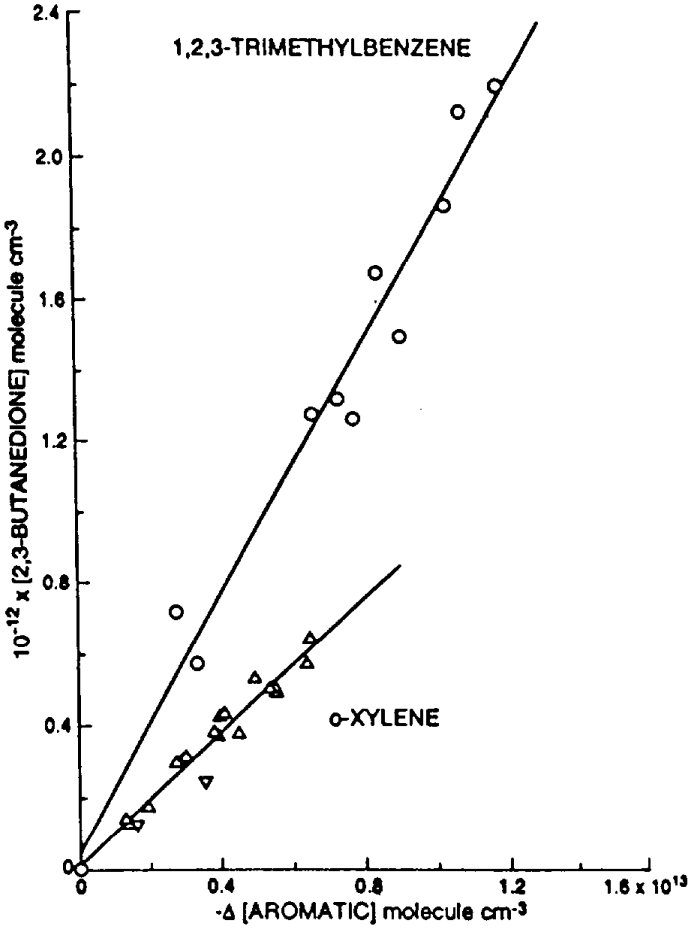

Figure 3. Plots of the amounts of 2,3-butanedione (biacetyl) formed against the amounts of *o*-xylene and 1,2,3-trimethylbenzene reacted in O_3-alkene-aromatic hydrocarbon-air mixtures. The alkenes were: ▽, propene; o, △, α-pinene.

Table 2. Experimental Conditions and *o*-Cresol Formation Yields from the OH Radical-Initiated Reaction of Toluene in Air.

NTC Run #	10^{-13} x Initial Concentration (molecule cm^{-3})			10^{-13} x $[NO_2]_{av}$ (molecule cm^{-3})	*o*-Cresol Yield[a]
	CH_3ONO	NO	NO_2		
120-123				0[b]	0.123 ± 0.022 (±0.026)[c]
134	9.4	9.19	0.37	3.48	0.145 ± 0.007 (±0.018)[c]
136	40.2	27.5	12.1	17.4	0.160 ± 0.008 (±0.020)[c]

[a] Corrected for secondary reaction with OH radicals (see text). Indicated errors are two least-squares standard deviations.

[b] OH radicals generated from the dark reactions of O_3 with propene or α-pinene in air (see text).

[c] Indicated errors are the two least-squares standard deviations combined with estimated overall uncertainties in the GC-FID calibration factors for toluene and *o*-cresol of ±5% and ±10%, respectively.

Table 3. Experimental Conditions and 2,3-Butanedione Formation Yields from the OH Radical-Initiated Reaction of *o*-Xylene.

NTC Run #	10^{-13} x Initial Concentration (molecule cm^{-3})			10^{-18} x $[O_2]$ (molecule cm^{-3})	10^{-13} x $[NO_2]_{av}$ (molecule cm^{-3})	2,3-Butanedione Yield[a]
	CH_3ONO	NO	NO_2			
125,126, 147-149				5.04	0[b]	0.092 ± 0.013
162	0.85	1.02	0.055	5.04	0.718	0.163 ± 0.009
150	1.12	1.16	0.036	5.04	0.828	0.158 ± 0.004
133	9.50	9.10	0.33	5.04	2.98	0.120 ± 0.009
160	9.14	10.9	0.48	5.04	3.34	0.115 ± 0.004
163	11.1	5.26	5.33	5.04	6.67	0.090 ± 0.003
161	21.8	19.6	1.64	5.04	7.70	0.095 ± 0.002
146	23.8	22.0	1.46	5.04	8.54	0.083 ± 0.005
164	0.92	1.06	0.046	1.03	0.574	0.129 ± 0.017

[a] Indicated errors are two least-squares standard deviations and do not include the estimated overall uncertainties in the GC-FID calibration factors for *o*-xylene (±5%) and 2,3-butanedione (±10%).

[b] OH radicals generated from the dark reactions of O_3 with propene or α-pinene (see text).

Table 4. Experimental Conditions and 2,3-Butanedione Formation Yields from the OH Radical-Initiated Reaction of 1,2,3-Trimethylbenzene.

NTC Run #	10^{-13} x Initial Concentration (molecule cm^{-3})			10^{-13} x $[NO_2]_{av}$ (molecule cm^{-3})	2,3-Butanedione Yield[a]
	CH_3ONO	NO	NO_2		
128,129				0[b]	0.180 ± 0.022
143	1.01	0.000	0.005	<0.18[c]	d
140	1.14	0.000	0.012	<0.20[c]	d
142	1.23	0.000	0.005	<0.21[c]	d
141	23.8	≤0.058	0.010	<0.9[c]	d
139	1.23	1.05	0.082	0.578	0.455 ± 0.016
138	2.26	2.21	0.055	0.775	0.478 ± 0.007
137	4.85	4.28	0.113	1.88	0.464 ± 0.023
132	9.36	8.40	0.274	2.36	0.433 ± 0.010

[a] Indicated errors are two least-squares standard deviations, and do not include the estimated uncertainties in the GC-FID calibration factors for 1,2,3-trimethylbenzene (±5%) and 2,3-butanedione (±10%).

[b] OH radicals generated from the dark reaction of O_3 with α-pinene in air (see text).

[c] Upper limit calculated assuming that all of the CH_3ONO photolyzed yields NO_2 via

$$CH_3ONO + h\upsilon \xrightarrow{O_2} HCHO + NO_2 + OH$$

(NO_2 is removed by reaction with OH radicals via $OH + NO_2 \rightarrow HNO_3$).

[d] See text and Figure 8.

NO_2 concentration is similar. These data suggest that *o*-cresol is formed from the two reaction pathways,

$$\text{HCHD} + O_2 \rightarrow o\text{-cresol} + HO_2 \qquad (2a)$$

$$\text{HCHD} + O_2 \rightarrow R\dot{O}_2 \qquad (2b)$$

$$\text{HCHD} + NO_2 \rightarrow o\text{-cresol} + \text{HONO} \qquad (3a)$$

$$\text{HCHD} + NO_2 \rightarrow \text{products} \qquad (3b)$$

where HCHD is the methylhydroxycyclohexadienyl radical formed from reaction (1b). Our present and previous (*35*) data suggest that reactions (2) and (3) are of comparable importance in an atmosphere of air for an NO_2 concentration in the range of (3-20) x 10^{13} molecule cm^{-3}. The kinetic data of Zetzsch and coworkers (*27,34*) for the reactions of the methylhydroxycyclohexadienyl radical with O_2 and NO_2 predict that reactions (2) and (3) will be of equal importance in one atmosphere of air at an NO_2 concentration of 8 x 10^{13} molecule cm^{-3}, consistent with our product data. Our data further indicate that the *o*-cresol formation yield from reactions (2) and (3) are reasonably similar, with the yield from reaction (2) $[k_{2a}/k_2]$ being $\sim$20% lower than the yield from reaction (3).

It should be noted, however, that the HO_2 and organic peroxy radical concentrations in these O_3-alkene-toluene experiments were undoubtedly significantly higher than those present in the ambient atmosphere, and the possibility of radical-radical reactions (for example, of HO_2 and organic peroxy radicals with the methylhydroxycyclohexadienyl radicals) leading to *o*-cresol fomation cannot be discounted. However, the *o*-cresol formation yields from the O_3-α-pinene-toluene-air and O_3-propene-toluene-air systems were similar (Figure 2) despite the factor of $\sim$8 difference in the O_3 reaction rate constants with propene and α-pinene (*4*).

<u>*o*-Xylene</u>. A series of CH_3ONO-NO-NO_2-*o*-xylene-air irradiations were carried out with differing initial CH_3ONO, NO and NO_2 concentrations (Table 3). Representative plots of the amounts of 2,3-butanedione formed against the amounts of *o*-xylene reacted are shown in

Figure 4 for three differing average NO_2 concentrations. As expected (*4*), the NO_2 concentrations generally varied during an experiment due to NO to NO_2 conversion caused by the reactions of NO with HO_2 and other peroxy radicals. The data in Figure 4 show that the 2,3-butanedione yield decreases with increasing average NO_2 concentration, and the formation yields from the individual experiments are given in Table 3 together with the initial NO and NO_2 and average NO_2 concentrations and the O_2 concentration.

The 2,3-butanedione formation yields are plotted as a function of the average NO_2 concentration in Figure 5, and the data shown in Figure 5 and given in Table 3 show that the determining factor for the 2,3-butanedione yield is the NO_2 concentration and not the NO or NO_x concentration. Additionally, an experiment (NTC-164) was carried out with a lower (by a factor of 5) O_2 partial pressure, and the 2,3-butanedione yield of 0.129 at an average NO_2/O_2 concentration ratio of 5.6×10^{-6} and average NO_2 concentration of 5.74×10^{12} molecule cm^{-3} is significantly lower than the 2,3-butanedione yields obtained in air (155 Torr partial pressure of O_2) at the same NO_2 concentration, but is similar to the yield obtained in air at the same NO_2 concentration and NO_2/O_2 concentration ratio. As also discussed below, these 2,3-butanedione formation yield data show that the yield depends on the NO_2/O_2 concentration ratio.

The 2,3-butanedione formation yield data shown in Figure 5 and Table 3 are consistent with differing 2,3-butanedione formation yields from the O_2 and NO_2 reactions with the dimethylhydroxycyclohexadienyl radical. With rate constants k_2 and k_3 for the reactions of the dimethylhydroxycyclohexadienyl radical(s) with O_2 and NO_2, respectively, and 2,3-butanedione formation yields of Y_{O_2} (with low but sufficient NO present that RO_2 radicals react with NO rather than with other peroxy radicals) and Y_{NO_2}, respectively, then the measured 2,3-butanedione formation yield Y is given by,

$$Y = \frac{k_2[O_2]Y_{O_2} + k_3[NO_2]Y_{NO_2}}{k_2[O_2] + k_3[NO_2]} \qquad \text{(I)}$$

and a plot of $(Y_{O_2}-Y)[O_2]/[NO_2]$ against Y should have a slope of k_3/k_2 and an intercept on the Y-axis of Y_{NO_2}. The experimental data shown in Figure 5 indicate that the value of Y_{O_2} is in

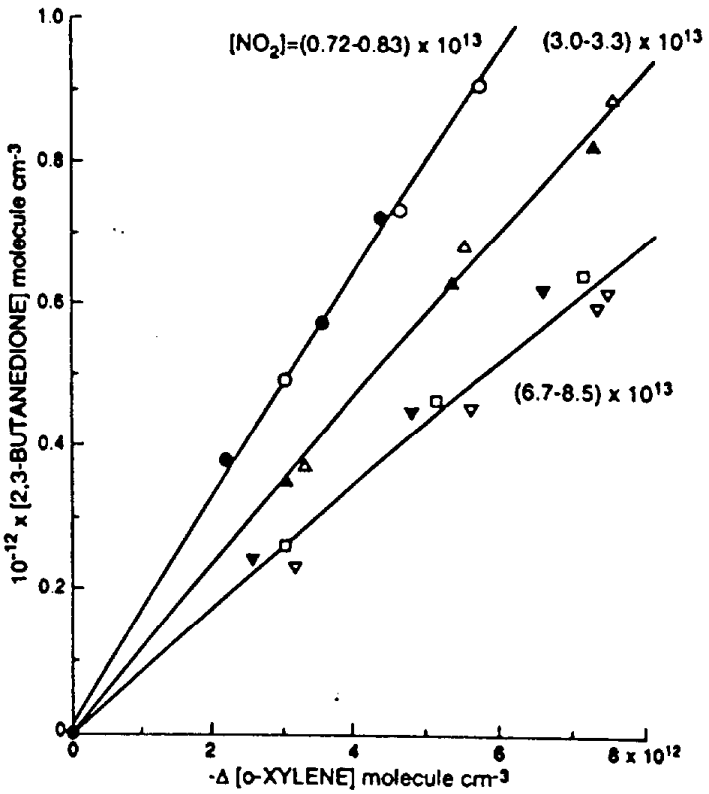

Figure 4. Plots of the amounts of 2,3-butanedione formed against the amounts of *o*-xylene reacted in irradiated CH_3ONO-NO-NO_2-*o*-xylene-air mixtures. Average NO_2 concentrations (in molecule cm^{-3} units) are given and the differing symbols identify different experiments. o, NTC-150; ●, NTC-162; △, NTC-133; ▲, NTC-160; ▽, NTC-146; □, NTC-163; ▼, NTC-161.

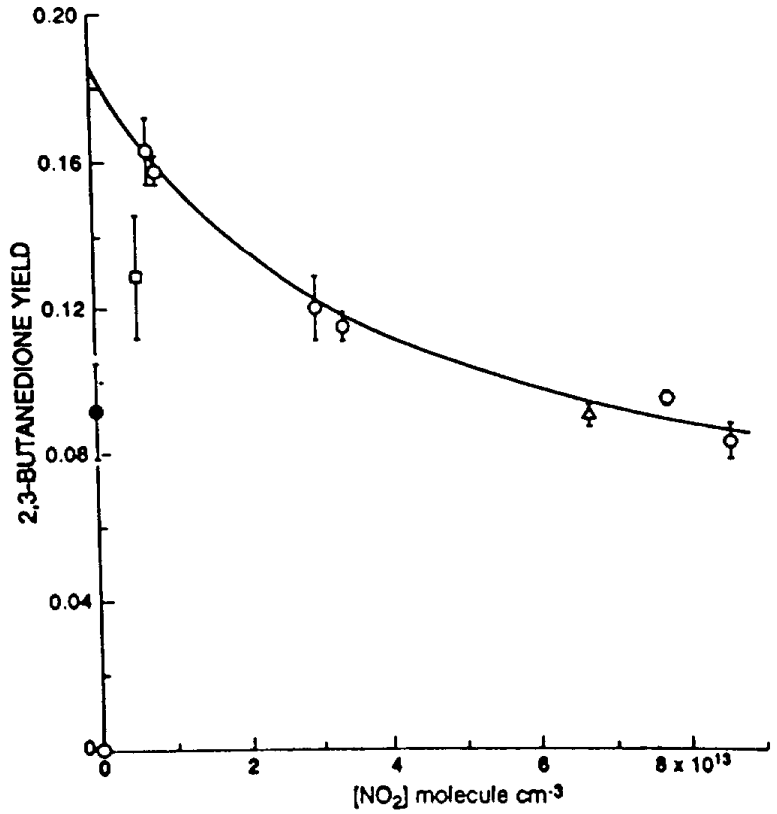

Figure 5. Plot of the 2,3-butanedione formation yields against the average NO_2 concentrations. o, Irradiations of CH_3ONO-NO-*o*-xylene-air mixtures; ▵, Irradiation of a CH_3ONO-NO-NO_2-*o*-xylene-air mixture (NTC-163); □, Irradiation of a CH_3ONO-NO-*o*-xylene-O_2 (4.3%)-N_2 (NTC-164) mixture; ●, Reaction of O_3-alkene-*o*-xylene-air mixtures. [See Table 3 for initial conditions]. (——), Calculated 2,3-butanedione yield for one atmosphere of air with $k_2 = 2.3 \times 10^{-16}$ cm^3 molecule^{-1} s^{-1}; $Y_{O_2} = 0.185$; $k_3 = 3.0 \times 10^{-11}$ cm^3 molecule^{-1} s^{-1}; $Y_{NO_2} = 0.04$ (see text).

the range 0.18-0.19. Use of Equation (I) with values of Y_{O_2} = 0.180, 0.185 and 0.190 leads to values of k_3/k_2 and Y_{NO_2} of (9.0 ± 2.7) x 10^4 and 0.018 ± 0.036; (1.30 ± 0.28) x 10^5 and 0.040 ± 0.028; and (1.70 ± 0.34) x 10^5 and 0.051 ± 0.027, respectively, where the indicated errors are two least-squares standard deviations. A plot of $(Y_{O_2}-Y)[O_2]/[NO_2]$ against Y is shown in Figure 6 for Y_{O_2} = 0.185, and the corresponding values of Y (with k_3/k_2 = 1.30 x 10^5 and Y_{NO_2} = 0.040) are shown by the solid curve in Figure 5. The data point obtained in 4.3% O_2 (run NTC-164) agrees with the data obtained in air with 21% O_2 (Figure 6), confirming the competition between the reactions of the dimethylhydroxycyclohexadienyl radical(s) with O_2 and NO_2.

Assuming that the rate constant for the reaction of NO_2 with the dimethyl-hydroxycyclohexadienyl radical formed from *o*-xylene is the same as those for the corresponding reactions of benzene and toluene, with k_3 = 3 x 10^{-11} cm^3 $molecule^{-1}$ s^{-1} (*27,34*), then our data shown in Figure 5 in the presence of NO_x in air are fit by 2,3-butanedione formation yields of 0.185 for the O_2 reaction and 0.040 for the NO_2 reaction and k_2 = 2.3 x 10^{-16} cm^3 $molecule^{-1}$ s^{-1}. This rate constant of k_2 = 2.3 x 10^{-16} cm^3 $molecule^{-1}$ s^{-1} is in the same range as those obtained by Zetzsch and coworkers (*27,34*) for the reactions of O_2 with the hydroxy-cyclohexadienyl and methylhydroxycyclohexadienyl radicals at room temperature, of (2-5) x 10^{-16} cm^3 $molecule^{-1}$ s^{-1}.

The lower 2,3-butanedione yield in the absence of NO_x is attributed to the occurrence of peroxy + peroxy radical reactions rather than peroxy radical reactions with NO. A speculative reaction sequence which is consistent with our data is (HCHD is the dimethyl-hydroxycyclohexadienyl radical):

$$OH + o\text{-xylene} \rightarrow H_2O + CH_3C_6H_4\dot{C}H_2 \qquad (1a)$$

$$OH + o\text{-xylene} \rightarrow HCHD \qquad (1b)$$

$$HCHD + O_2 \rightarrow \alpha\ R\dot{O}_2 \qquad (2b)$$

$$HCHD + NO_2 \rightarrow \beta\ R\dot{O} + NO \qquad (3b)$$

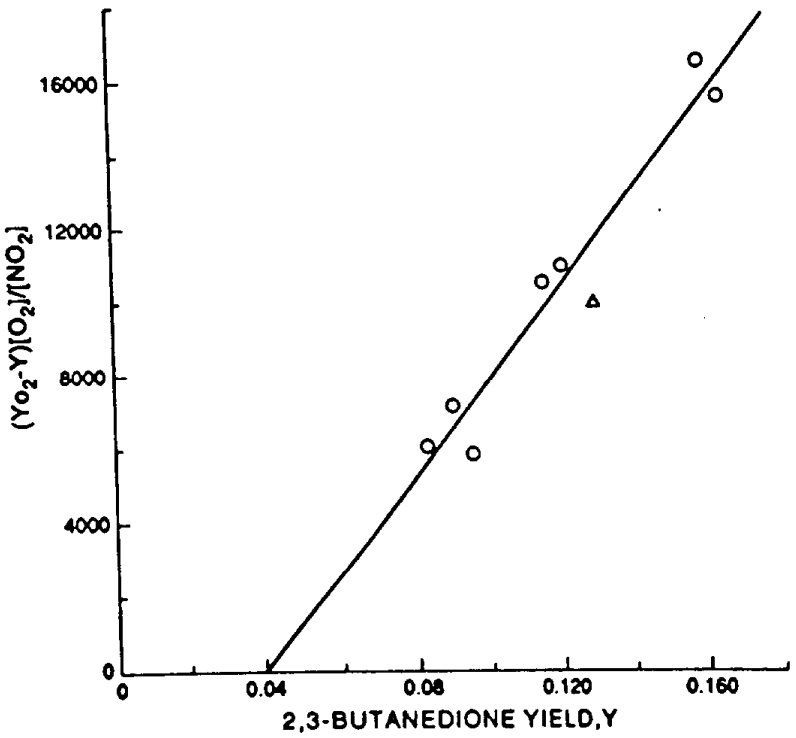

Figure 6. Plot of $(Y_{O_2}-Y)[O_2]/[NO_2]$ against Y for the OH radical-initiated reaction of *o*-xylene in the presence of NO_x. Y is the measured 2,3-butanedione yield and Y_{O_2} is the 2,3-butanedione yield from the reaction when the hydroxycyclohexadienyl radical(s) react with O_2. o - Irradiations of CH_3ONO-NO-NO_2-*o*-xylene-air mixtures; ▵, Irradiation of a CH_3ONO-NO-*o*-xylene-O_2 (4.3%)-N_2 mixture (NTC-164).

$$R\dot{O}_2 + R\dot{O}_2 \rightarrow 2\gamma\ R\dot{O} \quad (4)$$

$$R\dot{O}_2 + NO \rightarrow \delta\ R\dot{O} + NO_2 \quad (5)$$

$$R\dot{O} \rightarrow \rightarrow \epsilon\ \text{2,3-butanedione} \quad (6)$$

In the presence of NO, when reaction of the HCHD radical with O_2 dominates, the 2,3-butanedione formation yield is given by $k_{1b}/k_1\alpha\delta\epsilon = 0.185$, while when reaction of the HCHD radical with NO_2 dominates the 2,3-butanedione yield is given by $k_{1b}/k_1\beta\epsilon = 0.04$. In the absence of NO, peroxy + peroxy radical reaction [reaction (4)] dominates over peroxy radical + NO reaction [reaction (5)] and the 2,3-butanedione formation yield is given by $k_{1b}/k_1\alpha\gamma\epsilon = 0.09$. Since $k_{1b}/k_1 = 0.9$ (*4,26*), $\alpha\delta\epsilon = 0.21$, $\beta\epsilon = 0.044$ and $\alpha\gamma\epsilon = 0.10$. Furthermore, $\alpha = 0.82$ since reaction (2a) to form the 2,3- and 3,4-dimethylphenols accounts for 16% of the overall reaction (*36*).

The 2,3-butanedione formation yields obtained in this work are in good agreement with those previously reported from this laboratory by Darnall et al. (*41*), of 0.18 ± 0.04 at low concentrations of NO_x (1.2×10^{13} molecule cm^{-3}) at 283-323 K, and by Atkinson et al. (*42*) of 0.137 ± 0.016 for an NO_x concentration of 2.35×10^{13} molecule cm^{-3}. Additionally, Bandow and Washida (*43*) reported a 2,3-butanedione formation yield from *o*-xylene of 0.10 ± 0.02 from the irradiation of *o*-xylene-NO-NO_2-air mixtures with initial NO and NO_2 concentrations of 3.6×10^{13} and 1.2×10^{13} molecule cm^{-3}, respectively, although it should be noted that no corrections were made for any photolysis of the 2,3-butanedione during the irradiations.

While only limited studies were made, 2,3-dimethylphenol [the most abundant phenol formed from *o*-xylene (*36*)] was observed by GC/MS analyses in runs NTC-149 (an O_3-propene-*o*-xylene-air reaction mixture) and NTC-146 (an irradiated CH_3ONO-NO-*o*-xylene-air mixture). Identification of the small GC-FID peak due to 2,3-dimethylphenol was rendered difficult due to the small amounts present (and in NTC-149 due to the small amounts of *o*-xylene reacted). However, approximate 2,3-dimethylphenol formation yields (corrected to take into account reaction of 2,3-dimethylphenol with the OH radical) of 0.024 ± 0.009 in the absence of NO_x and 0.058 ± 0.010 for an average NO_2 concentration of 8.5×10^{13} molecule cm^{-3} were obtained.

The 2,3-dimethylphenol formation yield then appears to increase with increasing NO_2 concentration, as for *o*-cresol from toluene, although our 2,3-dimethylphenol yield from run NTC-146 is 40% lower than that of 0.097 ± 0.024 reported previously (*36*) for NO_2 concentrations $\geq 1.6 \times 10^{13}$ molecule cm^{-3}.

1,2,3-Trimethylbenzene. A series of CH_3ONO-NO-NO_2-1,2,3-trimethylbenzene-air irradiations were carried out, and the initial conditions, average NO_2 concentations and 2,3-butanedione formation yields obtained are given in Table 4. The 2,3-butanedione formation yields determined were independent of the average NO_2 concentrations over the range (0.58-2.4) x 10^{13} molecule cm^{-3} (Table 4 and Figure 7), with a mean 2,3-butanedione formation yield of 0.444 ± 0.053, where the indicated error is two least-squares standard deviations combined with the estimated overall uncertainties in the GC-FID calibration factors for 1,2,3-trimethylbenzene (±5%) and 2,3-butanedione (±10%). This 2,3-butanedione formation yield is a factor of 2.5 higher than that observed in the absence of NO_x (Table 4).

Figure 7 is a good straight-line plot, and no evidence for a lower 2,3-butanedione yield was observed even during the shortest irradiation period in run NTC-139, where the average NO_2 concentration was calculated to be $\sim 1.6 \times 10^{12}$ molecule cm^{-3}. This observation suggests that the 2,3-butanedione formation yield is independent of NO_2 concentration over the range (0.16-3.6) x 10^{13} molecule cm^{-3}, with the highest NO_2 concentration being that for the last of the three irradiation periods in run NTC-132. Our 2,3-butanedione yield of 0.444 ± 0.053 under these conditions is in excellent agreement with that reported by Bandow and Washida (*44*) of 0.45 ± 0.02 but is a factor of 1.4 higher than that previously determined in this laboratory by Tuazon et al. (*45*) of 0.316 ± 0.036 by GC with electron capture detection. Both of these studies were conducted in the presence of NO_x at concentrations of 5 x 10^{13} molecule cm^{-3} (*44*) and 1.2 x 10^{14} molecule cm^{-3} (*45*).

In contrast to the irradiations of CH_3ONO-NO-NO_2-1,2,3-trimethylbenzene-air mixtures, irradiations of CH_3ONO-1,2,3-trimethylbenzene-air mixtures (with NO_2 and NO being generated from the photolysis of CH_3ONO) led to initially lower formation yields of 2,3-butanedione (Figure 8). For low amounts of 1,2,3-trimethylbenzene reacted, corresponding to calculated upper limit NO_2 concentrations of $\leq 3.5 \times 10^{12}$ molecule cm^{-3}, the 2,3-butanedione formation yields are lower than the value of 0.44 obtained from the data shown in Figure 7.

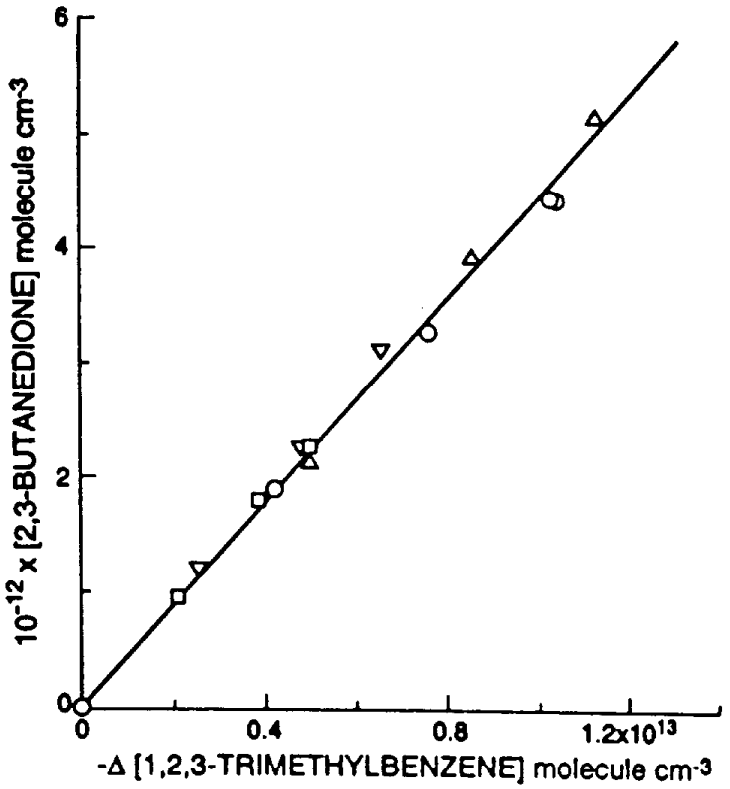

Figure 7. Plot of the amounts of 2,3-butanedione formed against the amounts of 1,2,3-trimethylbenzene reacted in irradiated CH_3ONO-NO-NO_2-1,2,3-trimethylbenzene-air mixtures with average NO_2 concentrations of (0.58-2.4) x 10^{13} molecule cm^{-3}. □, NTC-139; ▽, NTC-138; △, NTC-137; o, NTC-132.

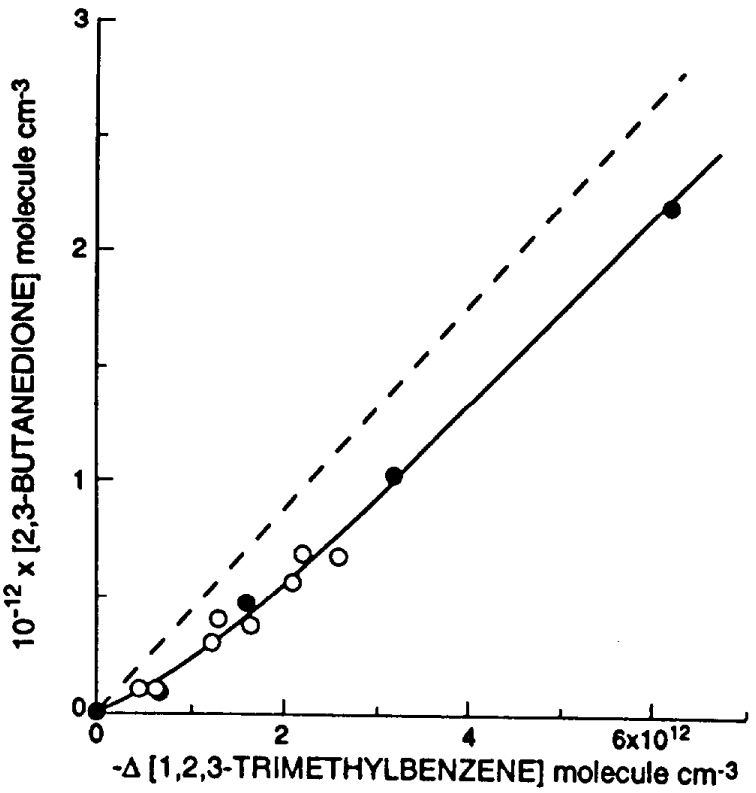

Figure 8. Plot of the amounts of 2,3-butanedione formed against the amounts of 1,2,3-trimethylbenzene reacted in irradiated CH_3ONO-1,2,3-trimethylbenzene-air mixtures. o, NTC-140, 142 and 143; ●, NTC-141. (- - -), 2,3-Butanedione yield from data obtained at NO_2 concentrations in the range (0.16-3.6) x 10^{13} molecule cm^{-3} (Figure 7).

These lower 2,3-butanedione yields at these low NO_2 concentrations could be due to (a) a lower 2,3-butanedione formation yield from the O_2 reaction than the NO_2 reaction with the trimethylhydroxycyclohexadienyl radical(s) or (b) under low NO_2 concentration conditions (and hence low NO concentrations), peroxy + peroxy radical reactions are in competition with peroxy radical + NO reactions (i.e., in a transition from the 2,3-butanedione formation yield of 0.18 in the absence of NO_x to a yield of 0.44 in the presence of sufficient NO that peroxy radicals react predominantly with NO). Whatever the reason, under our experimental conditions this transition appears to occur in the NO_2 concentration range $\sim$(1-3) x 10^{12} molecule cm^{-3}.

Reassessment of Nitroaromatic Formation Yield Data

Our previous nitroaromatic yield data from the OH radical-initiated reactions of benzene (*35*), toluene (*35*) and *o*-, *m*- and *p*-xylene (*36*) were interpreted in terms of reaction of the hydroxycyclohexadienyl radicals only with NO_2 for NO_2 concentrations $\geq 1.5 \times 10^{13}$ molecule cm^{-3}, and the O_2 reaction was not explicitly considered. Since our present product data are in agreement with the kinetic data of Zetzsch and coworkers (*27,34*) in that the hydroxycyclohexadienyl radicals react with both O_2 and NO_2, a reanalysis of our previous data (*35,36*) is necessary. With the general reaction scheme,

$$\text{HCHD} + O_2 \rightarrow \text{products} \qquad (2)$$

$$\text{HCHD} + NO_2 \begin{cases} \rightarrow \text{nitroaromatic} & (3c) \\ \rightarrow \text{other products} & (3a + 3b) \end{cases}$$

we have reanalyzed our previous data for the formation of nitrobenzene from benzene (*35*) and m-nitrotoluene from nitrotoluene (*35*). The rate constants reported by Zetzsch and coworkers (*27,34*) for the reactions of the hydroxycyclohexadienyl and methylhydroxycyclohexadienyl radicals with O_2 and NO_2 were used.

Figures 9 and 10 compare our previous experimental data (*35*) with calculated curves using nitroaromatic yields from reaction (3) [k_{3c}/k_3] of 0.07-0.09. The fits are reasonable,

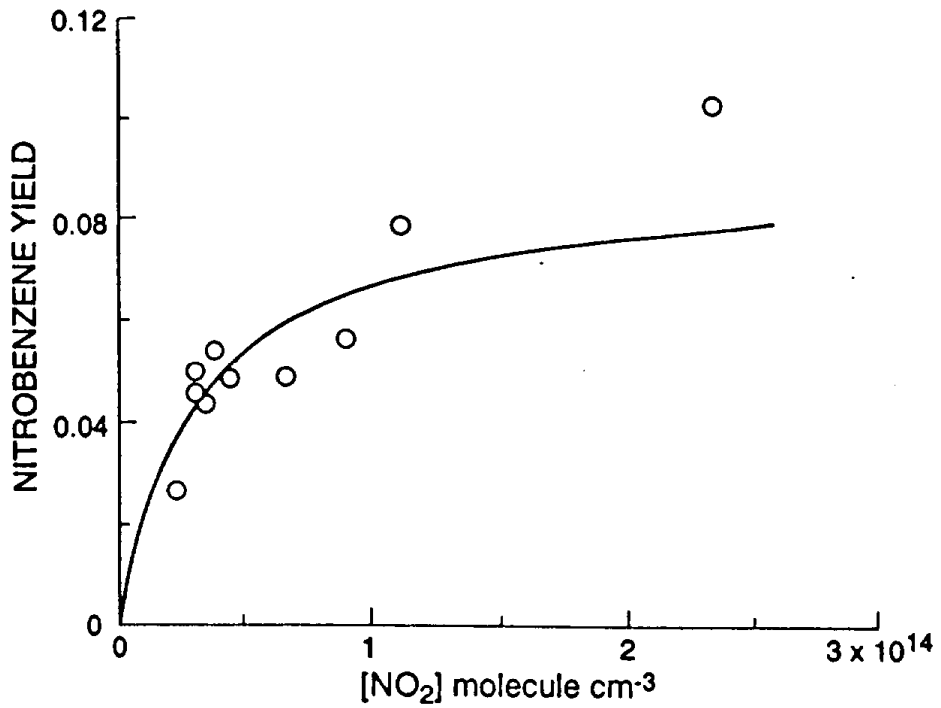

Figure 9. Plot of the nitrobenzene formation yield against NO_2 concentration (taken from ref. *35*). (——) Fit with $k_2 = 1.7 \times 10^{-16}$ cm^3 molecule^{-1} s^{-1}, $k_3 = 2.5 \times 10^{-11}$ cm^3 molecule^{-1} s^{-1} and a nitrobenzene yield from reaction (3) of 0.09.

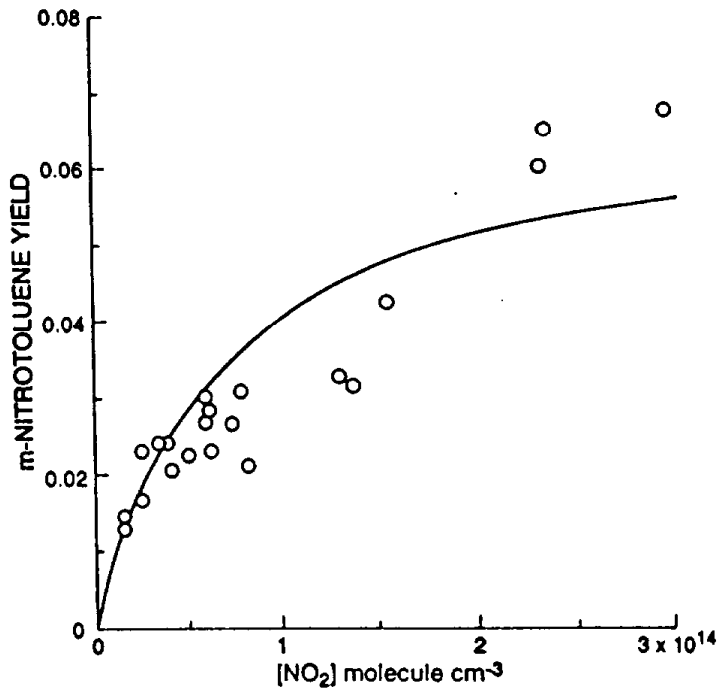

Figure 10. Plot of the *m*-nitrotoluene formation yield against the NO_2 concentration (taken from ref. *35*). (——), Fit with $k_2 = 5.2 \times 10^{-16}$ cm^3 molecule^{-1} s^{-1}, $k_3 = 3.6 \times 10^{-11}$ cm^3 molecule^{-1} s^{-1} and a *m*-nitrotoluene yield from reaction (3) of 0.076 (using $k_{1b}/k_1 = 0.92$ for toluene (*4*); $k_{3c}k_{1b}/k_1k_3 = 0.07$).

although there appear to be discrepancies at high NO_2 concentrations for both the benzene and toluene systems and at intermediate NO_2 concentrations for the toluene system. Whether these discrepancies are random or systematic (the latter case implying disagreement with the reaction scheme used to derive the curves drawn in Figures 9 and 10) remains to be determined.

C. Conclusions

The formation yields of selected products have been determined for the OH radical-initiated reactions of toluene, *o*-xylene and 1,2,3-trimethylbenzene in the presence and absence of NO_x. The experimental data for the formation of *o*-cresol from toluene and of 2,3-butanedione from *o*-xylene are consistent with the reactions of the intermediate hydroxycyclohexadienyl-type radicals with O_2 and NO_2. In particular, the formation yields of 2,3-butanedione from *o*-xylene lead to a rate constant ratio for the reactions of the dimethylhydroxycyclohexadienyl radical(s) with NO_2 and O_2 of 1.3×10^5 and yields from the O_2 and NO_2 reactions of 0.21 and 0.044, respectively. Our data and those of Zetzsch and coworkers (*27,34*) then show that under typical tropospheric conditions the hydroxycyclohexadienyl-type radicals formed from benzene, toluene, the xylenes and trimethylbenzenes react predominantly with O_2.

III. PRODUCTS OF THE GAS-PHASE REACTIONS OF SELECTED KETONES

As noted in Section I above, the degradation reactions of alkanes (and alkenes) in the troposphere proceed through the intermediary of alkyl (R) radicals, alkyl peroxy ($R\dot{O}_2$) radicals and alkoxy ($R\dot{O}$) radicals, or their hydroxy- or nitrato- substituted homologs (*4*). A major uncertainty in these degradation schemes, which affects the products formed, concerns the reactions of the alkoxy radicals, and especially the relative importance of their thermal decomposition, unimolecular isomerization, or reaction with O_2 (*4,46*). For the 2-pentoxy radical, these reactions are,

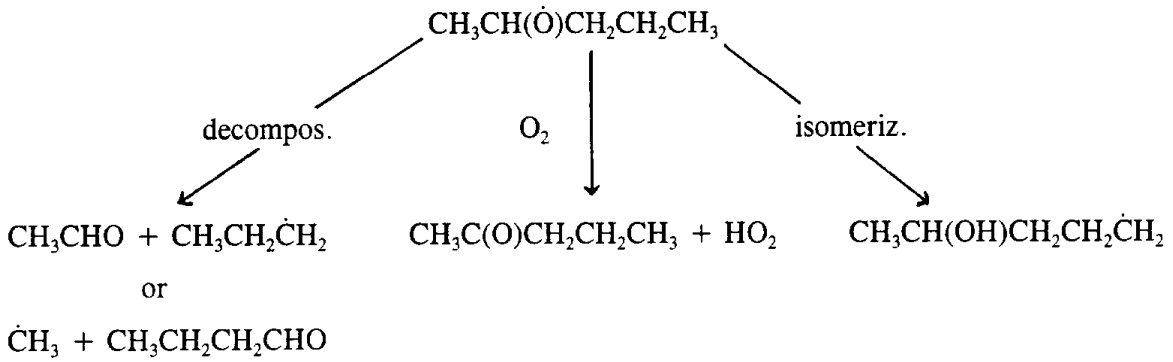

with the isomerization reaction proceeding via a 6-membered transition state and involving intramolecular H-atom abstraction from a C-H bond on the δ-carbon (*20,47,48*). To date, the occurrence of the isomerization reaction at room temperature has been inferred by the lack of the products expected from the competing alkoxy radical decomposition and reaction with O_2 (*24,25,47*).

To attempt to provide unambiguous evidence for the occurrence of the alkoxy radical isomerization reaction, we investigated the formation of selected products from the OH radical reactions with 4-methyl-2-pentanone [$CH_3C(O)CH_2CH(CH_3)_2$] and 2,6-dimethyl-4-heptanone [$(CH_3)_2CHCH_2C(O)CH_2CH(CH_3)_2$]. For 2,6-dimethyl-4-heptanone, it was expected that the majority of the OH radical reaction would occur by H-atom abstraction from the tertiary $>$CH-bonds (*49*), with the resulting alkoxy radical either undergoing decomposition to form acetone

as a primary product (plus other products) or isomerization to yield 2-methylpropanal (isobutyraldehyde) as a primary product (*4*) (these primary products are underlined below).

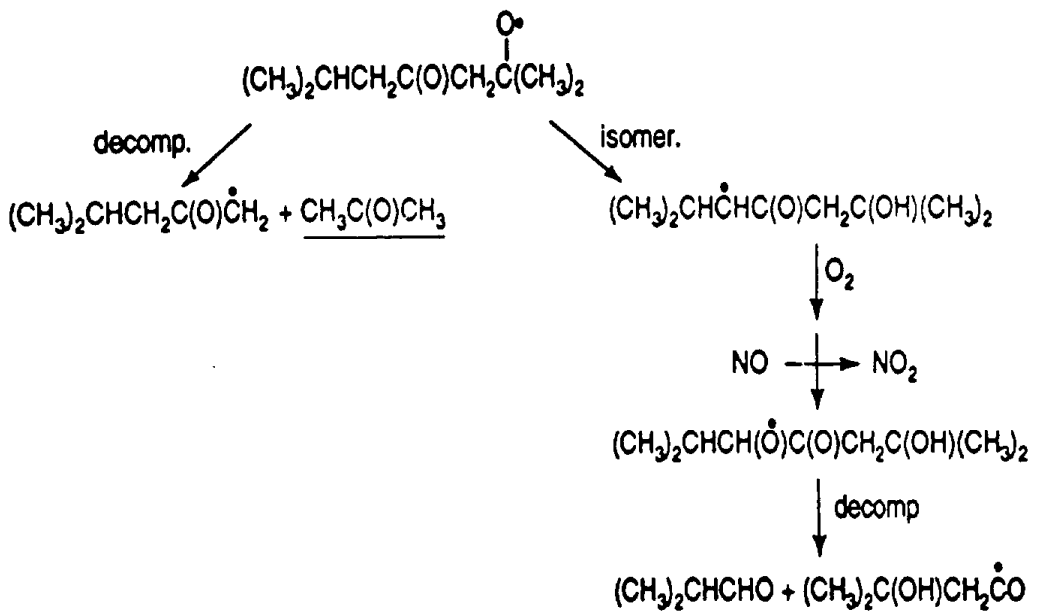

As discussed below, the data obtained were more complex, but provide useful insights into the relative importance of the various alkoxy radical reaction pathways.

A. Experimental

Experiments were carried out at 296 ± 2 K and 740 Torr total pressure of purified air (3-5% relative humidity) in a 7900 liter all-Teflon chamber (Figure 1) equipped with two parallel banks of blacklamps. Hydroxyl radicals were generated by the photolysis of methyl nitrite (CH_3ONO) in air at wavelengths >300 nm (*37*), and NO and NO_2 were included in the reactant mixtures to either avoid the formation of O_3 (and hence of NO_3 radicals) or provide information concerning the reaction mechanism(s) [see Results section below]. The initial reactant concentrations (in molecule cm^{-3} units) were: CH_3ONO, (2.4-2.6) x 10^{14}; NO, (0.75-2.4) x 10^{14}; NO_2, (0-1.5) x 10^{14}; 4-methyl-2-pentanone or 2,6-dimethyl-4-heptanone, (4.03-4.44) x 10^{13}.

Irradiations were carried out at 50% of the maximum light intensity for 5-15 mins (4-methyl-2-pentanone) or 3-9 mins (2,6-dimethyl-4-heptanone). In certain experiments, 4.8×10^{14} molecule cm^{-3} of NO was added to the chamber after the irradiations had been completed in order to assess whether or not the carbonyl products being monitored were formed through the intermediary of acyl and/or acyl peroxy radicals (*4*).

The ketone reactants and selected carbonyl products were analyzed during the experiments by gas chromatography with flame ionization detection (GC-FID). For the analyses of 4-methyl-2-pentanone, 2,6-dimethyl-4-heptanone and 2-methylpropanal (isobutyraldehyde), gas samples were collected from the chamber in 100 cm^3 all-glass, gas-tight syringes and introduced via a 1 cm^3 gas sampling loop onto a 30 m DB-5 megabore column in a Hewlett Packard (HP) 5890 GC, initially held at -25 °C and then temperature programmed to 200 °C at 8 °C min^{-1}. For the analyses of acetone, 100 cm^3 volume samples were collected from the chamber onto Tenax-TA solid adsorbent, with subsequent thermal desorption at 225 °C onto a 30 m DB-5.625 megabore column in a HP 5710 GC, initially held at 0 °C and then temperature programmed to 200 °C at 8 °C min^{-1}. Gas samples were also collected onto Tenax-TA solid adsorbent for subsequent thermal desorption and analysis by combined gas chromatography-mass spectrometry (GC-MS), using a 60 m DB-5MS fused silica capillary column, temperature programmed from -80 °C at 10 °C min^{-1} to 250 °C, in a HP 5890 GC interfaced to a HP 5970 mass selective detector operated in the scanning mode. The NO concentrations and initial NO_2 concentrations were monitored during these experiments using a chemiluminescence NO-NO_x analyzer.

The GC-FID instruments were re-calibrated several times during this study, using the methods described above, and good agreement was obtained except for the Tenax solid adsorbent/thermal desorption system during one time period when gas flow problems to the GC were encountered; experiments carried out during these time periods were not used in the data analysis discussed below. The NO-NO_x analyzer was calibrated with a National Institute of Standards and Technology NO in N_2 gas mixture. All analytical instruments were maintained as recommended and their performance checked on a daily basis.

The chemicals used, and their stated purities, were: acetone (>99.6%), Fisher Scientific; 4-methyl-2-pentanone (99+%) and 2-methylpropanal [isobutyraldehyde] (99+%), Aldrich Chemical Company; 2,6-dimethyl-4-heptanone (99%), Chem Samples; and NO (≥99.0%), Matheson Gas Products. Methyl nitrite was prepared and stored as described previously (*37*). NO_2 was prepared just prior to use by reacting NO with an excess of O_2.

B. Results and Discussion

4-Methyl-2-pentanone. A series of CH_3ONO-NO-NO_2-4-methyl-2-pentanone-air irradiations were carried out, and the products observed by GC-FID and GC-MS analyses were acetone and 2-methylpropanal. In order to determine whether these products, or a fraction of these products, were formed through the intermediary of acyl or acyl peroxy radicals, NO was added to the reactant mixtures after the OH radical reactions were completed and analyses conducted, and repeat analyses carried out 1-3 hrs later. This procedure allowed any acyl peroxynitrates to thermally decompose.

$$RC(O)OONO_2 \rightarrow RC(O)O\dot{O} + NO_2 \qquad (7)$$

$$RC(O)O\dot{O} + NO_2 \rightarrow RC(O)OONO_2 \qquad (8)$$

$$RC(O)O\dot{O} + NO \rightarrow RC(O)\dot{O} + NO_2 \qquad (9)$$

$$\downarrow$$

$$\dot{R} + CO_2$$

The concentrations of acetone and 2-methylpropanal showed no increase after the addition of NO to the reacted mixtures, indicating that no significant fraction of these two products were formed through the intermediary of acyl or acyl peroxy radicals [through reactions (7)-(9)].

Since acetone and 2-methylpropanal react with the OH radical (*4*), the measured concentrations of acetone and 2-methylpropanal were corrected to take into account their reaction with OH radicals (*40*), using rate constants for the OH radical reactions (in units of 10^{-12} cm^3 $molecule^{-1}$ s^{-1}) of: 4-methyl-2-pentanone, 14.1 (*4,26*); acetone, 0.219 (*4*); and 2-methylpropanal, 26.3 (*4,26*). The multiplicative factors to account for reactions of the products with OH radicals during the reactions were <1.01 for acetone and ≤ 1.99 for 2-methylpropanal, and the amounts of acetone and 2-methylpropanal formed, corrected for reaction with the OH radical, are plotted against the amounts of 4-methyl-2-pentanone reacted in Figure 11. Good straight line plots are observed, and least-squares analyses of these data lead to the formation yields given in Table 5. Secondary formation of acetone from the reaction of the OH radical with 2-methylpropanal (*4*) was of minor importance, accounting for $<4.7\%$ of the observed acetone.

The acetone yield determined here of 0.78 ± 0.06 is in reasonable agreement with the yields reported by Cox et al. (*24,50*) of 0.68 (*50*) and 0.90 (*24*). Cox et al. (*24,50*) also reported the formation of peroxyacetyl nitrate (PAN; $CH_3C(O)OONO_2$) (*24,50*), indicating the formation of $CH_3\dot{C}O$ radicals (*4,24*), and a lack of formation of methylglyoxal ($CH_3C(O)CHO$) (*24*). The OH radical reaction with 4-methyl-2-pentanone proceeds by H-atom abstraction from the various $-CH_3$, $-CH_2-$ and $>CH-$ groups, and the estimation method of Atkinson (*49*) allows the rate constants for H-atom abstraction from these groups, and hence the distribution of alkyl radicals formed, to be calculated. The percentage of the overall OH radical reaction occurring by H-atom abstraction from the C-H bonds at the various carbon atoms are then calculated to be: from the $-CH_3$ group at the 1-position, 1%; from the $-CH_2-$ group at the 3-position, 9%; from the $>CH-$ group at the 4-position, 86%; and from the two equivalent $-CH_3$ groups at the 5-positions, 4%. The estimated overall reaction rate constant of 9.4×10^{-12} cm^3 $molecule^{-1}$ s^{-1} at 298 K can be compared to the recommended value of 1.41×10^{-11} cm^3 $molecule^{-1}$ s^{-1} (*4,26*).

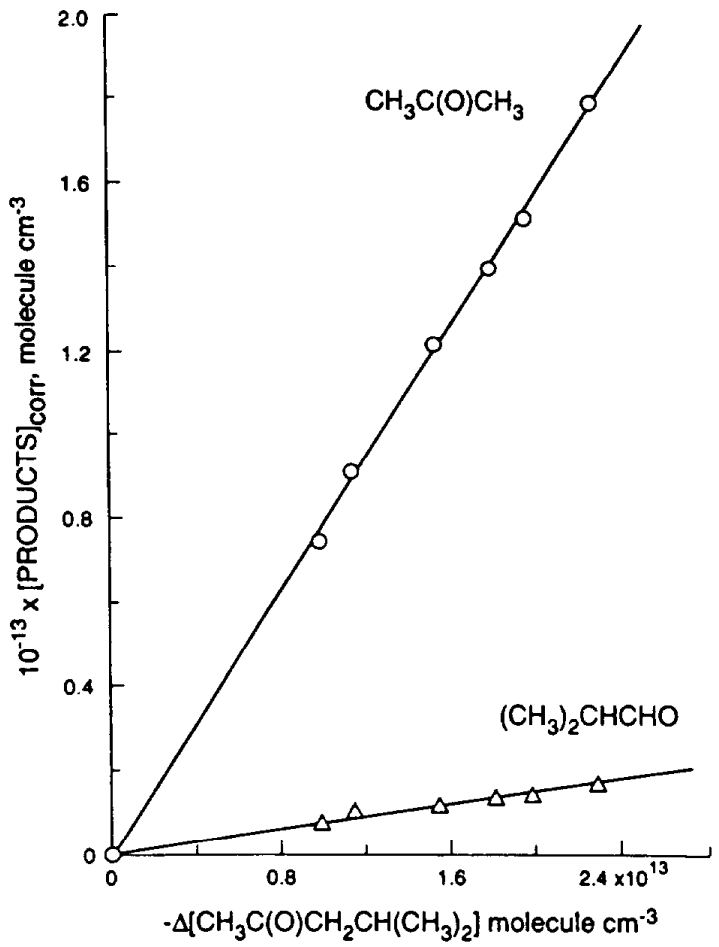

Figure 11. Plots of the amounts of acetone and 2-methylpropanal formed, corrected for reaction with the OH radical (see text), against the amounts of 4-methyl-2-pentanone reacted with the OH radical.

Table 5. Experimental Yields of Acetone and 2-Methylpropanal from the Reactions of the OH Radical with 4-Methyl-2-pentanone and 2,6-Dimethyl-4-heptanone at 296 ± 2 K and 740 Torr Total Pressure of Air.

Ketone	Formation Yield[a]	
	Acetone	2-Methylpropanal
4-Methyl-2-pentanone	0.78 ± 0.06	0.071 ± 0.011
2,6-Dimethyl-4-heptanone	0.82 ± 0.11[b] 0.68 ± 0.11[c]	0.385 ± 0.034

[a]Indicated errors are two least-squares standard deviations combined with estimated overall uncertainties in the GC-FID response factors for the reactant and products of ±5% each.

[b]Amount formed increased after addition of NO to reacted mixtures (see text). This yield is from data obtained after addition of NO.

[c]Corrected to take into account secondary formation from the OH radical reaction with 2-methylpropanal (see text).

After addition of O_2 and reaction with NO, neglecting organic nitrate formation (*4,20,40*) from the $R\dot{O}_2$ + NO reaction, the alkoxy radicals formed and their expected possible reactions are as shown in Reaction Schemes (Ia-Id). In these reaction schemes, the alkyl and alkyl peroxy radicals have been omitted for clarity and only the alkoxy and acyl radicals involved are shown. Based on experimental data (*4,46,50,51*) and thermochemical estimations (*4*) concerning the alkoxy radical reactions with O_2 and decomposition, the expected relative importance of thepossible alkoxy radical reaction pathways are indicated by the arrows [with the relative importance being given by (⟶) > (→) > (- - →)]. The estimates for alkoxy radical reactions with O_2 and decomposition used thermochemical data from the NIST thermochemical data computer program (*52*), which for molecules for which experimental data are not available uses the group additivity method of Benson (*53*). The alkoxy radicals $(CH_3)_2CH\dot{O}$ and $CH_3C(O)CH_2\dot{O}$ are known (*50,51,54*) and calculated (*4*) to predominantly react with O_2 and decompose, respectively, at room temperature and one atmosphere of air, while the $(CH_3)_2CHCH_2\dot{O}$ radical is calculated (*4*) to predominantly react with O_2 at room temperature and atmospheric pressure of air. The intermediary of acyl and/or acyl peroxy radicals are indicated in Reaction Scheme (Ia-Id) by multiple arrows and the symbol @.

The $(CH_3)_2CHCH_2C(O)CH_2\dot{O}$ and $CH_3C(O)CH_2CH(CH_3)CH_2\dot{O}$ radicals formed after H-atom abstraction from the $-CH_3$ groups at the 1- and 5-positions, respectively, are calculated to account for 1% and 4%, respectively, of the overall reaction, with the $CH_3C(O)CH_2CH(CH_3)CH_2\dot{O}$ radical formed after H-atom abstraction from the $-CH_3$ groups at the 5-position not being expected to lead to acetone or 2-methylpropanal (Reaction Scheme Id). Hence the observed acetone and 2-methylpropanal must arise almost totally after H-atom abstraction from the $-CH_2-$ and/or $>CH-$ groups.

The $CH_3C(O)CH(\dot{O})CH(CH_3)_2$ radical formed after H-atom abstraction from the $-CH_2-$ group at the 3-position cannot undergo isomerization via a 6-membered transition state, and hence decomposition and reaction with O_2 are expected to dominate (*4,46*). Thermochemical calculations (*4*) indicate that decomposition will dominate for lower tropospheric conditions, leading to 2-methylpropanal (Reaction Scheme Ib). The $CH_3C(O)CH_2C(\dot{O})(CH_3)_2$ radical formed after H-atom abstraction from the $>CH-$ group at the 4-position cannot react with O_2, leaving decomposition and isomerization as possible pathways (Reaction Scheme Ic). Isomerization

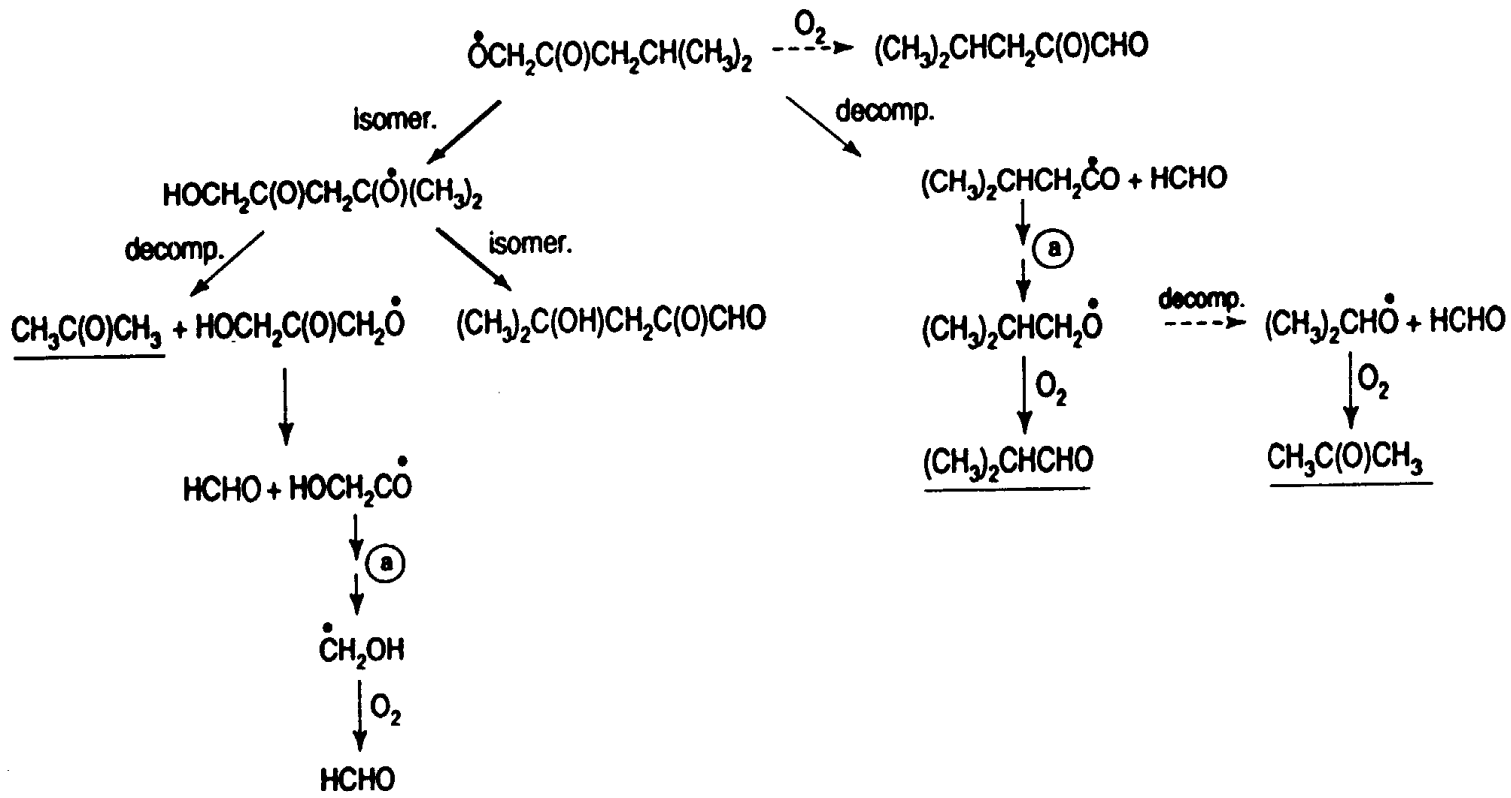

Reaction Scheme Ia.

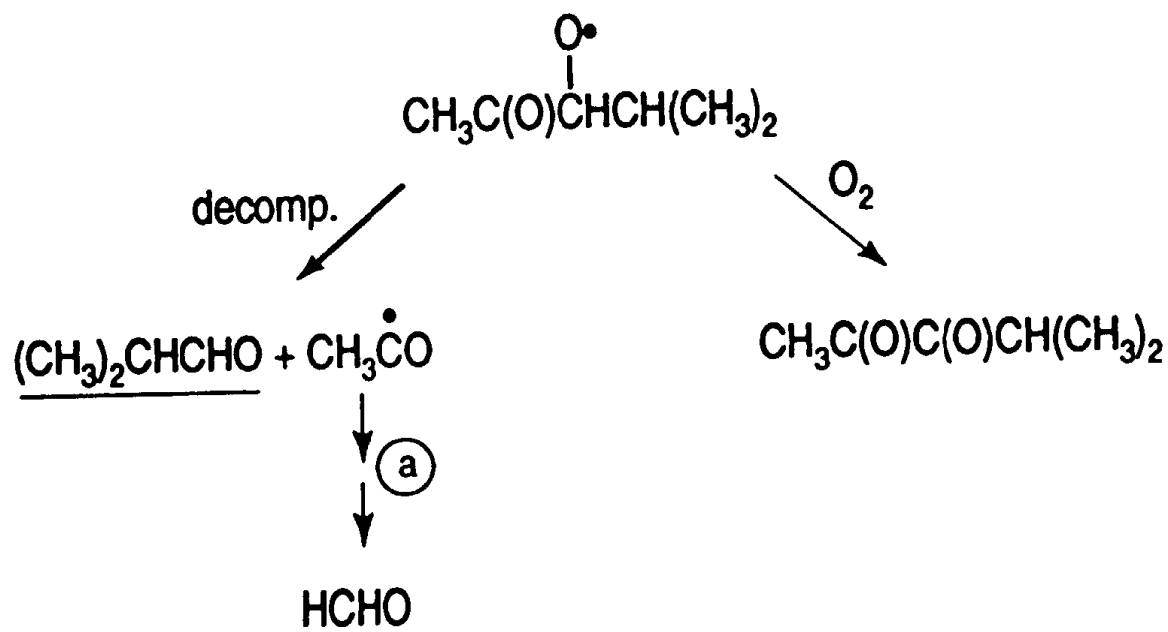

Reaction Scheme Ib.

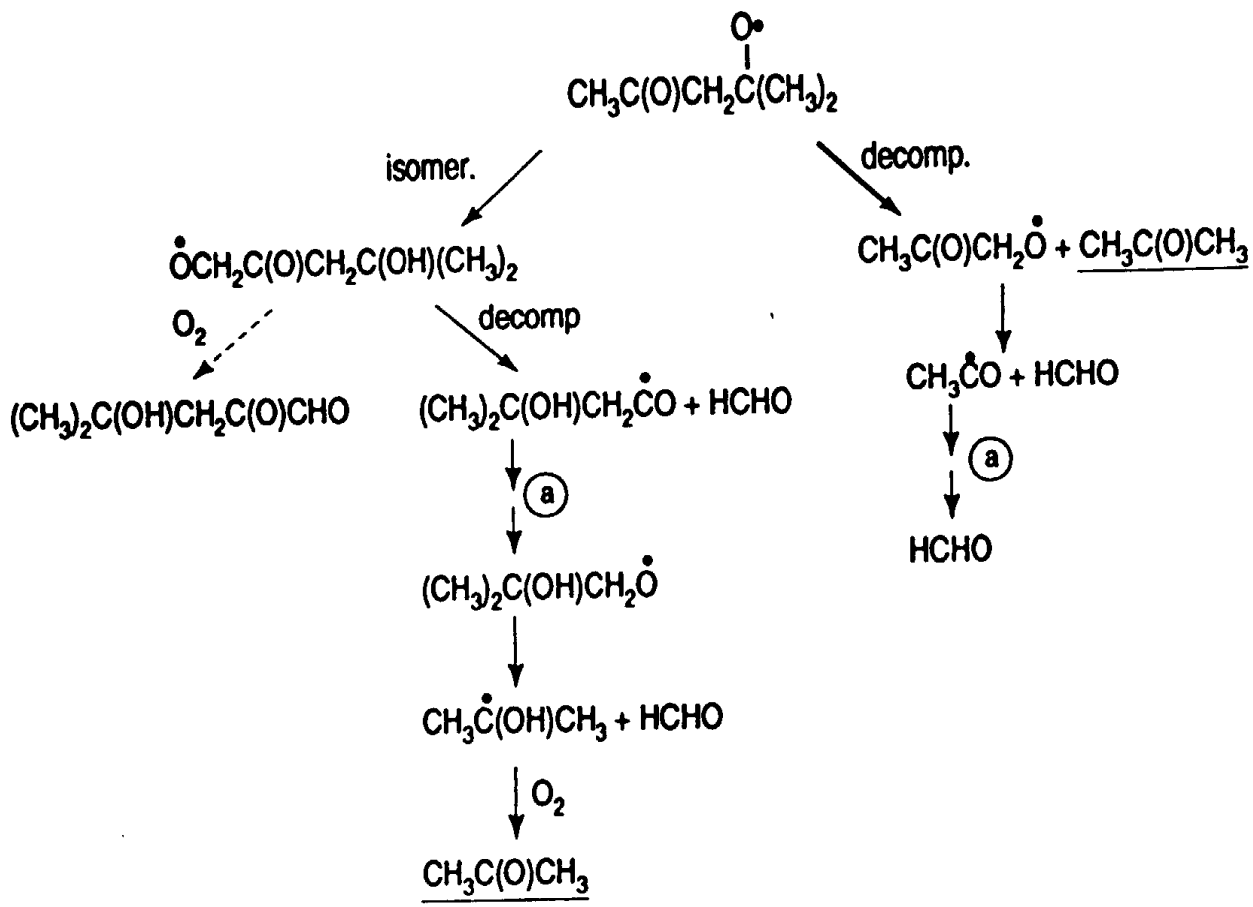

Reaction Scheme Ic.

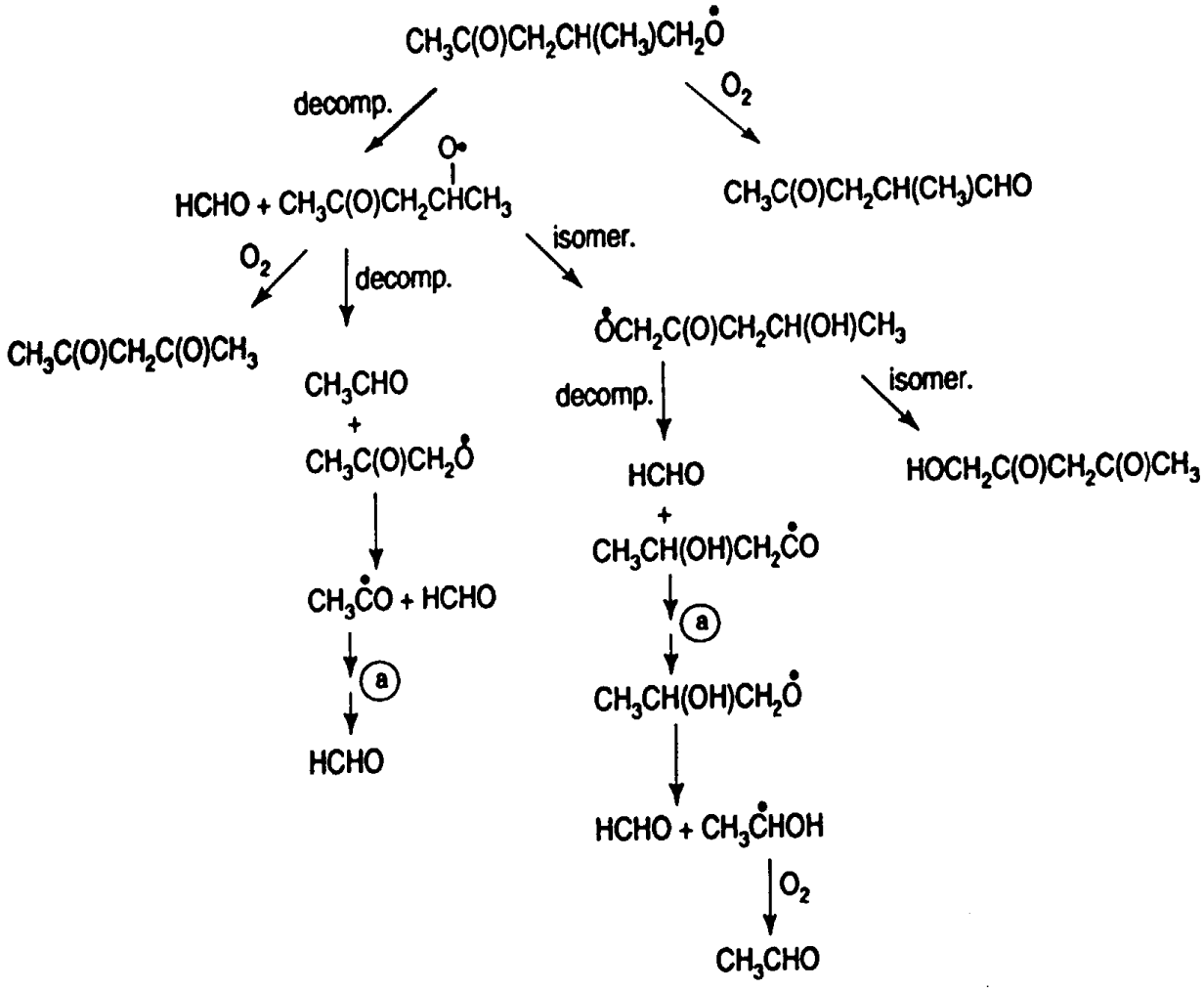

Reaction Scheme Id.

would lead, by decomposition of the intermediate alkoxy radical $(CH_3)_2C(OH)CH_2C(O)CH_2\dot{O}$ (isomerization of this radical cannot occur via a 6-membered transition state), to formation of acetone through the intermediary of an acyl radical. The observed lack of an effect of adding NO to the reaction system shows that an acyl radical is not a precursor to the acetone, and hence that decomposition of the $CH_3C(O)CH_2C(\dot{O})(CH_3)_2$ radical must occur (Reaction Scheme Ic).

Based on Reaction Schemes (Ia-Id) and the calculated relative importance of the various alkoxy radical pathways, our acetone and 2-methylpropanal yields indicate that 2-methylpropanal is formed after H-atom abstraction from the $-CH_2-$ group and that acetone is formed after H-atom abstraction from the $>CH-$ group. Furthermore, our measured 2-methylpropanal and acetone yields of 0.071 ± 0.011 and 0.78 ± 0.06, respectively, are close to the estimate that 9% and 86% of the overall OH radical reaction with 4-methyl-2-pentanone proceeds by H-atom abstraction from the $-CH_2-$ and $>CH-$ groups, respectively (*49*). Organic nitrate formation from the reactions of $R\dot{O}_2$ radicals with NO (*4*) then appears to be of minor ($\sim 10\%$ or less) importance, consistent with the alkyl nitrate yields from C_5 and C_6 alkanes (*4,22*). As discussed further below, it is of interest that decomposition of the $CH_3C(O)CH_2C(\dot{O})(CH_3)_2$ radical appears to dominate over isomerization since present estimation methods suggest that both processes should be of similar importance, with the decomposition and isomerization rates being $\sim 7 \times 10^4$ s^{-1} each at 298 K (*4*).

<u>2,6-Dimethyl-4-heptanone</u>. A series of irradiations of CH_3ONO-NO-NO_2-2,6-dimethyl-4-heptanone-air mixtures were carried out. As for 4-methyl-2-pentanone, the major products observed by GC-FID and GC-MS analyses were acetone and 2-methylpropanal. Secondary reactions of acetone and 2-methylpropanal with the OH radical were taken into account using the rate constants given above for acetone and 2-methylpropanol and a rate constant for the reaction of the OH radical with 2,6-dimethyl-4-heptanone of 2.75×10^{-11} cm^3 $molecule^{-1}$ s^{-1} (*4,26*). In these experiments, the multiplicative factors to take into account OH radical reaction were <1.01 for acetone and ≤ 1.63 for 2-methylpropanal. In contrast to the OH radical reaction with 4-methyl-2-pentanone, addition of NO to reacted 2,6-dimethyl-4-heptanone mixtures led to an increase in the acetone yields (Figure 12), showing that acetone was formed, at least in part, through the intermediate formation of an acyl radical. No effect on NO addition was noted for 2-methylpropanal, indicating that 2-methylpropanal was not formed through an

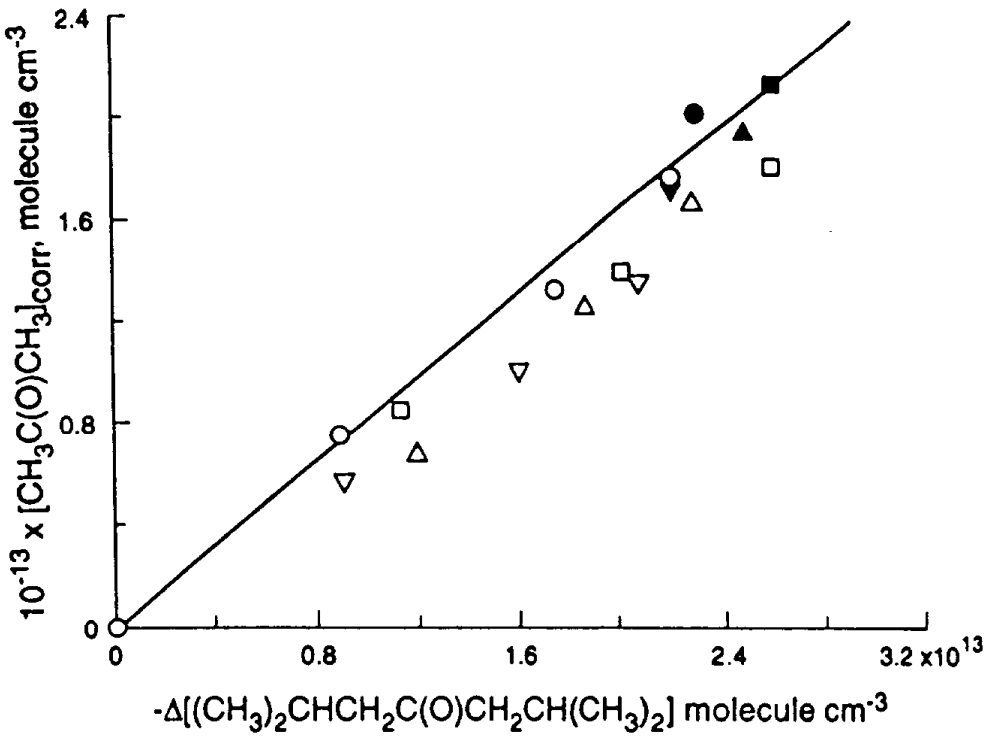

Figure 12. Plots of the amounts of acetone formed, corrected for reaction with the OH radical (see text), against the amounts of 2,6-dimethyl-4-heptanone reacted with the OH radical. Initial NO and NO_2 concentrations (in units of 10^{14} molecule cm^{-3}) were: o, ●, 1.9 and 0.3, respectively; △, ▲, 1.2 and 1.3, respectively; ▽, ▼, 0.7 and 1.5, respectively; □, ■, 2.4 and 0, respectively. ●, ▲, ▼, ■, Analysis ≥1 hr after addition of NO to reacted mixture. Line is from a least-squares analysis of data shown by filled symbols.

acyl radical intermediate. Plots of the amounts of acetone and 2-methylpropanal formed [the acetone being after the addition of NO (Figure 12)], corrected for reaction with the OH radical, against the amounts of 2,6-dimethyl-4-heptanone reacted are shown in Figure 13. The acetone and 2-methylpropanal yields obtained from least-squares analyses of these data are given in Table 5. Secondary formation of acetone from the OH radical reaction with 2-methylpropanal was calculated, assuming an acetone yield of unity, to account for up to 18% of the measured acetone concentrations in these experiments and the acetone yield corrected for secondary formation from 2-methylpropanal is also given in Table 5.

Three other product peaks were observed by GC-MS (two being much smaller than the third) with two (one being the major of the three) having mass spectra suggestive of dimethylheptenones [highest mass ions at m/z 140 and similar fragment ions to those of parent 2,6-dimethyl-4-heptanone (which is of molecular weight 142)] and the other with a m/z 141 ion as the highest mass observed. At least one of the m/z 140 peaks may arise from decomposition of a tertiary alkyl nitrate during the thermal desorption process. If this is the case, then assuming a similar GC-FID response for the observed dimethylheptenone(s) as for 2,6-dimethyl-4-heptanone (*55*), the single GC-FID peak observed would account for 10-15% of the overall reaction products.

The OH radical reaction with 2,6-dimethyl-4-heptanone proceeds by H-atom abstraction from the $-CH_3$, $-CH_2$ and $>CH-$ groups, with the estimation method of Atkinson (*49*) leading to calculated percentages of H-atom abstraction of 4% from the four equivalent $-CH_3$ groups, 9% from the two equivalent $-CH_2-$ groups and 87% from the two equivalent $>CH-$ groups. The measured OH radical reaction rate constant for 2,6-dimethyl-4-heptanone is almost exactly a factor of 2 higher than that for 4-methyl-2-pentanone (*4,26*), as expected (*49*), showing that with respect to the initial OH radical reaction 2,6-dimethyl-4-heptanone can be viewed as being similar to two molecules of 4-methyl-2-pentanone. Neglecting alkyl nitrate formation from the reactions of the organic peroxy radicals with NO (*4,40*), then the possible reaction schemes for the three initially formed alkoxy radicals formed after H-atom abstraction from the $-CH_3$, $-CH_2-$ and $>CH-$ groups are shown in Reaction Schemes II(a-c). The relative importance of certain of the alkoxy radical reactions, as either known from experimental studies (*4,46,50,51,54*) or estimated (*4,52*), have been indicated as noted for Reaction Scheme I, and only the alkoxy and

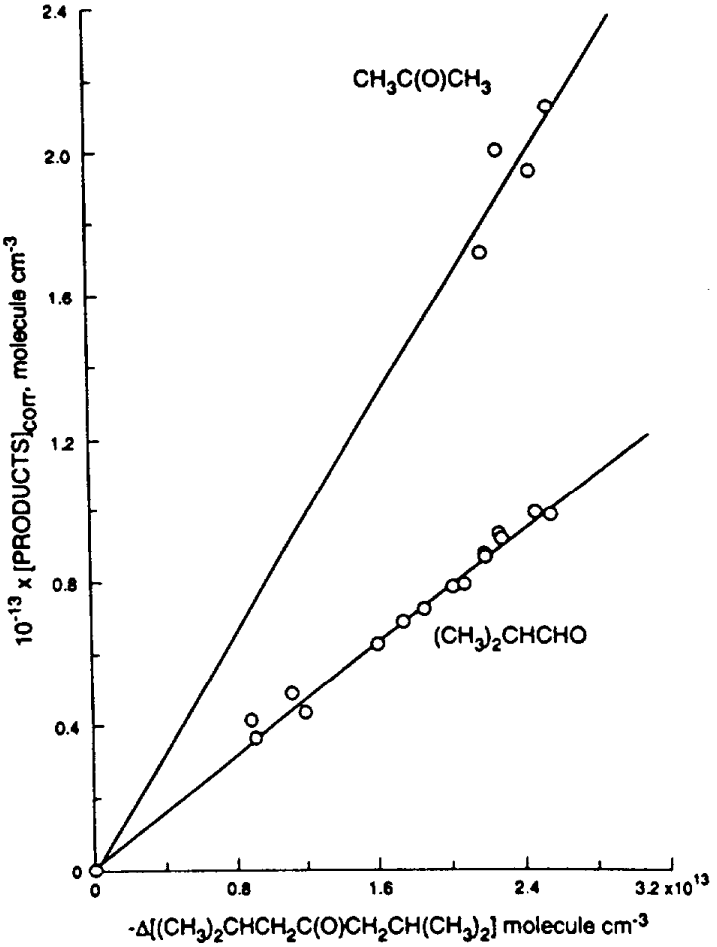

Figure 13. Plots of the amounts of acetone [after addition of NO to the reacted mixtures (data shown as ●, ▲, ▼, ■ in Figure 12)] and 2-methylpropanal, corrected for reaction with the OH radical (see text), against the amounts of 2,6-dimethyl-4-heptanone reacted with the OH radical.

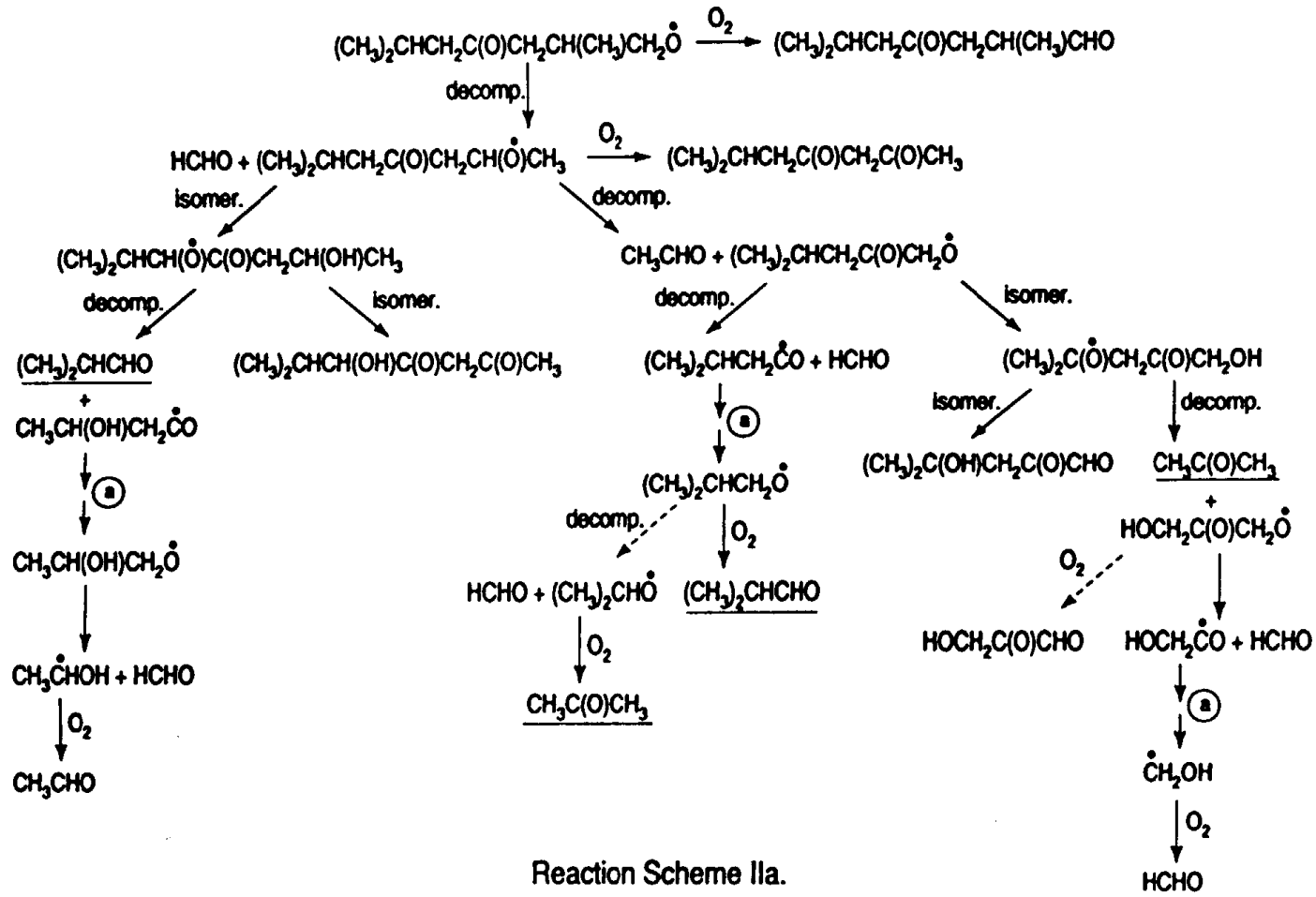

Reaction Scheme IIa.

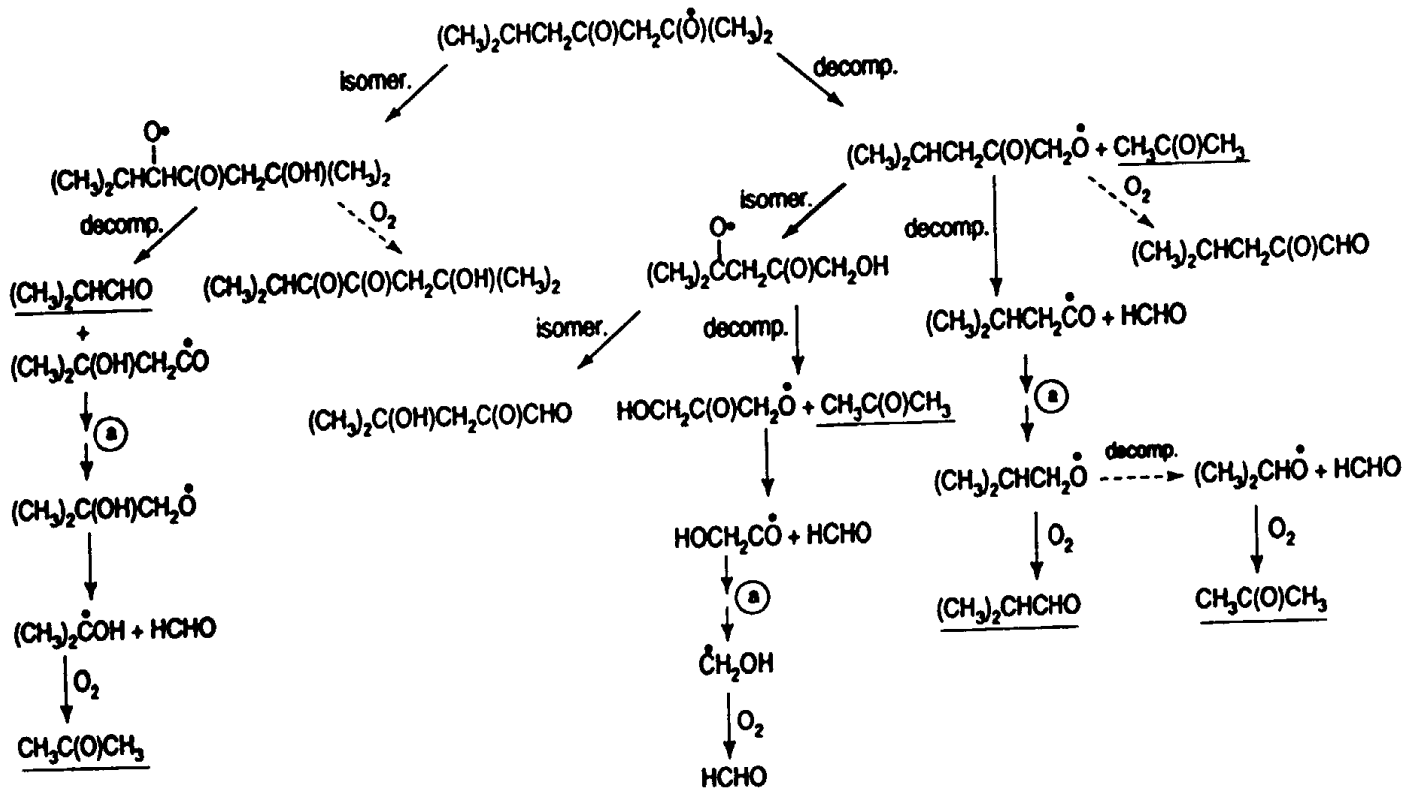

Reaction Scheme IIb.

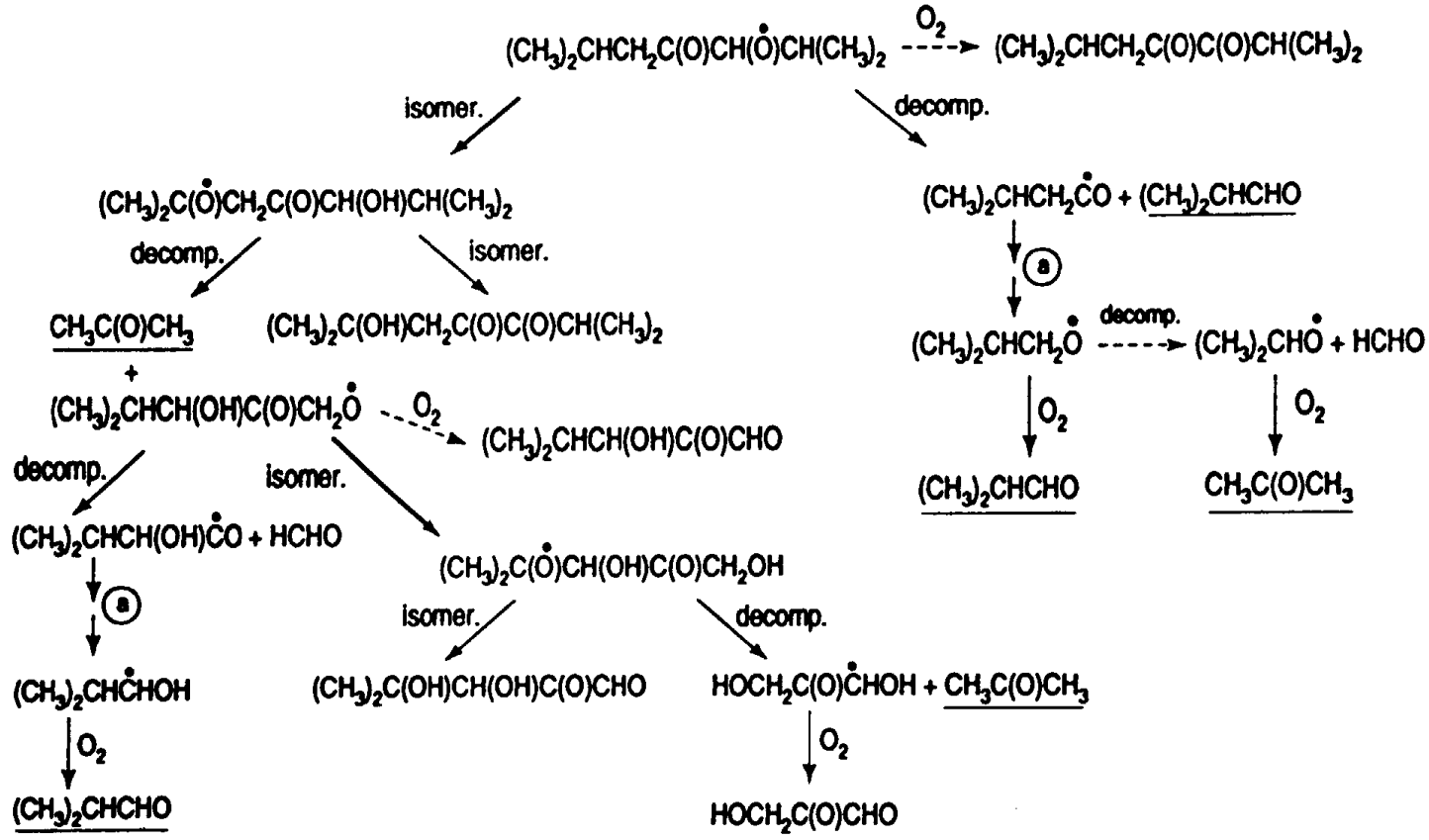

Reaction Scheme IIc.

acyl radicals are shown for clarity. Furthermore, the reaction of the $(CH_3)_2CHCH_2C(O)CH_2\dot{O}$ radical with O_2, estimated to be of minor importance relative to decomposition, has been omitted for clarity in Reaction Scheme IIa.

While these reaction schemes are complex, the experimental data allow certain conclusions to be drawn. Since the $(CH_3)_2CHCH_2C(O)CH_2CH(CH_3)CH_2\dot{O}$ radical formed after H-atom abstraction from the $-CH_3$ groups accounts for only $\leq 4\%$ of the overall reaction (depending on the importance of nitrate formation from the $R\dot{O}_2$ + NO reaction), any acetone or 2-methylpropanal formation from this radical (Reaction Scheme IIa) can only account for a minor fraction of the acetone and 2-methylpropanal observed.

The $(CH_3)_2CHCH_2C(O)CH(\dot{O})CH(CH_3)_2$ radical accounts for $\leq 9\%$ of the overall OH radical reaction, depending on the importance of nitrate formation from the $R\dot{O}_2$ + NO reaction. Based on the observation that the yield of 2-methylpropanal was not affected by NO addition to the reacted mixtures and the expectation that the decomposition of the $(CH_3)_2CHCH_2C(O)CH(\dot{O})CH(CH_3)_2$ radical dominates over reaction with O_2 (*4*), then this alkoxy radical must predominantly react by isomerization to lead to 0-2 molecules of acetone (Reaction Scheme IIc), with the number of molecules of acetone formed depending on the reactions subsequent to the first isomerization reaction (Reaction Scheme IIc).

Therefore, the major amount of 2-methylpropanal formed must arise after H-atom abstraction from the $>CH-$ groups. From Reaction Scheme IIb and noting that (a) 2-methylpropanal formation does not involve an acyl radical precursor, (b) H-atom abstraction from the $>CH-$ groups is estimated to account for 87% of the overall OH radical reaction with 2,6-dimethyl-4-heptanone, and (c) that the 2-methylpropanal yield is 0.385 ± 0.034 (Table 4), then the $(CH_3)_2CHCH_2C(O)CH_2C(\dot{O})(CH_3)_2$ alkoxy radical must undergo both isomerization and decomposition. These considerations show that 2-methylpropanal must be formed mainly from the isomerization reaction of the $(CH_3)_2CHCH_2C(O)CH_2CH(\dot{O})(CH_3)_2$ radical.

Reaction Scheme IIb indicates that this formation of 2-methylpropanal via isomerization of the $(CH_3)_2CHCH_2C(O)CH_2C(\dot{O})(CH_3)_2$ radical, followed by decomposition of the resulting $(CH_3)_2CHCH(\dot{O})C(O)CH_2C(OH)(CH_3)_2$ alkoxy radical (isomerization by a 6-membered transition state cannot occur), should be accompanied by acetone formation through the intermediary of an acyl radical. The remainder of the measured acetone yield, of ~ 0.30, is significantly higher

than can be formed after initial H-atom abstraction from the $-CH_2-$ groups (9% of the overall OH radical reaction) [Reaction Scheme IIc] and hence acetone must also be formed from decomposition of the alkoxy radical formed after H-atom abstraction from the $>CH-$ groups (Reaction Scheme IIb).

Relative Importance of Alkoxy Radical Isomerization vs. Decomposition. For the reaction of the OH radical with 2,6-dimethyl-4-heptanone in the presence of NO_x, the initially formed alkoxy radicals and the yields of acetone and 2-methylpropanal formed from these alkoxy radicals via the various reaction pathways shown in Reaction Schemes II(a-c) are summarized in Table 6. Comparison of the data in Table 6 with our experimental data show that isomerization of the $(CH_3)_2CHCH_2C(O)CH_2C(\dot{O})(CH_3)_2$ radical must occur and that for this alkoxy radical isomerization and decomposition must be of comparable importance at room temperature.

Our present acetone and 2-methylpropanal formation yield data from the OH radical-initiated reactions of 4-methyl-2-pentanone and 2,6-dimethyl-4-heptanone in the presence of NO_x allow the relative importance of isomerization *versus* decomposition for the alkoxy radicals $CH_3C(O)CH_2C(\dot{O})(CH_3)_2$, $(CH_3)_2CHCH_2C(O)CH_2\dot{O}$ and $(CH_3)_2CHCH_2C(O)CH_2C(\dot{O})(CH_3)_2$ to be obtained. These alkoxy radicals are given in Table 7 together with ratios of k(decomposition)/k(isomerization) derived from our experimental data and from present estimation methods (*4*). As indicated by Atkinson (*4*), these estimates for the decomposition and isomerization rates are subject to significant uncertainties.

The decomposition and isomerization reactions for each of the three alkoxy radicals listed in Table 7 can be respectively viewed as:

$CH_3C(O)CH_2C(\dot{O})(CH_3)_2$ radical

$$>C(\dot{O})CH_2C(O)CH_3 \rightarrow >CO + \dot{C}H_2C(O)CH_3 \quad \text{(decomposition)} \qquad (10)$$

$$>C(\dot{O})CH_2C(O)CH_3 \rightarrow >C(OH)CH_2C(O)\dot{C}H_2 \quad \text{(isomerization)} \qquad (11)$$

Table 6. Initially Formed Alkoxy Radicals in the OH Radical-Initiated Reaction of 2,6-Dimethyl-4-heptanone, and the Possible Production of Acetone and 2-Methylpropanal from the Reactions of these Alkoxy Radicals (Reaction Schemes IIa-IIc).

Alkoxy radical	Percentage formed[a] %	Reaction with	Possible Yields of	
			Acetone	2-Methylpropanal
$(CH_3)_2CHCH_2C(O)CH_2CH(CH_3)CH_2\dot{O}$	≤4	O_2	0	0
		decomposition	0 0 1 0	0 1[b,c] 0 1
$(CH_3)_2CHCH_2C(O)CH_2C(\dot{O})(CH_3)_2$	≤87	decomposition	1 2 1	0 0 1[b,c]
		isomerization	0 1[b]	0 1
$(CH_3)_2CHCH_2C(O)CH(\dot{O})CH(CH_3)_2$	≤9	O_2	0	0
		decomposition	0	2[c,d]
		isomerization	0 1 1 2	0 0 1[b,c] 0

[a]Upper limit if organic nitrate yield from $R\dot{O}_2$ + NO reaction is zero (see text).

[b]Formed via intermediary of an acyl radical.

[c]Not consistent with the experimental data.

[d]One molecule of these two formed via intermediary of an acyl radical.

Table 7. Experimental and Estimated Relative Importances of Decomposition *versus* Isomerization for Selected Alkoxy Radicals at 298 K.

	k(decomposition)/k(isomerization)		
Alkoxy radical	Experimental[a]	Estimated[b]	k(isomerization)[b] s^{-1}
$CH_3C(O)CH_2C(\dot{O})(CH_3)_2$	>5	~1	7×10^4
$(CH_3)_2CHCH_2C(O)CH_2C(\dot{O})(CH_3)_2$	~1	~0.01	8×10^6
$(CH_3)_2CHCH_2C(O)CH_2\dot{O}$	<1[c]	~7	4×10^6

[a]This work.

[b]Estimated as discussed in ref. (*4*) [using Equation (III) on p. 22 of ref. (*4*) to estimate the thermal decomposition rate of the $(CH_3)_2CHCH_2C(O)CH_2\dot{O}$ radical].

[c]Based on the experimental data indicating that $(CH_3)_2CHCHO$ formation from 2,6-dimethyl-4-heptanone does not involve an acyl radical precursor (see text and Reaction Scheme IIb).

$(CH_3)_2CHCH_2C(O)CH_2C(\dot{O})(CH_3)_2$ radical

$$>C(\dot{O})CH_2C(O)CH_2\text{-} \rightarrow >CO + \dot{C}H_2C(O)CH_2\text{-} \quad \text{(decomposition)} \quad (12)$$

$$>C(\dot{O})CH_2C(O)CH_2\text{-} \rightarrow >C(OH)CH_2C(O)\dot{C}H\text{-} \quad \text{(isomerization)} \quad (13)$$

$(CH_3)_2CHCH_2C(O)CH_2\dot{O}$ radical

$$>C(\dot{O})C(O)CH_2CH< \rightarrow >CO + \dot{C}(O)CH_2CH< \quad \text{(decomposition)} \quad (14)$$

$$>C(\dot{O})C(O)CH_2CH< \rightarrow >C(OH)C(O)CH_2\dot{C}< \quad \text{(isomerization)} \quad (15)$$

The decomposition reactions (10) and (12) are expected to have very similar decomposition rates, since they involve identical C-C bond scissions, while the isomerization reactions (11) and (13) differ in that reaction (11) involves H-atom abstraction from a $-CH_3$ group and reaction (13) involves H-atom abstraction from a $-CH_2-$ group, both being α to the $>C(O)$ group. Since H-atom abstraction from a $-CH_3$ group has a lower exothermicity than H-atom abstraction from a $-CH_2-$ group (all other things being equal) (*4*), then the rate of reaction (11) is expected to be lower than that for reaction (13), consistent with our experimental data which show that (11) is minor compared to reaction (10) [with no evidence for the occurrence of reaction (11)] but that reactions (12) and (13) are of comparable importance. However, as shown in Table 7, the isomerization reactions (11) and (13) are less important than expected based on estimations for the analogous alkoxy radicals formed from alkanes (*4,20,46*).

The thermal decomposition reaction (14) is expected to be significantly more rapid than the decomposition reactions (10) and (12), since reaction (14) involves a $>C(\dot{O})C(O)$-carbon-carbon bond scission rather than a $>C(\dot{O})CH_2-$ carbon-carbon bond scission (*20,46,48*), yet the isomerization reaction for the $(CH_3)_2CHCH_2C(O)CH_2\dot{O}$ radical [reaction (15)] still appears to dominate (Table 7). The alkoxy radical isomerization reaction (15) involves H-atom abstraction from a $>CH-$ group β to the $>CO$ group, and it hence appears that, totally analogous to OH radical reaction with the ketones (*49*), H-atom abstraction from C-H bonds β to the $>CO$ group

in the isomerization reaction is significantly faster than H-atom abstraction from C-H bonds α to the >CO group. In fact, the empirical estimation method of Atkinson (*49*) for H-atom abstraction by OH radicals from ketones at 298 K has H-atom abstraction from C-H bonds at the β carbon being a factor of 5.8 faster than H-atom abstraction from C-H bonds at the α carbon (*49*). All of the alkoxy radical isomerization pathways in Reaction Schemes (Ia-Id) and (IIa-IIc) are consistent with such an β/α effect of the >CO group.

C. Conclusions

The experimental product data obtained in this study provide direct evidence for the occurrence of isomerization of alkoxy radicals. However, these data also indicate that estimates of the alkoxy radical isomerization rates derived from alkane reactions need to be refined to be applicable to alkoxy radicals formed from ketones. Analogous to H-atom abstraction by OH radicals from ketones (*49*), the alkoxy radicals formed from the ketones have isomerization rates which depend on the position of the $-CH_3$, $-CH_2-$ and >CH- groups relative to the >CO group; in particular, whether these groups are α or β to the >CO group, with H-atom abstraction from alkyl groups β to the >CO group being significantly more rapid than from alkyl groups α to the >CO group.

IV. PRODUCT STUDIES OF THE GAS-PHASE REACTIONS OF THE OH RADICAL WITH SELECTED ALCOHOLS

In Section III, product studies of the OH radical reactions (in the presence of NO_x) with 4-methyl-2-pentanone and 2,6-dimethyl-4-heptanone were described, with the goal being to obtain unambiguous evidence for the occurrence of the alkoxy radical isomerization reaction through identification and quantification of products which could only arise from the isomerization pathway. While evidence for alkoxy radical isomerization was obtained, the products targeted could be formed from other pathways, rendering the interpretation of the data obtained difficult. Therefore, other reaction systems were sought, and it was expected that the products of the reactions of the OH radical, in the presence of NO_x, with 2,4-dimethyl-2-pentanol and 3,5-dimethyl-3-hexanol could provide unambiguous evidence for alkoxy radical isomerization. Taking 3,5-dimethyl-3-hexanol as an example and showing only the alkoxy radicals involved, the major reactions expected (*4*) are as shown in Reaction Schemes IIIa through IIIc, where organic nitrate formation (*4*) has been neglected and H-atom abstraction from the four $-CH_3$ groups neglected. The formation of 4-hydroxy-4-methyl-2-pentanone should therefore be conclusive proof of the occurrence of isomerization of the alkoxy radical formed after H-atom abstraction from the 5-position >CH- group.

A similar analysis of the expected reactions for 2,4-dimethyl-2-pentanol (*4*) leads to the formation of acetone + 2-methylpropanal (via decomposition) after H-atom abstraction from the 3-position $-CH_2-$ group; and 4-hydroxy-4-methyl-2-pentanone (via isomerization) or acetone + HCHO + acetone (via decomposition) after H-atom abstraction from the 4-position >CH-group. Again, the formation of 4-hydroxy-4-methyl-2-pentanone would be proof of isomerization of the alkoxy radical formed after H-atom abstraction from the 4-position >CH-group.

A. Experimental

Experiments were carried out at 295 ± 2 K and 740 Torr total pressure of purified (3-5% relative humidity) air in a 7900 liter all-Teflon chamber equipped with two parallel banks of blacklamps. Hydroxyl radicals were generated by the photolysis of methyl nitrite (CH_3ONO) in air at wavelengths >300 nm (*37*), and NO was included in the reactant mixtures to avoid the formation of O_3, and hence of NO_3 radicals. The initial reactant concentrations (in

After H-atom abstraction from the 2-position -CH_2- group.

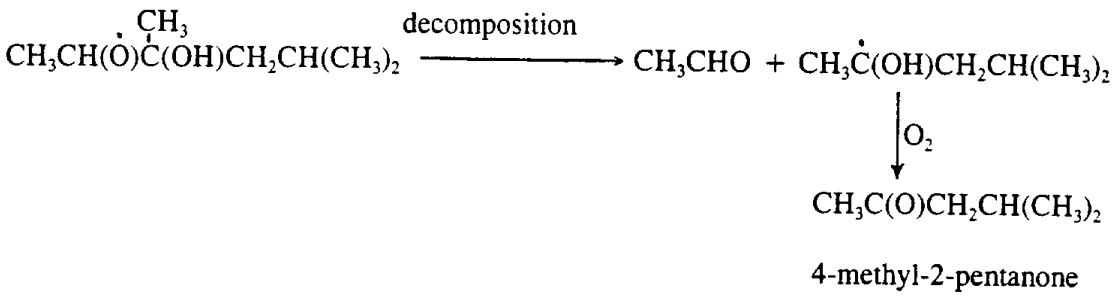

Reaction Scheme IIIa

After H-atom abstraction from the 4-position -CH_2- group.

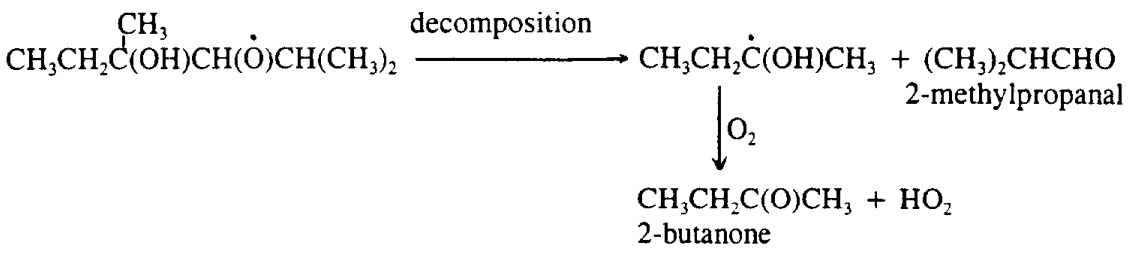

Reaction Scheme IIIb

After H-atom abstraction from the 5-position >CH-group.

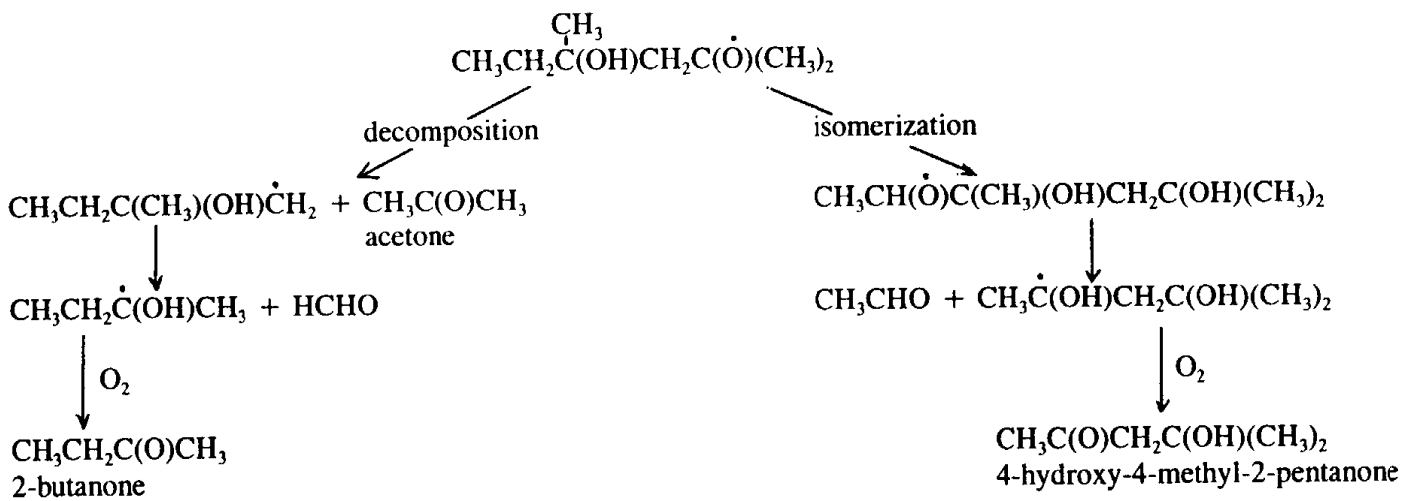

Reaction Scheme IIIc

molecule cm^{-3} units) were: CH_3ONO, $\sim 2.4 \times 10^{14}$; NO, $\sim 2.4 \times 10^{14}$; 2,4-dimethyl-2-pentanol or 3,5-dimethyl-3-hexanol, $\sim 2.4 \times 10^{13}$. Irradiations were carried out at 20% the maximum light intensity for 8-30 mins.

The alcohol reactants and products were analyzed during the experiments by gas chromatography with flame ionization detection (GC-FID). Gas samples of 100 cm^3 volume were collected from the chamber onto Tenax-TA solid adsorbent, with subsequent thermal desorption at 225 °C onto a 30 m DB-5.625 megabore column in a HP 5710 GC, initially held at 0 °C and then temperature programmed to 200 °C at 8 °C min^{-1}. GC-FID calibrations were carried out by measuring known pressures of the compound, using an MKS Baratron 0-100 Torr sensor head, into a 2.03 liter Pyrex bulb (acetone, 2-methylpropanal, 2,4-dimethyl-2-pentanol, 3,5-dimethyl-3-hexanol and 4-hydroxy-4-methyl-2-pentanone) or by introducing measured volumes of the liquids (2-butanone and 4-methyl-2-pentanone) into a 1 liter Pyrex bulb, and flushing the contents of these bulbs into the 7900 liter chamber by a stream of N_2 gas. On a relative basis, the GC-FID response factors agreed with the Equivalent Carbon Numbers, as calculated by Scanlon and Willis (*55*), to within ±9%, giving confidence that the calibration factors were accurate and that the sample collection and thermal desorption procedures were quantitative.

Gas samples were also collected onto Tenax-TA solid adsorbent for subsequent thermal desorption and analysis by combined gas chromatography-mass spectrometry (GC-MS), using a 60 m DB-5MS fused silica capillary column, temperature programmed from -80 °C at 10 °C min^{-1} to 250 °C, in a HP 5890 GC interfaced to a HP 5970 mass selective detector operated in the scanning mode. The NO concentrations and initial NO_2 concentrations were monitored during these experiments using a chemiluminescence NO-NO_x analyzer. All instruments were maintained as recommended and their performance checked on a daily basis.

The chemicals used, and their stated purities, were: acetone (>99.6%), Fisher Scientific; 4-hydroxy-4-methyl-2-pentanone (99%); 4-methyl-2-pentanone (99+%) and 2-methylpropanal [isobutyraldehyde] (99+%), Aldrich Chemical Company; 2,4-dimethyl-2-pentanol, ICN; 3,5-dimethyl-3-hexanol, Pfaltz and Bauer; and NO (≥99.0%), Matheson Gas Products. Methyl nitrite was prepared and stored as described previously (*37*).

B. Results and Discussion

An initial set of experiments were carried out prior to the end of this Contract. Three irradiations of CH_3ONO-NO-2,4-dimethyl-2-pentanol-air mixtures and one irradiation of a CH_3ONO-NO-3,5-dimethyl-3-hexanol-air mixture were carried out, and GC/MS and GC-FID analyses showed the formation of the following products: from 2,4-dimethyl-2-pentanol, acetone, 2-methylpropanal and 4-hydroxy-4-methyl-2-pentanone; and from 3,5-dimethyl-3-hexanol, acetone, 2-butanone, 2-methylpropanal, 4-methyl-2-pentanone and 4-hydroxy-4-methyl-2-pentanone. An additional product was observed from each reaction system which was not identified but is ascribed to a tertiary nitrate which decomposes during the thermal desorption procedure to yield an unsaturated alcohol (for example, 3,5-dimethylhex-4-en-3-ol from the 3,5-dimethyl-3-hexanol reaction).

Since the products observed also react with the OH radical, their secondary reactions must be taken into account in determining their formation yields, and hence the rate constants for the gas-phase reactions of the OH radical with 2,4-dimethyl-2-pentanol, 3,5-dimethyl-3-hexanol and 4-hydroxy-4-methyl-2-pentanone need to be determined (rate constants are available for the other products for which authentic standards are available). Due to time constraints, these kinetic experiments have not been carried out during this Contract, and hence only approximate product formation yields can be derived, especially for the more reactive products such as 4-methyl-2-pentanone from 3,5-dimethyl-3-hexanol and, especially, for 2-methylpropanal from both alcohols. The necessary kinetic experiments, the remainder of the product experiments and the final data analysis will be completed under a Cooperative Agreement with the U.S. Environmental Protection Agency (Cooperative Agreement CR 821787-01-0).

Based on the estimation method of Atkinson (*49*), as updated by Kwok and Atkinson (*56*), 4-hydroxy-4-methyl-2-pentanone should be less reactive towards OH radicals than either of the precursor alcohols, and hence corrections to take into account secondary reactions of 4-hydroxy-4-methyl-2-pentanone should be minor. Similarly with acetone, although the usefulness of acetone as a product to define the reaction channels is negated by the fact that acetone is formed from the secondary reactions of 2-methylpropanal (formed from the reactions of both alcohols) and from 4-methyl-2-pentanone [Section III] (formed from the 3,5-dimethyl-3-hexanol reaction). Based on the measured concentrations of 4-hydroxy-4-methyl-2-pentanone and the

alcohols during these reactions, the approximate 4-hydroxy-4-methyl-2-pentanone formation yields from 2,4-dimethyl-2-pentanol and 3,5-dimethyl-3-hexanol are ~0.11 and ~0.23, respectively. The estimated rate constants for reactions of the OH radical with the various -OH, $-CH_3$, $-CH_2-$ and >CH- groups in 2,4-dimethyl-2-pentanol and 3,5-dimethyl-3-hexanol (*49,56*) imply that the fractions of the overall OH radical reactions with 2,4-dimethyl-2-pentanol and 3,5-dimethyl-3-hexanol proceeding via H-atom abstraction from the >CH- group are 0.52 and 0.41, respectively [note that the accurate determination of the 2-methylpropanal, 2-butanone, 4-methyl-2-pentanone and 4-hydroxy-4-methyl-2-pentanone formation yields from the OH radical reaction with 3,5-dimethyl-3-hexanol should allow all of the major alkoxy radical reaction pathways to be quantitatively defined]. The preliminary data obtained in this program show unambiguously that alkoxy radical isomerization does occur at room temperature, and further shows, as expected, that isomerization of the $CH_3CH_2C(CH_3)(OH)CH_2C(\dot{O})(CH_3)_2$ radical, proceeding via H-atom abstraction from the weaker C-H bonds of a $-CH_2-$ group, is more rapid than isomerization of the $(CH_3)_2C(OH)CH_2C(\dot{O})(CH_3)_2$ radical, proceeding via H-atom abstraction from the C-H bonds of a $-CH_3$ group (assuming that decomposition of the $RC(CH_3)(OH)CH_2C(O)(CH_3)_2$ radical to acetone plus the $RC(CH_3)(OH)CH_2$ radical has the same rate for R = CH_3 or C_2H_5).

V. PRODUCTS OF THE GAS-PHASE REACTIONS OF OH RADICALS WITH A SERIES OF *n*-ALKANES

In an attempt to observe the products of the alkoxy radical isomerization in the alkanes, a product study of the gas-phase OH radical reactions, in the presence of NO_x, with the *n*-alkanes, *n*-butane through *n*-octane was carried out. The products of the gas-phase OH radical-initiated reactions of *n*-pentane through *n*-octane were studied using gas chromatographic analyses, while the reactions of OH radicals with *n*-butane through *n*-octane and selected of their perdeuterated analogs were studied using a SCIEX API III MS/MS direct air sampling, atmospheric pressure ionization tandem mass spectrometer. Because of other commitments and needed maintenance on the SCIEX API MS/MS, only preliminary data using this *in situ* analysis method were obtained during this Contract. The experiments carried out during this ARB-funded Contract are described below and a very preliminary analysis of the data obtained is made. As for the experiments described in Section IV, the study described here will be completed under funding from the U.S. Environmental Protection Agency Cooperative Agreement CR 821787-01-0.

A. Experimental

Experiments were carried out in a ~7900 liter all-Teflon chamber (Figure 1) and a ~6500 liter all-Teflon chamber interfaced to a SCIEX API III MS/MS system (Figure 14). In both chambers, hydroxyl radicals were generated by the photolysis of methyl nitrite (CH_3ONO) in air at wavelengths >300 nm (*37*).

Analyses by API MS/MS. As noted above, the ~6500 liter all-Teflon chambers was interfaced directly to a SCIEX API III MS/MS (Figure 14). In these experiments, the chemical ionization reagents were mainly protonated hydrates ($H_3O^+[H_2O]_n$) or anionic oxygen species such as superoxide anions (O_2^-) in the atmospheric pressure chemical ionization (APCI) source which directly sampled the chamber diluent gas (which was purified air at ~5% relative humidity). These ions were generated by electrons created in a corona discharge operated at a constant discharge current. Chemical ionization may occur as a charge transfer (positive or negative ion mode), or as protonation (positive ion mode) or deprotonation (negative ion mode).

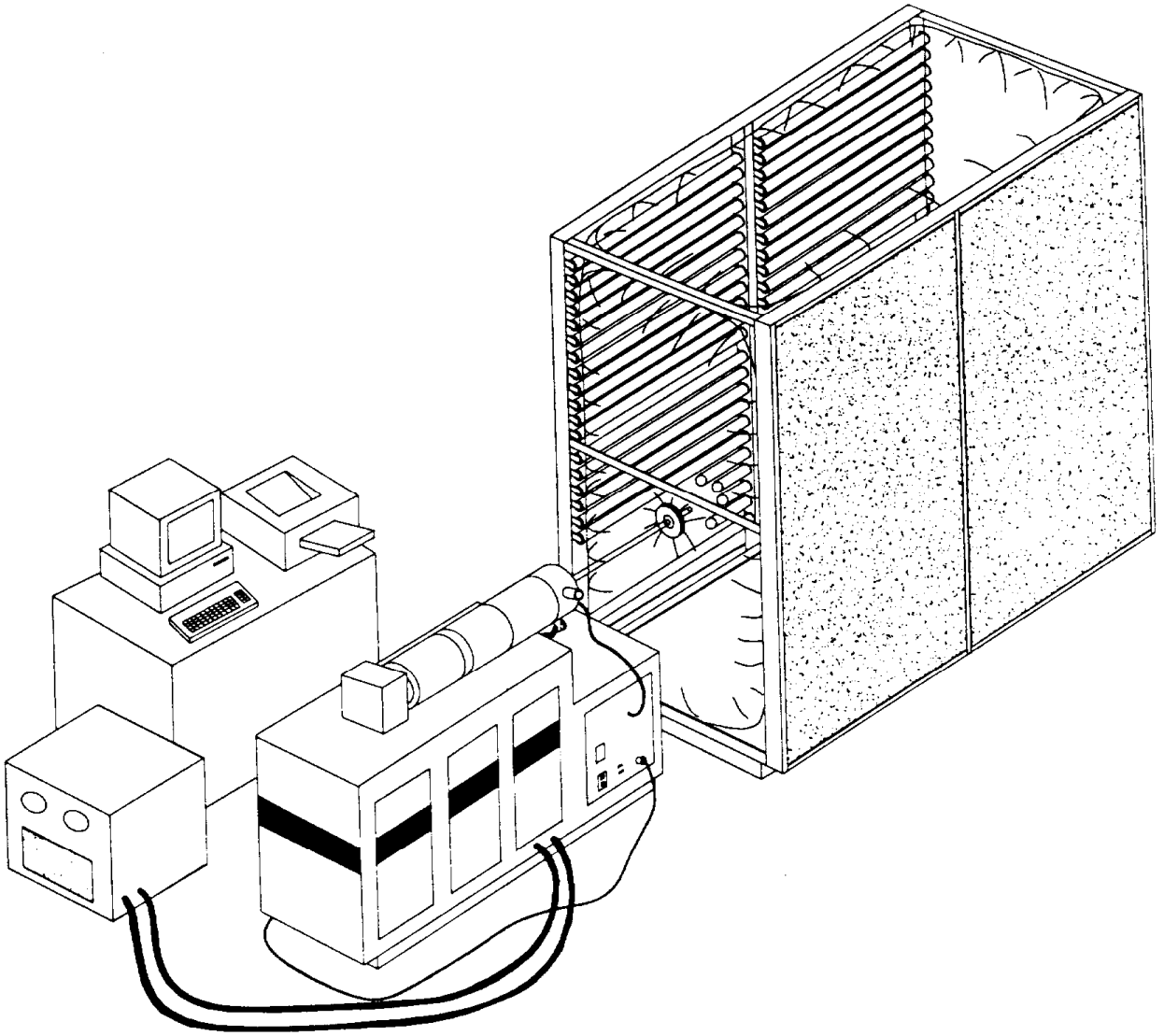

Figure 14. Schematic of ~6500 liter all-Teflon chamber interfaced to SCIEX API mass spectrometer.

Some compounds are more sensitive in positive ion mode than in the negative ion mode, and vice versa. For the alkanes studied here and their reaction products, positive ion mode was the most useful, although spectra were routinely obtained in the negative ion mode.

In the MS mode, mass spectra (each being the sum of 10 scans) of the reactants and the reacted mixtures were obtained by the first quadrupole (Q1), with the second and third quadrupoles (Q2 and Q3) being operated in the "total-ion" mode (RF-only mode). Each scan was acquired over the range 60-300 amu using a step of 0.2 amu and a dwell time of 30 ms. In the MS/MS mode, the precursor ion was selected by Q1 and was scanned by Q3. Argon was used as the collision gas in an open Q2 collision cell, with the collision gas thickness being equal to $\sim 3 \times 10^{14}$ molecule cm^{-2}. The collision-activated dissociation (CAD) spectrum of an analyte (sum of 20 scans) was acquired using a step of 0.2 amu and a dwell time of 20 ms. The lower and upper limits of the mass range used for acquiring parent and daughter ion spectra, respectively, was determined by the molecular weight of the ion of interest.

The initial reactant concentrations were (in molecule cm^{-3} units): CH_3ONO, $\sim 1.2 \times 10^{13}$; NO, $\sim 1.2 \times 10^{13}$; alkane, $\sim 1.2 \times 10^{13}$. Irradiations were carried out at 20% of the maximum light intensity for 1-10 mins. While the API MS/MS system was almost totally insensitive to the alkanes, in these preliminary experiments no GC-FID analyses were carried out and hence no quantitative alkane concentration data are available.

Analyses by GC-FID. These experiments were carried out in the 7900 liter all-Teflon chamber. The initial reactant concentrations (in molecule cm^{-3} units) were: CH_3ONO, 2.4×10^{14}; NO, 2.4×10^{14}; and alkane, $(4.2\text{-}4.5) \times 10^{13}$. Irradiations were carried out at the maximum light intensity for 3-15 mins. For all four *n*-alkanes, experiments were carried out in air [740 Torr total pressure, 21% (155 Torr) of O_2] and in "high-O_2" diluent gas, obtained by filling the majority of the (almost empty) chamber with O_2. Based on the amounts of O_2 introduced into the chamber from cylinders, the percentages of O_2 were in the range 75-85% (550-630 Torr O_2).

The alkane reactants and selected products were analyzed during the experiments by gas chromatography with flame ionization detection (GC-FID). For the analyses of the alkanes, gas samples were collected from the chamber in 100 cm^3 all-glass, gas-tight syringes and introduced

via a 1 cm^3 gas sampling loop onto a 30 m DB-5 megabore column in a Hewlett Packard (HP) 5890 GC, initially held at -25 °C and then temperature programmed to 200 °C at 8 °C min^{-1}. For the analyses of the carbonyl and alkyl nitrate products, 100 cm^3 volume samples were collected from the chamber onto Tenax-TA solid adsorbent, with subsequent thermal desorption at 225 °C onto a 30 m DB-5.625 megabore column in a HP 5710 GC, initially held at 0 °C and then temperature programmed to 200 °C at 8 °C min^{-1}. Gas samples were also collected onto Tenax-TA solid adsorbent for subsequent thermal desorption and analysis by combined gas chromatography-mass spectrometry (GC-MS), using a 60 m DB-5MS fused silica capillary column, temperature programmed from -80 °C at 10 °C min^{-1} to 250 °C, in a HP 5890 GC interfaced to a HP 5970 mass selective detector operated in the scanning mode. The NO concentrations and initial NO_2 concentrations were monitored during these experiments using a chemiluminescence NO-NO_x analyzer.

Calibrations of the CG-FID instruments and the NO-NO_x analyzer were carried out as described in Sections III and IV above. All instruments, including the direct air sampling atmospheric pressure ionization MS/MS, were maintained as recommended and their performance checked on a daily basis.

The chemicals used, and their stated purities, were: *n*-heptane-d_{16} (99+%), 2-heptanone (98%), 3-heptanone (98%), 4-heptanone (98%), *n*-hexane, (99+%), *n*-hexane-d_{14} (99% D), 2-hexanone (99+%), 3-hexanone (98%), *n*-octane (99+%), *n*-octane-d_{18} (98+% D), 2-octanone (98%), 3-octanone (98+%), *n*-pentane (99+%), Aldrich Chemical Company; *n*-pentane-d_{12} (98% D), Cambridge Isotope Laboratories; 4-octanone (98%), Pfaltz and Bauer; 2-pentanone and 3-pentanone, MCB; *n*-heptane (Reagent Grade), Mallinckrodt; *n*-butane ($\geq$99.0%) and NO ($\geq$99.0%), Matheson Gas Products.

B. Results and Discussion

GC-FID Analyses

n-Pentane. The majority of the experiments dealt with the products formed from *n*-pentane. GC/MS and GC-FID analyses of irradiated CH_3ONO-NO-*n*-pentane-air mixtures showed the formation of 2-pentanone, 3-pentanone and 2- and 3-pentyl nitrate. While the pentyl nitrates were not baseline resolved with the DB-5.625 megabore column used, their

concentrations were integrated individually. Since these observed products also react with the OH radical, their secondary reactions must be taken into account in determining the product formation yields. Secondary reaction were taken into account as described by Atkinson et al. (*40*), using rate constants for the OH radical reactions of (in units of 10^{-12} cm^3 $molecule^{-1}$ s^{-1}): *n*-pentane, 3.91; 2-pentanone, 5.07; 3-pentanone, 2.09; 2-pentyl nitrate, 1.85; and 3-pentyl nitrate, 1.12 (*4,26*). The multiplicative correction factors to take into account secondary reactions were ≤ 1.30 for 2-pentanone, ≤ 1.12 for 3-pentanone, ≤ 1.12 for 2-pentyl nitrate, and ≤ 1.06 for 3-pentyl nitrate.

Plots of the 2-pentanone and 3-pentanone data, corrected to take into account secondary reactions with the OH radical, are shown in Figure 15. Least squares analysis of the data leads to the formation yields given in Table 8. The relative yields of the 2- and 3-pentanones determined here at room temperature and one atmosphere of air, of (2-pentanone)/(2- + 3-pentanone) = 0.18, are in agreement with the values for this ratio of 0.16-0.21 reported by Carter et al. (*47*). Figure 15 and Table 8 shows that the 2-pentanone and 3-pentanone formation yields increase with increasing O_2 concentration, with the effect being most marked for 2-pentanone. In contrast, the 2- and 3-pentyl nitrate yields were independent of the O_2 concentrations, as expected (*4*) since these nitrates are formed from the reactions of the 2- and 3-pentyl peroxy radicals with NO

$$R\dot{O}_2 + NO \xrightarrow{M} RONO_2$$

in competition with the pathway forming the alkoxy radical plus NO_2

$$R\dot{O}_2 + NO \rightarrow RO + NO_2$$

The nitrate yields are dependent on the temperature (increasing with decreasing temperature) and total pressure (increasing with increasing total pressure) (*4*), but should be independent of the O_2 concentration providing that O_2 and N_2 have similar third-body efficiencies for the $R\dot{O}_2$ + NO $\rightarrow$ $RONO_2$ reactions.

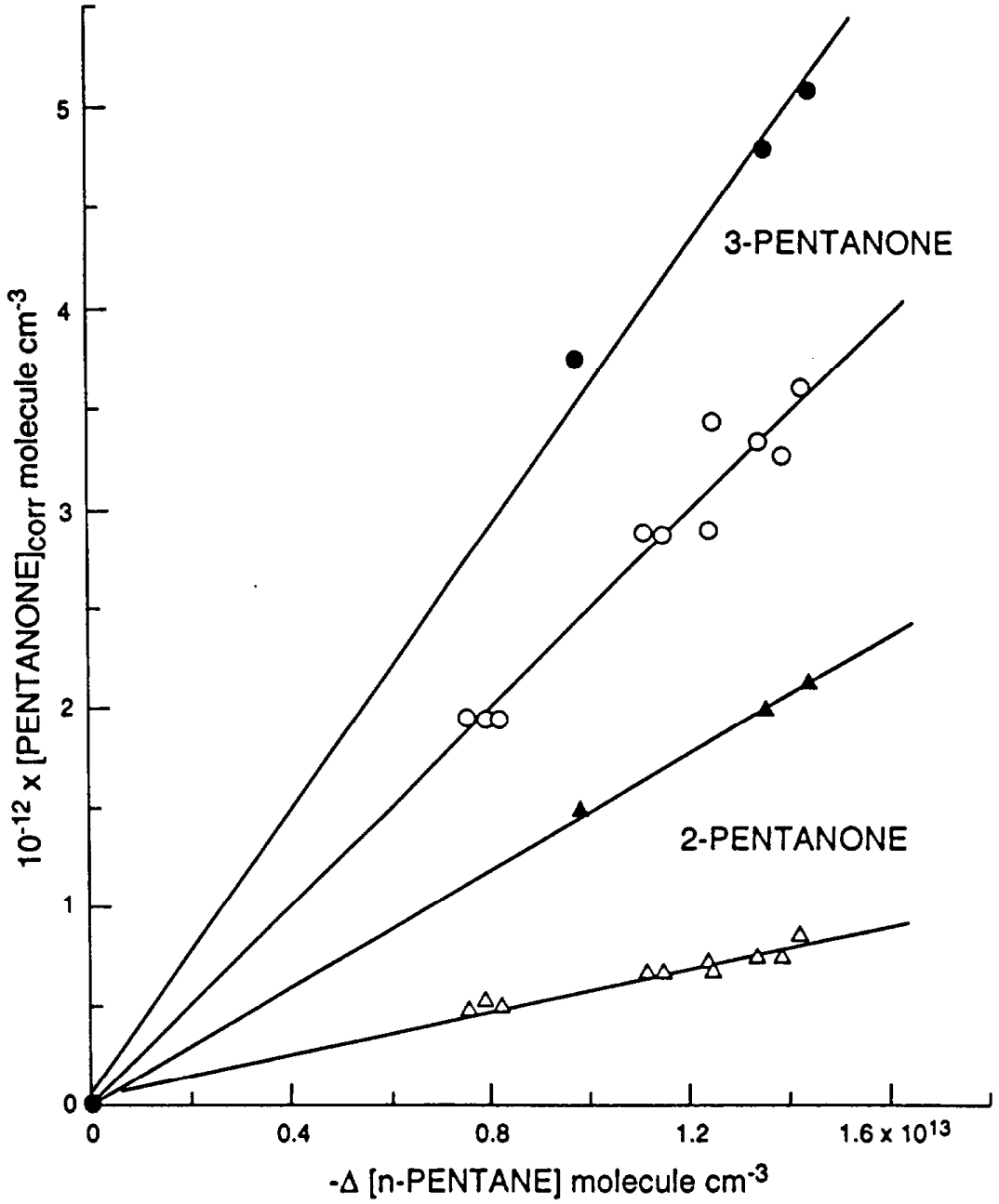

Figure 15. Plots of the amounts of 2- and 3-pentanone formed, corrected for reaction with the OH radical, against the amount of *n*-pentane reacted. o, ▵ - In air diluent; ●, ▲, in a 75% O_2 25% N_2 mixture.

Table 8. Measured Formation Yields of 2-Pentanone, 3-Pentanone, 2-Pentyl Nitrate and 3-Pentyl Nitrate at 296 ± 2 K and 760 Torr Total Pressure.

O_2 Pressure (Torr)	Formation Yields[a]			
	2-Pentanone	3-Pentanone	2-Pentyl nitrate	3-Pentyl nitrate
155	0.054 ± 0.008	0.250 ± 0.030	0.062 ± 0.012	0.047 ± 0.006
590	0.149 ± 0.017	0.353 ± 0.032	0.064 ± 0.009	0.043 ± 0.004
			0.060 ± 0.010[b]	0.044 ± 0.006[b]

[a] Indicated errors are the two least-squares standard deviations combined with the estimated overall uncertainties in the GC-FID response factors of ±5% for *n*-pentane and the products.
[b] Combined data.

The formation yields of the 2- and 3-pentyl nitrates obtained from a least-squares analysis of the entire data set (Table 8) are 0.060 ± 0.010 for 2-pentyl nitrate and 0.044 ± 0.006 for 3-pentyl nitrate. These formation yields can be compared to our previous yields at room temperature (299-300 K) and atmospheric pressure (735-740 Torr) of 0.071 ± 0.009 and 0.046 ± 0.006, respectively, (*40*) and 0.074 ± 0.002 and 0.052 ± 0.004, respectively (*57*), where the indicated errors in the Atkinson et al. (*40,57*) data are two least-squares standard deviations. The agreement is reasonably good.

The expected reactions of the 2- and 3-pentoxy radicals formed after H-atom abstraction from the 2- and 3-positions in *n*-pentane are reaction with O_2, decomposition and isomerization for the 2-pentoxy radical, and O_2 reaction and decomposition for the 3-pentoxy radical (isomerization via a 6-member transition state cannot occur). The 2-pentanone and 3-pentanone formation yields should therefore exhibit a dependence on the O_2 concentration, and a plot of $(\text{yield})^{-1}$ against $[O_2]^{-1}$ should be a straight line, with an intercept of (yield of pentoxy radical from *n*-pentane)$^{-1}$ and a slope/intercept of $[(k_{decomp} + k_{isomer})/k_{O2}]$. Such plots are shown in Figure 16, and the intercepts lead to fraction yields of pentoxy radicals from *n*-pentane of 0.403 for the 2-pentoxy radical and 0.415 for the 3-pentoxy radical.

Combining the 2- and 3-pentanone yields extrapolated to $[O_2]^{-1} = 0$ with the measured 2- and 3-pentyl nitrate yields implies a yield of 2-pentyl radicals from *n*-pentane of 0.46, and of the 3-pentyl radical from *n*-pentane of 0.46. Since the calculated formation yield of 1-pentyl radicals from *n*-pentane is 0.009 ± 0.001, then a complete accounting of the pentyl radicals has been obtained. However, the formation yields of 2- and 3-pentyl radicals derived from this product study of 0.46 each are in significant disagreement with expectations based on the Atkinson (*49*) estimation technique of formation yields of 0.56 and 0.35, respectively (though the combined yield is identical). This observation implies that the empirical Atkinson (*49*) estimation method for OH radical reaction rate constants and group rate constants may be incorrect at this level of detail.

The values of $[(k_{decomp} + k_{isomer})/k_{O2}]$ obtained from the slopes of the lines in Figure 16 are 3.3×10^{19} molecule cm^{-3} (± 15-20%) for the 2-pentoxy radical and 3.3×10^{18} molecule cm^{-3} (±50%) for the 3-pentoxy radical, both at 296 ± 2 K and 740 Torr total pressure. Literature data are available for the corresponding ratios for the 1-butoxy radical (corresponding to the

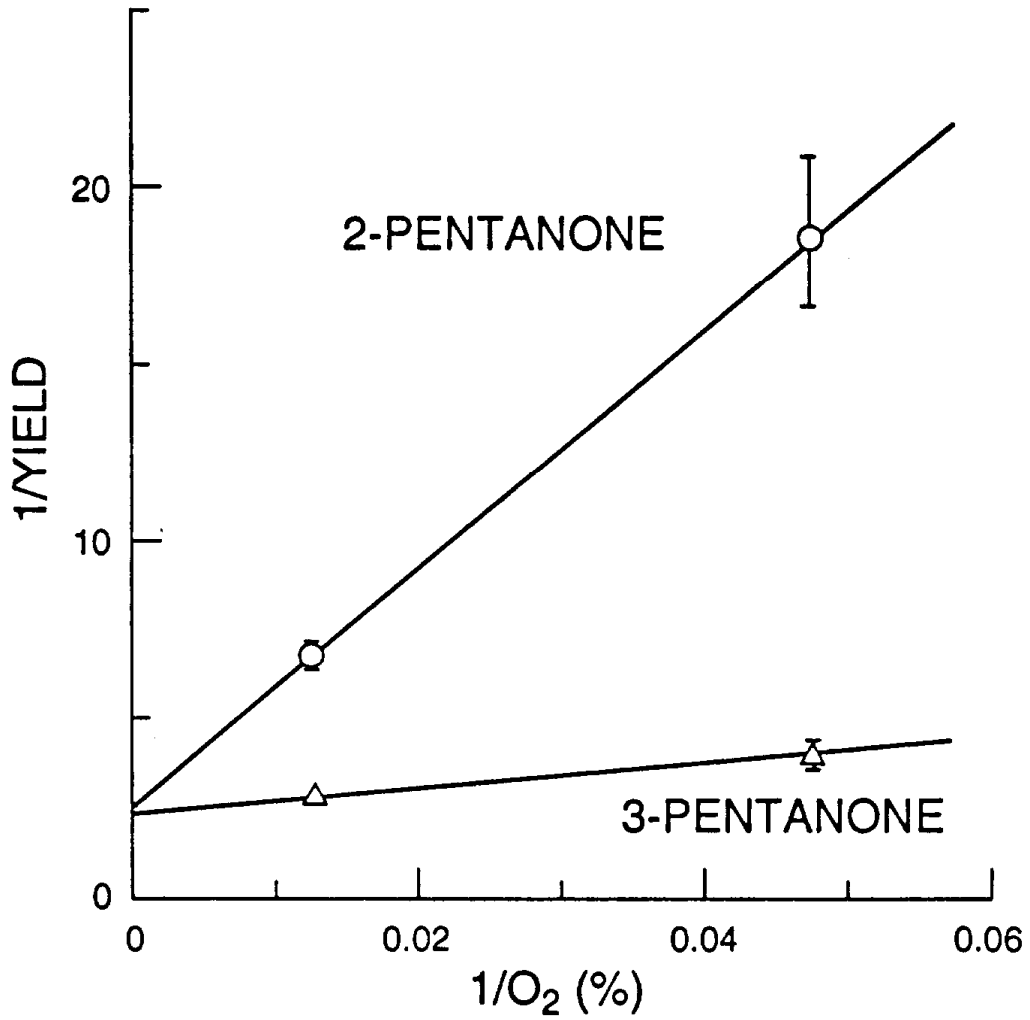

Figure 16. Plots of $(\text{yield})^{-1}$ for 2- and 3-pentanone against $[O_2]^{-1}$.

2-pentoxy radical) and the 2-butoxy radical (corresponding to the 3-pentoxy radical). For the 1-butoxy radical (decomposition being expected to be less important for the 1-butoxy radical than for the 2-pentoxy radical), Carter et al. (*23*), Cox et al. (*24*) and Niki et al. (*25*) derived a ratio of $[(k_{decomp} + k_{isomer})/k_{O2}] = 1.7 \times 10^{19}$ molecule cm^{-3} at ~299 K (*4*), while for the 2-butoxy radical, Carter et al. (*23*) and Cox et al. (*24*) obtained values of $[(k_{decomp} + k_{isomer})/k_{O2}] = 3.1 \times 10^{18}$ molecule cm^{-3} at 303 K and 2.6×10^{18} molecule cm^{-3} at 296 K, respectively. These ratios of $[(k_{decomp} + k_{isomer})/k_{O2}]$ for the 1- and 2-butoxy radicals are similar to the ratios obtained here for the 2- and 3-pentoxy radicals, respectively, which is gratifying since it is expected that to a reasonable approximation the 2-pentoxy radical should correspond to the 1-butoxy radical (but with decomposition of the 1-butoxy being of minor importance) and that the 3-pentoxy radical should correspond to the 2-butoxy radical.

Assuming that the rate constants k_{O2} for the O_2 reactions with the 2- and 3-pentoxy radicals are both 9×10^{-15} cm^3 $molecule^{-1}$ s^{-1} at 298 K (*4*), then the values of $(k_{decomp} + k_{isomer})$ are 3.0×10^4 s^{-1} ($\pm$50%) for the 3-pentoxy radical and 3.0×10^5 s^{-1} for the 2-pentoxy radical, both at 296 $\pm$ 2 K. The decomposition rate for the 2-pentoxy radical is expected to be a factor of 2 less than that for the 3-pentoxy radical (due to the degeneracy factor of 2 for the 3-pentoxy radical), and hence the value of $(k_{decomp} + k_{isomer})$ for the 2-pentoxy radical is expected to be close to that for k_{isomer}. The resulting value of $k_{isomer} = 2.85 \times 10^5$ s^{-1} at 296 K is a factor of 4 higher than the isomerization rate for the 1-butoxy radical (*4,23-25*), but a factor of 2 lower than the value predicted by Baldwin et al. (*48*). Hence our data for the ketone and alkyl nitrate products from the OH radical-initiated reaction of *n*-pentane are in agreement with previous literature data for *n*-pentane and consistent with our present knowledge of alkoxy radical reactions, and provide important additional data to the rather meager data base.

n-Hexane, n-heptane and n-octane. The products of the OH radical reactions with *n*-hexane, *n*-heptane and *n*-octane, in the presence of NO_x, were carried out in air (21% O_2) and in elevated O_2 mixtures. For *n*-hexane, the 2- and 3-hexyl nitrates were observed in ~12-13% yield (combined), consistent with previous data (*40*). In air, only 3-hexanone was identified and quantified, with a formation yield of ~6%. Under elevated O_2 conditions, 2-hexanone was also observed in low (~1%) yield together with 3-hexanone in ~12% yield. No useful data were obtained from the *n*-heptane or *n*-octane experiments.

Analyses by API MS/MS. Reactions of the OH radical with a series of *n*-alkanes and their fully deuterated analogs were carried out, in the presence of NO_x, in a 6500 liter all-Teflon chamber interfaced to a SCIEX API III MS/MS system. The data obtained are preliminary and will be repeated with concurrent GC-FID analyses during the next several months under funding from the U.S. Environmental Protection Agency. In positive ion mode carbonyl compounds exhibit a peak at $[MH]^+$, while alcohols show small peaks at $[MH]^+$ and $[M-H]^+$, together with a more abundant peak at ($[MH-H_2O]^+$ (see, for example, Figure 17 for 4-octanol). Therefore, for the non-deuterated alkanes, the carbonyls would be observed by ion peaks at 73, 87, 101, 115 and 129 amu for *n*-butane through *n*-octane, while the three peaks mentioned above for the hydroxycarbonyls expected from alkoxy radical isomerization would be expected at 89, 87 and 71 for *n*-butane, 103, 101 and 85 for *n*-pentane, 117, 115 and 99 for *n*-hexane, 131, 129 and 113 for *n*-heptane and 145, 143 and 127 for *n*-octane.

The major product ion observed from the OH radical reaction with *n*-butane (molecular weight 58) was a peak at 73 amu, corresponding to the expected carbonyls (butanal + 2-butanone). For *n*-pentane, product ion peaks were observed at 101 amu (possibly with a very weak 103 amu peak), 87 amu and 85 amu (Figure 18). Based on the above discussion, the 87 amu peak would correspond to the pentanones (the authentic standards had 87 amu $[MH]^+$ peaks) and the 85/101 amu peaks may belong to the expected δ-hydroxycarbonyls. In a similar manner, *n*-hexane showed product ion peaks at 97, 99, 101, and 115 amu, with the weak 101 peak corresponding to hexanones and the 99/115 peaks possibly belonging to the δ-hydroxycarbonyls. The daughter ion spectrum of the 99 amu peak showed ions at 29, 43 and 57 amu, corresponding to $HCO^+/C_2H_5^+$, $CH_3CO^+/C_3H_7^+$ and $CH_3CH_2CO^+/C_4H_9^+$.

n-Heptane showed major product ions at 113 and 129 amu (Figure 19), which could correspond to the hydroxycarbonyls expected after heptoxy radical isomerization. The expected heptanone product ion peak at 115 amu was minor, at best (Figure 19). Use of different API operating parameters, while markedly changing the appearance of the product ion spectrum, also showed the formation of ion peaks at 129 (very weak) and 113 amu, as well as a peak at 131 amu, the position of the $[MH]^+$ ion. Similarly, reaction of *n*-octane gave product peaks at 127, 143 and 145 amu, with the intensities of the individual peaks of these depending on the API conditions. Again, no evidence for the octanone 129 amu peak was observed.

DI	5
ISV	8000
IN	850
OR	35
R0	30
M1	200
RE1	123
DM1	0.140
R1	28
L7	-40
R2	-41
M3	200
RE3	123
DM3	0.110
R3	-50
L9	-250
FP	-250
MU	-4600
CC	10
CG	Off
DI µA	3.7
CGT	3.05
ISv	5520.3
UV	664.4

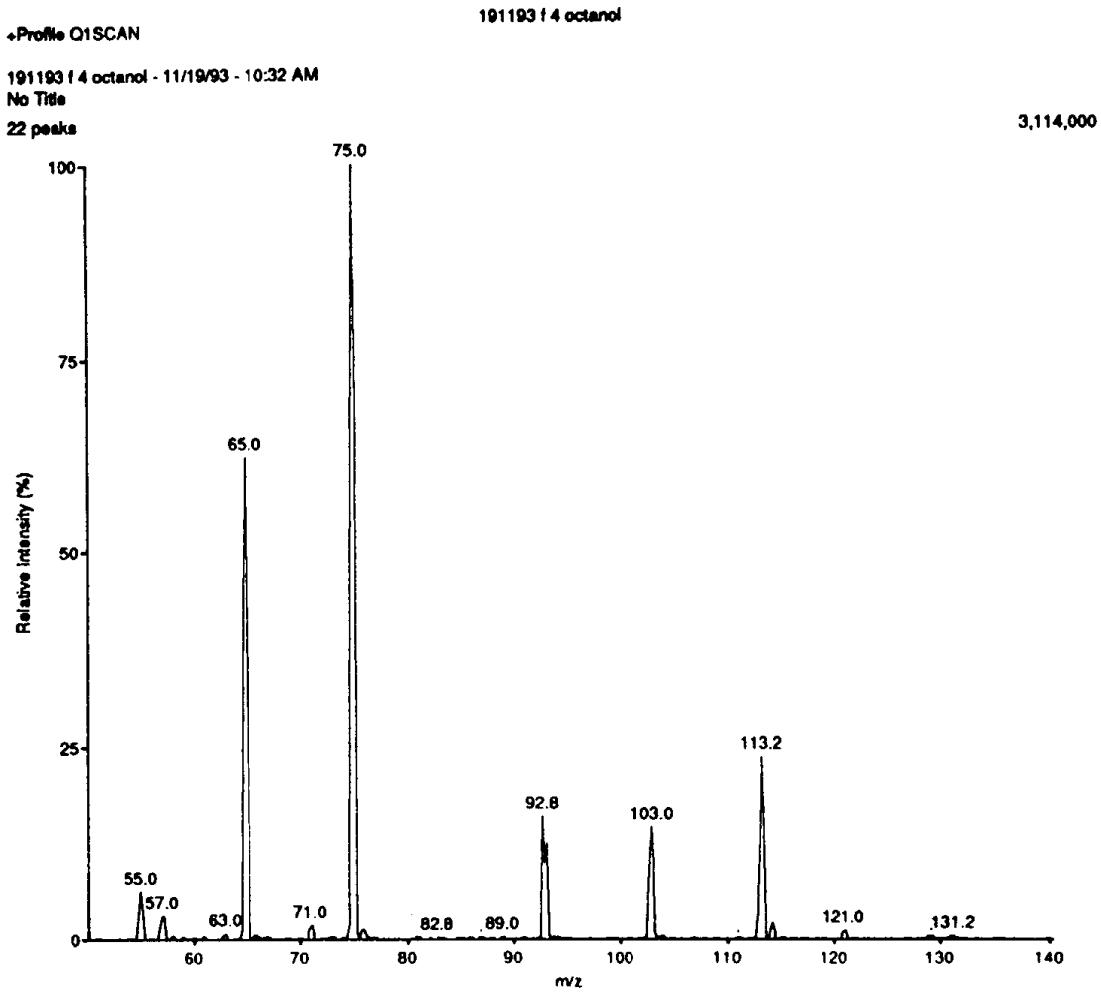

Figure 17. API MS spectrum for 4-octanol.

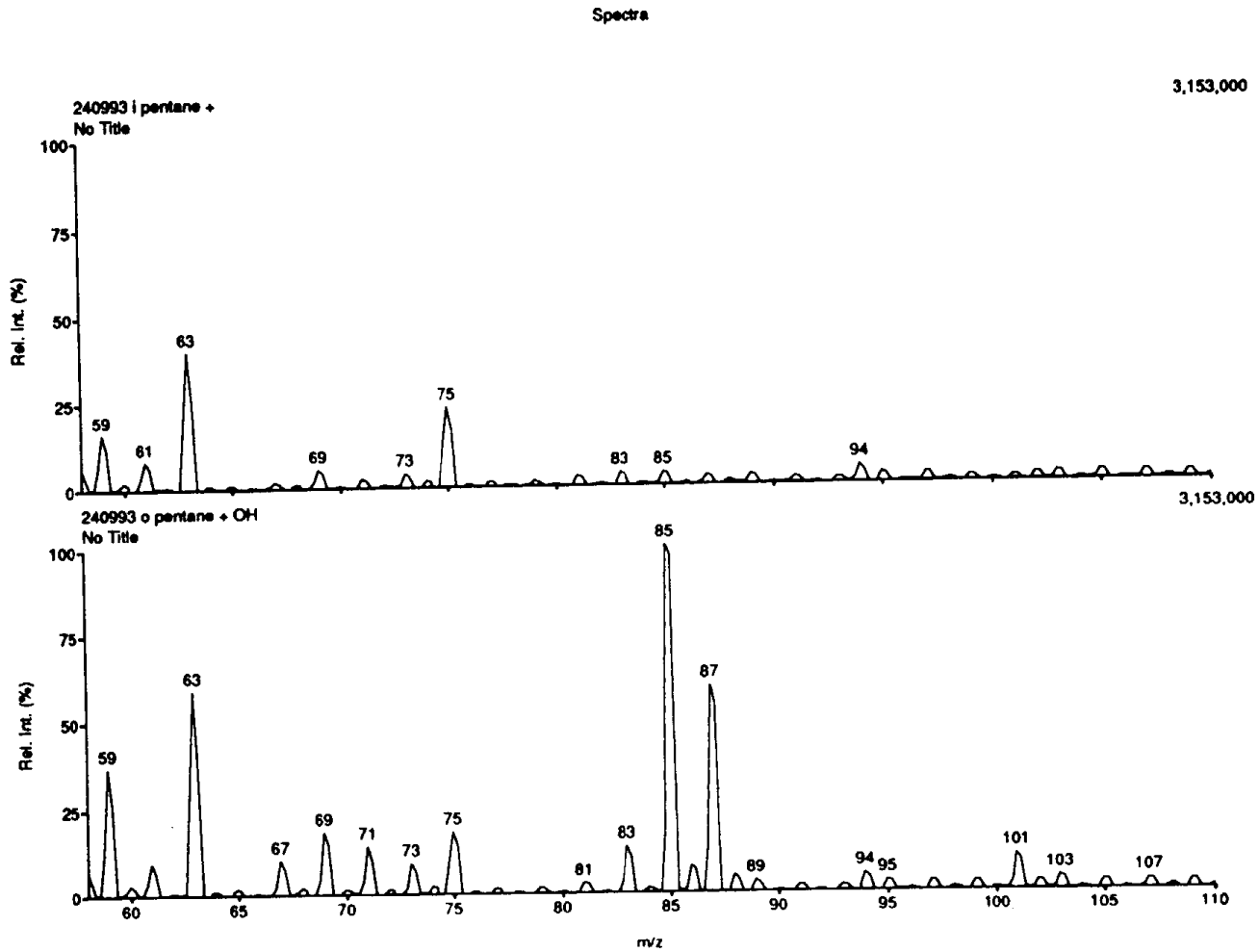

Figure 18. API MS spectra obtained before (top) and after (bottom) irradiation of a CH_3ONO-NO-*n*-pentane-air mixture.

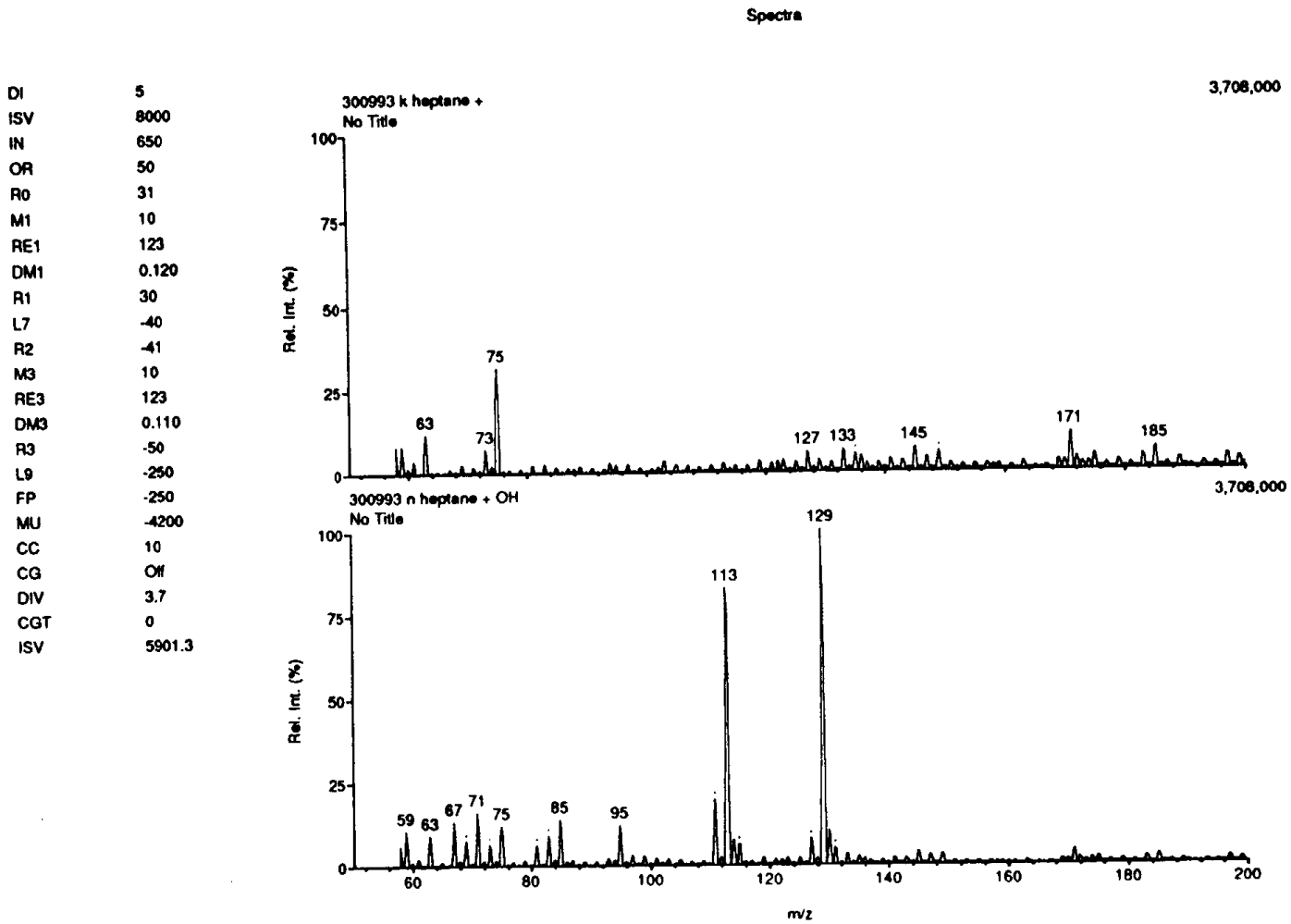

Figure 19. API MS spectra obtained before (top) and after (bottom) irradiation of a CH_3ONO-NO-*n*-heptane-air mixture.

The API MS data for the OH radical-initiated reactions of the C_4 - C_8 *n*-alkanes are consistent with, but do not prove, the formation of carbonyls and hydroxycarbonyls of the same carbon number as the *n*-alkane, with the importance of the carbonyl decreasing with increasing carbon number and with the importance of the hydroxycarbonyl increasing with carbon number. Reactions of the perdeuterated *n*-alkanes were therefore carried out to attempt to verify this "postulate." To date, preliminary experiments have been carried out with *n*-hexane-d_{14},*n*-heptane-d_{16} and *n*-octane-d_{18}. The obvious product peaks for the *n*-hexane-d_{14} reaction were at 110, 113, and 125 amu. The 113 amu peak is at the mass expected for the hexanones/hexanal product $[MH]^+$. Since D atoms on alcohol -OD groups are expected to rapidly H/D exchange to -OH, then the hydroxycarbonyls would be $C_6D_{11}O_2H$, and the $[MH]^+$ ion would be at 128 amu and the $[MH\text{-}H_2O]^+$ ion at 110 amu (for example, $[CD_3C(O)CD_2CD_2CDCD_3]^+$). The ion corresponding to the $[M\text{-}H]^+$ ion could be at 126 amu (for example, $CD_3C(O)CD_2CD_2CDO^+CD_3$) or, if $[M\text{-}D]^+$, at 125 amu (for example, $CD_3C(O)CD_2CD_2COH^+CD_3$). The observed 110 and 125 amu peaks are consistent with hydroxycarbonyl formation and, although the expected δ-hydroxycarbonyls are not commercially available, we will use our authentic standard of 4-hydroxy-4-methyl-2-pentanone to record the API MS spectrum. The spectra obtained from the *n*-heptane-d_{16} and *n*-octane-d_{18} reactions were analogous to these from *n*-hexane-d_{14}, with the mass numbers 16 and 32 amu higher, respectively.

VI. SUMMARY AND CONCLUSIONS

The experimental product studies of the atmospherically-important reactions of selected aromatic hydrocarbons and alkanes, and of ketones and alcohols designed to provide unambiguous evidence for alkoxy radical isomerization, have led to important new findings:

- Our product study of the OH radical-initiated reactions of toluene, 1,2,3-trimethylbenzene and, especially, *o*-xylene, has shown that in the troposphere the OH-*o*-xylene adduct will react with O_2 and not with NO_2. The O_2 and NO_2 reactions will be equally important at an NO_2 mixing ratio of 1.6 ppm, a concentration often encountered in laboratory product studies but not in ambient air. Our data for *o*-xylene are in agreement with the kinetic data of Zetzsch and coworkers (*27*) for benzene and toluene; further research is needed to elucidate the products and reaction mechanisms of the O_2 and NO_2 reactions with the OH-aromatic adducts. Since laboratory studies have often been carried out at NO_2 concentrations such that the OH-aromatic adducts react at least partially with NO_2, care must be taken in using these laboratory product data for ambient atmospheric purposes.

- We have unambiguously observed the products arising after alkoxy radical isomerization in the OH radical-initiated reactions of the two alcohols 2,4-dimethyl-4-pentanol and 3,5-dimethyl-3-hexanol and, less unambiguously, from the OH radical-initiated reactions of the two ketones 4-methyl-2-pentanone and 2,6-dimethyl-4-heptanone. Preliminary *in situ* atmospheric pressure ionization mass spectrometric data for the reactions of the OH radical with a series of *n*-alkanes provides evidence for the formation of the expected δ-hydroxycarbonyls after alkoxy radical isomerization, and gas chromatographic analysis of the products formed from the OH radical reaction with *n*-pentane yields rate constant ratios for the decomposition, isomerization and O_2 reaction rate constants which are consistent with the literature data for the 1- and 2-butoxy radicals (the only other data available).

The experimental data described above in this report answer the two questions which were the basis for this program: "Do the OH-aromatic adducts react with O_2 or with NO_2 in the atmosphere?" and "Do alkoxy radicals undergo isomerization?" While a vast amount of research remains to be done to elucidate the details of the aromatic and alkanes degradation reaction sequences in the atmosphere, progress is being made which enables the chemical mechanisms formulated and tested for use in urban and regional airshed computer models to be placed on an increasingly firm scientific basis.

References

1. J. H. Seinfeld, Urban air pollution: State of the science, *Science,* **243**, 745-752 (1989).

2. "Rethinking the Ozone Problem in Urban and Regional Air Pollution," National Academy Press, Washington, D.C. (1991).

3. S. N. Pandis, R. A Harley, G. R. Cass, and J. H. Seinfeld, Secondary organic aerosol formation and transport, *Atmos. Environ.*, **26A**, 2269-2282 (1992).

4. R. Atkinson, Gas-phase tropospheric chemistry of organic compounds, *J. Phys. Chem. Ref. Data*, **Monograph 2**, 1-216 (1994).

5. SCAQMD, South Coast Air Quality Management District, "Pollution Sources by Activity Data for 1985" (1989).

6. R. A. Harley, M. P. Hannigan, and G. R. Cass, Respeciation of organic gas emissions and the detection of excess unburned gasoline in the atmosphere, *Environ. Sci. Technol.*, **26**, 2395-2408 (1992).

7. W. A. Lonneman, R. L. Seila, and S. A. Meeks, Non-methane organic composition in the Lincoln Tunnel, *Environ. Sci. Technol.*, **20**, 790-796 (1986).

8. J. E. Sigsby, Jr., S. Tejada, W. Ray, J. M. Lang, and J. W. Duncan, Volatile organic compound emissions from 46 in-use passenger cars, *Environ. Sci. Technol.*, **21**, 466-475 (1987).

9. R. B. Zweidinger, J. E. Sigsby, Jr., S. B. Tejada, F. D. Stump, D. L. Dropkin, W. D. Ray, and J. W. Duncan, Detailed hydrocarbon and aldehyde mobile source emissions from roadway studies, *Environ. Sci. Technol.*, **22**, 956-962 (1988).

10. F. Stump, S. Tejada, W. Ray, D. Dropkin, F. Black, W. Crews, R. Snow, P. Siudak, C. O. Davis, L. Baker, and N. Perry, The influence of ambient temperature on tailpipe emissions from 1984-1987 model year light-duty gasoline motor vehicles, *Atmos. Environ.*, **23**, 307-320 (1989).

11. S. K. Hoekman, Speciated measurements and calculated reactivities of vehicle exhaust emissions from conventional and reformulated gasolines, *Environ. Sci. Technol.*, **26**, 1206-1216 (1992).

12. D. Grosjean, and K. Fung, Hydrocarbons and carbonyls in Los Angeles air, *J. Air Pollut. Control Assoc.*, **34**, 537-543 (1984).

13. S. A. Edgerton, M. W. Holdren, D. L. Smith, and J. J. Shah, Inter-urban comparison of ambient volatile organic compound concentrations in U.S. cities, *J. Air Pollut. Control Assoc.*, **39**, 729-732 (1989).

14. R. L. Seila, W. A. Lonneman, and S. A. Meeks, "Determination of C_2 to C_{12} ambient air hydrocarbons in 39 U.S. cities, from 1984 through 1986." EPA 600/3-89/058, U.S. Environmental Protection Agency, Research Triangle Park, NC, September, 1989.

15. "Analysis of the Ambient VOC Data Collected in the Southern California Air Quality Study," Final Report, prepared by F. W. Lurmann and H. H. Main, California Air Resources Board Contract No. A832-130, Sacramento, CA, February 1992.

16. M. W. Gery, G. Z. Whitten, J. P. Killus, and M. C. Dodge, A photochemical kinetics mechanism for urban and regional scale computer modeling, *J. Geophys. Res.*, 94, 12925-12956 (1989).

17. M. C. Dodge, M. C., A comparison of three photochemical oxidant mechanisms, *J. Geophys. Res.*, **94**, 5121-5136 (1989).

18. M. C. Dodge, Formaldehyde production in photochemical smog as predicted by three state-of-the science chemical oxidant mechansisms, *J. Geophys. Res.*, **95**, 3635-3648 (1990).

19. W. P. L. Carter, A detailed mechanism for the gas-phase atmospheric reactions of organic compounds, *Atmos. Environ.*, **24A**, 481-518 (1990).

20. W. P. L. Carter and R. Atkinson, Atmospheric chemistry of alkanes, *J. Atmos. Chem.*, **3**, 377-405 (1985).

21. R. Atkinson, Gas-phase tropospheric chemistry of organic compounds: A review, *Atmos. Environ.*, **24A**, 1-41 (1990).

22. W. P. L. Carter, and R. Atkinson, Alkyl nitrate formation from the atmospheric photooxidation of alkanes: A revised estimation method, *J. Atmos. Chem.*, **8**, 165-173 (1989).

23. W. P. L. Carter, A. C. Lloyd, J. L. Sprung, and J. N. Pitts, Jr., Computer modeling of smog chamber data: Progress in validation of a detailed mechanism for the photooxidation of propene and *n*-butane in photochemical smog, *Int. J. Chem. Kinet.*, **11**, 45-101 (1979).

24. R. A. Cox, K. F. Patrick, and S. A. Chant, Mechanism of atmospheric photooxidation of organic compounds. Reactions of alkoxy radicals in oxidation of *n*-butane and simple ketones, *Environ. Sci. Technol.*, **15**, 587-592 (1981).

25. H. Niki, P. D. Maker, C. M. Savage, and L. P. Breitenbach, An FT IR study of the isomerization and O_2 reaction of *n*-butoxy radicals, *J. Phys. Chem.*, **85**, 2698-2700 (1981).

26. R. Atkinson, Kinetics and mechanisms of the gas-phase reactions of the hydroxyl radical with organic compounds, *J. Phys. Chem. Ref. Data*, **Monograph 1**, 1-246 (1989).

27. R. Knispel, R. Koch, M. Siese, and C. Zetzsch, Adduct formation of OH radicals with benzene, tolluene and phenol and consecutive reactions of the adducts with NO_x and O_2, *Ber. Bunsenges. Phys. Chem.*, **94**, 1375-1379 (1990).

28. R. Zellner, B. Fritz, and M. Preidel, A cw UV laser absorption study of the reactions of the hydroxy-cyclohexadienyl radical with NO_2 and NO, *Chem. Phys. Lett.*, **121**, 412-416 (1985).

29. N. Bourmada, P. Devolder, and L.-R. Sochet, Rate constant for the termolecular reaction of OH + toluene + helium in the fall-off range below 10 torr, *Chem. Phys. Lett.*, **149**, 339-342 (1988).

30. N. Bourmada, M. Carlier, J.-F. Pauwels, and P. Devolder, Mesure de la constante de vitesse de la reáction du radical OH avec le toluène par la technique du tube à écoulement rapide et décharge microonde, *J. Chim. Phys.*, **85**, 881-887 (1988).

31. C. Zetzsch, R. Koch, M. Siese, F. Witte, and P. Devolder, "Adduct formation of OH with benzene and toluene and reaction of the adducts with NO and NO_2," Proc. 5th European Symposium on the Physico-Chemical Behaviour of Atmospheric Pollutants. Kluwer Academic Pub., Dordrecht, The Netherlands, 1990, pp. 320-327.

32. A. Gourmi, J.-P. Sawerysyn, J.-F. Pauwels, and P. Devolder, "Tropospheric oxidation of toluene: Reactions of some intermediate radicals," Proc. 5th European Symposium on the Physico-Chemical Behavior of Atmospheric Pollutants, Kluwer Academic Pub., Dordrecht, The Netherlands, 1990, pp. 315-319.

33. A. Goumri, J. F. Pauwels, and P. Devolder, Rate of the OH + C_6H_6 + He reaction in the fall-off range by discharge flow and OH resonance fluorescence. *Can. J. Chem.*, **69**, 1057-1064 (1991).

34. C. Zetzsch, M. Elend, R. Knispel, R. Koch, J. Nowack, and M. Siese, "Hydroxyl and Aromatics: Rate of the Adducts in the Presence of O_2," EUROTRAC Annual Report, 1991, Part 8, LACTOZ, pp. 207-215, Commission of the European Communities.

35. R. Atkinson, S. M. Aschmann, J. Arey, and W. P. L. Carter, Formation of ring-retaining products from the OH radical-initiated reactions of benzene and toluene, *Int. J. Chem. Kinet.*, **21**, 801-827 (1989).

36. R. Atkinson, S. M. Aschmann, and J. Arey, Formation of ring-retaining products from the OH radical-initiated reactions of *o*- *m*-, and *p*-xylene, *Int. J. Chem. Kinet.*, **23**, 77-97 (1991).

37. R. Atkinson, W. P. L. Carter, A. M. Winer, and J. N. Pitts, Jr., An experimental protocol for the determination of OH radical rate constants with organics using methyl nitrite photolysis as an OH radical source, *J. Air Pollut. Control Assoc.*, **31**, 1090-1092 (1981).

38. R. Atkinson, S. M. Aschmann, J. Arey, and B. Shorees, Formation of OH radicals in the gas-phase reactions of O_3 with a series of terpenes, *J. Geophys. Res.*, **97**, 6065-6073 (1992).

39. R. Atkinson and S. M. Aschmann, OH radical production from the gas-phase reactions of O_3 with a series of alkenes under atmospheric conditions, *Environ. Sci. Technol.*, **27**, 1357-1363 (1993).

40. R. Atkinson, S. M. Aschmann, W. P. L. Carter, A. M. Winer, and J. N. Pitts, Jr., Alkyl nitrate formation from the NO_x-air photooxidations of C_2-C_8 *n*-alkanes, *J. Phys. Chem.*, **86**, 4563-4569 (1982).

41. K. R. Darnall, R. Atkinson, and J. N. Pitts, Jr., Observation of biacetyl from the reaction of OH radicals with *o*-xylene. Evidence for ring cleavage, *J. Phys. Chem.*, **83**, 1943-1946 (1979).

42. R. Atkinson, W. P. L. Carter, and A. M. Winer, Effects of pressure on product yields in the NO_x photooxidations of selected aromatic hydrocarbons, *J. Phys. Chem.*, **87**, 1605-1610 (1983).

43. H. Bandow and N. Washida, Ring-cleavage reactions of aromatic hydrocarbons studied by FT-IR spectroscopy. II. Photooxidation of *o*-, *m*-, and *p*-xylenes in the NO_x-air system, *Bull. Chem. Soc. Jpn.*, **58**, 2541-2548 (1985).

44. H. Bandow and N. Washida, Ring-cleavage reactions of aromatic hydrocarbons studied by FT-IR spectroscopy. III. Photooxidation of 1,2,3- 1,2,4- and 1,3,5-trimethylbenzenes in the NO_x-air system, *Bull. Chem. Soc. Jpn.*, **58**, 2549-2555 (1985).

45. E. C. Tuazon, H. Mac Leod, R. Atkinson, and W. P. L. Carter, α-Dicarbonyl yields from the NO_x-air photooxidations of a series of aromatic hydrocarbons in air, *Environ. Sci. Technol.*, **20**, 383-387 (1986).

46. R. Atkinson and W. P. L. Carter, Reactions of alkoxy radicals under atmospheric conditions: The relative importance of decomposition versus reaction with O_2, *J. Atmos. Chem.*, **13**, 195-210 (1991).

47. W. P. L. Carter, K. R. Darnall, A. C. Lloyd, A. M. Winer, and J. N. Pitts, Jr., Evidence for alkoxy radical isomerization in photooxidations of C_4-C_6 alkanes under simulated atmospheric conditions, *Chem. Phys. Lett.*, **42**, 22-27 (1976).

48. A. C. Baldwin, J. R. Barker, D. M. Golden, and D. G. Hendry, Photochemical smog. Rate parameter estimates and computer simulations, *J. Phys. Chem.*, **81**, 2483-2492 (1977).

49. R. Atkinson, A structure-activity relationship for the estimation of rate constants for the gas-phase reactions of OH radicals with organic compounds, *Int. J. Chem. Kinet.*, **19**, 799-828 (1987).

50. R. A. Cox, R. G. Derwent, and M. R. Williams, Atmospheric photooxidation reactions. Rates, reactivity, and mechanism for reaction of organic compounds with hydroxyl radicals, *Environ. Sci. Technol.*, **14**, 57-61 (1980).

51. G. Heimann and P. Warneck, OH radical induced oxidation of 2,3-dimethylbutane in air, *J. Phys. Chem.*, **96**, 8403-8409 (1992).

52. National Institute of Standards and Technology Standard Reference Database 25 "Structures and Properties Database and Estimation Program," Version 2.0, S.E. Stein, Chemical Kinetics and Thermodynamics Division, NIST, Gaithersburg, MD, 1994.

53. S. W. Benson, *Thermochemical Kinetics, 2nd Ed.*, Wiley, New York, NY (1976).

54. M. E. Jenkin, R. A. Cox, M. Emrich, and G. K. Moortgat, Mechanisms of the Cl-atom-initiated oxidation of acetone and hydroxyacetone in air, *J. Chem. Soc. Faraday Trans.*, **89**, 2983-2991 (1993).

55. J. T. Scanlon and D. E. Willis, Calculation of flame ionization detector relative response factors using the Effective Carbon Number concept, *J. Chromat. Sci.*, **23**, 333-340 (1985).

56. E. S. C. Kwok and R. Atkinson, "Estimation of Hydroxyl Radical Reaction Rate Constants for Gas-Phase Organic Compounds Using a Structure-Reactivity Relationship: An Update," Final Report to the Chemical Manufacturers Association, Washington, D.C. (1994).

57. R. Atkinson, W. P. L. Carter, and A. M. Winer, Effects of temperature and pressure on alkyl nitrate yields in the NO_x photooxidation of *n*-pentane and *n*-heptane, *J. Phys. Chem.*, **87**, 2012-2018 (1983).

Glossary of Terms, Abbreviations, and Symbols

APCI	Atmospheric pressure chemical ionization
API MS/MS	Atmospheric pressure ionization tandem mass spectrometry
ARB	Air Resources Board
CAD	Collision-activated dissociation
FID	Flame ionization detection
GC	Gas chromatography
GC/MS	Combined gas chromatography-mass spectrometry
NMOC	Non-methane organic compounds
NO	Nitric oxide
NO_2	Nitrogen dioxide
NO_3	Gaseous nitrate radical
O_3	Ozone
PAN	Peroxyacetyl nitrate
SAPRC	Statewide Air Pollution Research Center